A MECHANISTIC STUDY OF UMPOLUNG AMIDE SYNTHESIS, THE STRAIGHTFORWARD SYNTHESIS OF ^{18}O-LABELED AMIDES, AND THE DEVELOPMENT OF CATALYTIC UMPOLUNG AMIDE SYNTHESIS

By

Jessica P. Shackleford

Thesis

Submitted to the Faculty of the

Graduate School of Vanderbilt University

in partial fulfillment of the requirements

for the degree of

MASTER OF SCIENCE

in

Chemistry

May, 2012

Nashville, TN

Approved

Dr. Jeffrey N. Johnston

Dr. Charles M. Lukehart

ACKNOWLEDGMENTS

This work would not have been possible without funding from the National Science Foundation Graduate Research Fellowship program, Amgen, and the National Institute of Health. I also want to specifically thank my advisor, Dr. Jeffrey Johnston, for his constant support and encouragement. His passion for science and teaching serves as an inspiration to me, and I hope to one day inspire students the way he has inspired me. He has always pushed me to do my best and then do even better, and I will be a better scientist and teacher because of that encouragement.

Additionally, I would like to thank my committee members Dr. Charles Lukehart and Dr. Brian Bachmann for their support and critical feedback. I would also like to thank our excellent NMR staff at Vanderbilt University, Dr. Don Stec and Dr. Markus Voehler, for all their help interpreting and developing NMR experiments. I also owe a huge debt of thanks to Jonathan Karty, Angela Hanson, and the Indiana University Mass Spectrometry department for all of their considerable time and effort in analyzing my numerous ^{18}O-enriched samples.

I would like to specifically thank Dr. Bo Shen for his collaborative efforts on these projects, a lot of which would not be possible without his contributions. In addition, my thanks to Dawn Makley and Matt Leighty for providing thoughtful discussions, helpful advice, and a listening ear throughout my thesis work. Other members of the Johnston group I would like to thank for their support and encouragement are Amanda Doody, Priya Mathew, Hubert Muchalski, Mark Dobish, Tyler Davis, and Aroop Chandra.

I would also like to thank my husband, Trey Flinn, for his encouragement throughout my research and for being willing to listen to me talk about my work even though it wasn't always the easiest conversation to follow. Lastly, I would like to thank my parents for always supporting and encouraging my dreams and aspirations. They raised me to believe that I was capable of doing anything I put my mind toward doing, and without their faith, none of this would be possible.

TABLE OF CONTENTS

ACKNOWLEDGMENTS ..... **ii**

LIST OF SCHEMES ..... **viii**

LIST OF FIGURES ..... **xi**

LIST OF EQUATIONS ..... **xiii**

1. Umpolung Amide Synthesis Mechanistic Study **1**

1.1 Introduction 1

1.1.1. Current Methods and Problems in Amide Coupling 1

1.1.2. Syntheses of ^{18}O-Labeled Peptides and Their Use 4

1.2 Umpolung Amide Bond Synthesis Mechanistic Study 10

1.2.1 Initial Determination of Oxygen Donor 11

1.2.2 Optimization of ^{18}O-Labeling Method 17

1.2.3 NMR, IR, and Mass Spectrometric Analysis of Compounds 25

1.2.4 Formation of Doubly Labeled ^{18}O Peptides Through Standard Coupling 33

2. Catalytic Umpolung Amide Synthesis **38**

2.1 Introduction 38

2.1.1 Alternatives to NIS 38

2.1.2 Oxygen-Catalyzed Turnover of NIS 40

2.2 Catalytic Umpolung Amide Bond Synthesis 42

2.3 Catalytic Umpolung Amide Coupling Using Disubstituted Amines 49

2.3.1 Current Methods and Challenges of Coupling Disubstituted Amines 51

2.3.2 Reaction Optimization of Disubstituted Amine Coupling 55

2.3.3 Coupling Examples Featuring N-Me Amino Esters 68

3. Experimental 75

LIST OF TABLES

Table 1. Method Comparison for $^{18}O_2$ Gas Amide Synthesis 23

Table 2. Substrate Scope for $^{18}O_2$ Gas Amide Bond Formation 23

Table 3. Peptidic Substrate Scope of ^{18}O-Labeled Peptides 24

Table 4. Comparison of N-Halosuccinimide Halonium Sources 39

Table 5. Full Halogenating Reagent Screen 40

Table 6. Catalytic Umpolung Amide Synthesis: Substrate Scope of α-Bromo Nitroalkane Donors 43

Table 7. Catalytic Umpolung Amide Synthesis: Substrate Scope of *N*-Boc α-Bromo Nitroamines 44

Table 8. Optimization of NIS Equivalents for Entry 5 46

Table 9. Temperature Variation Studies on Entry 5 46

Table 10. Catalytic Umpolung Amide Synthesis: Substrate Scope of Amines 48

Table 11. Effect of Amine Equivalents on Disubstituted Amide Synthesis 56

Table 12. Effect of Additional NIS Addition 56

Table 13. Reaction Conversion with Additional NIS Monitored by NMR Aliquot 57

Table 14. Acidic Workup and Temperature Effects on the Disubstituted Amide Synthesis 58

Table 15. Base Screen for the Monosubstituted Amine Coupling 60

Table 16. Effect of Water on the Monosubstituted Amine Coupling 61

Table 17. Potential Water Substitutes for the Monosubstituted Amine Coupling 62

Table 18. Solvent Screen for the Monosubstituted Amine Coupling 63

Table 19. Temperature Variations of the Monosubstituted Amine Coupling 64

Table 20. Reaction Time Evaluation for Disubstituted Amine Couplings 64

Table 21. Excess Reagent Screen for Disubstituted Amine Couplings 66

Table 22. Variations in NIS Equivalents for Disubstituted Amine Couplings 67

Table 23. Halogenating Agent Screen for the Disubstituted Amine Couplings 67

Table 24. Optimization of *N*-Methylalanine Methyl Ester Coupling 72

Table 25. The Effect of the Side Chain on Coupling *N*-Methylamino Esters 74

LIST OF SCHEMES

Scheme 1. Amide Bond Formation: Examples of Coupling Reagents 2

Scheme 2. Solid Phase Peptide Synthesis 3

Scheme 3. Novel Methods for Amide Bond Synthesis 4

Scheme 4. Traditional Preparation of ^{18}O-Labeled Peptides 6

Scheme 5. Potential Back-Exchange Using $H_2{}^{18}O$/Acid Hydrolysis 7

Scheme 6. Method for ^{18}O Enrichment of FMOC Protected Amino Acids 7

Scheme 7. Method for ^{18}O Enrichment Preventing Back-Exchange 8

Scheme 8. Alternative Methods for the Preparation of ^{18}O-Labeled Amides 9

Scheme 9. Umpolung Amide Synthesis Using NIS 10

Scheme 10. Proposed Mechanism Featuring H_2O as the Amide Carbonyl Oxygen Donor 11

Scheme 11. ^{18}O-Labeled H_2O Amide Bond Synthesis 12

Scheme 12. Nitro Group Based Hydrolysis 13

Scheme 13. Proposed Mechanism Featuring the Nitro Group as the Amide Carbonyl Oxygen Donor 13

Scheme 14. Formation of ^{18}O-Labeled α-Bromo Nitroalkane 15

Scheme 15. Evaluation of Potential Oxygen Sources 16

Scheme 16. $^{18}O_2$ Gas Amide Bond Synthesis 16

Scheme 17. Proposed Aerobic and Anaerobic Pathways of Amide Bond Synthesis 17

Scheme 18. $^{18}O_2$ Gas Addition Methods Comparison 19

Scheme 19. Formation of the Doubly ^{18}O-Labeled Pentapeptide..... 35

Scheme 20. Comparison of Coupling Reagent Effectiveness 36

Scheme 21. Formation of a Doubly ^{18}O-Labeled Tetrapeptide 37

Scheme 22. Proposed Aerobic Pathway Featuring Turnover of Iodide to Iodonium 41

Scheme 23. Umpolung Amide Synthesis Using Catalytic NIS (5 mol %) 42

Scheme 24. Mechanism of Racemization in *N*-Methyl Amino Acid Couplings 51

Scheme 25. HOBt Racemization Suppressant Mechanism 52

Scheme 26. Mechanism for Diketopiperazine Formation 53

Scheme 27. Recent Advances in the Synthesis of Disubstituted Amides..... 54

Scheme 28. Model Reaction for Disubstituted Amide Formation Optimization..... 55

Scheme 29. The ter Meer Reaction 58

Scheme 30. Acidic Workup vs. Filtration Workup for Monosubstituted Amine Coupling..... 59

Scheme 31. Synthesis of *N*-Methyl Amino Ester Derivatives 68

Scheme 32. UmAS Couplings Featuring *N*-Methyl Phenylalanine Methyl Ester 69

Scheme 33. Purification Results for the *N*-Methyl Phenylalanine Methyl Ester..... 69

Scheme 34. Formation of the *N*-Methyl Alanine Methyl Ester Amide 71

Scheme 35. Potential Intermediates in Disubstituted UmAS 73

Scheme 36. Synthesis of *N*-Methyl Glycine Methyl Ester 73

Scheme 37. Formation of the *N*-Methyl Glycine Methyl Ester Amide 73

LIST OF FIGURES

Figure 1. Rate-Enhancers and Racemization Suppressants 2

Figure 2. Umpolung Amide Bond Synthesis 11

Figure 3. $^{18}O_2$ Gas Delivery System 20

Figure 4. Optimized $^{18}O_2$ Gas Amide Synthesis Set Up 22

Figure 5. IR Data for ^{18}O-Labeled-2-Phenyl-*N*-(1-phenylethyl)acetamide 26

Figure 6. ^{13}C NMR Data (expansion and integration) for ^{18}O-Labeled-2-Phenyl-*N*-(1-phenylethyl)acetamide 27

Figure 7. IR Data for ^{18}O-Labeled-*N*-Boc-4-Cl-Phenylglycine-Ala-Phe-OMe 29

Figure 8. HMBC Data Expansion of the Carbonyl Region of ^{18}O-Labeled-*N*-Boc-4-Cl-Phenylglycine-Ala-Phe-OMe 30

Figure 9. HMBC Data Expansion Featuring the Carbamate Carbonyl of the Boc Group 30

Figure 10. ^{13}C NMR data (expansion) for ^{18}O-Labeled-*N*-Boc-4-Cl-Phenylglycine-Ala-Phe-OMe 31

Figure 11. ^{13}C NMR for ^{18}O-Labeled-*N*-Boc-4-Cl-Phenylglycine-Ala-Phe-OMe at 0% and 93% Incorporation 31

Figure 12. ^{13}C NMR for ^{18}O-Labeled-*N*-Boc-4-Cl-Phenylglycine-Ala-Phe-OMe at 27% and 93% Incorporation 32

Figure 13. Hydrolysis, Deprotection, and Formation of a Doubly-^{18}O-Labeled Pentapeptide 34

Figure 14. Coupling Reagents Used in the Standard Coupling 35

Figure 15. Protecting Group Change 47

Figure 16. Protecting Group Change over a Longer Reaction Time 47

Figure 17. Natural Product Examples Featuring Disubstituted Amides..... 49

Figure 18. Mixed Pivalic and BOP Anhydride Activated Carboxylic Acids 54

Figure 19. NMR Comparison of *N*-Methylphenylalanine Methyl Ester to its Altered Derivative..... 70

LIST OF EQUATIONS

Equation 1. Theoretical ^{18}O Incorporation Mass Spectrometry Calculation 28

Equation 2. Mass Spectrometry Calculation for ^{18}O-Labeled-2-Phenyl-*N*-(1-phenylethyl)acetamide 28

Equation 3. Mass Spectrometry Calculation for ^{18}O-Labeled-*N*-Boc-4-Cl-Phenylglycine-Ala-Phe-OMe..... 33

Chapter 1

Umpolung Amide Synthesis Mechanistic Study

1.1 Introduction

Amide bond formation is a strategically important process in the synthesis of proteins and many pharmaceutical drugs. In 2007 proteins and peptides made up 18% of the top 200 drugs sold.[1] Nature forms these bonds through enzyme-catalyzed condensations of amines and thioesters. In the absence of enzymes, synthetic methods for this condensation have been developed using coupling reagents. While these methods are widely used, there remain problems inherent to these methods that still need to be overcome.

1.1.1. Current Methods and Problems in Amide Coupling

Classical amide bond synthesis consists of the condensation of an amine and carboxylic acid.[2] This process occurs quite readily in nature due to enzymes, but it is much more difficult at the bench top due to the high amount of energy required to remove a molecule of water. This has led to the use of coupling reagents to promote amide bond formation (Scheme 1).[3] While these coupling reactions are widely used and very successful when working with simple amides, their effectiveness begins to degrade as substrates become larger and more complex. This has led to low conversions and high

[1] www.arizona.edu/njardarson/group/Top200PharmaceuticalProductsbyWorldwideSalesin2009.pdf
[2] Jones, J. *Amino Acid and Peptide Synthesis*, Oxford Science Publications: Oxford, 1992.
[3] For recent reviews, see: Han, S.Y.; Kim, Y.A. *Tetrahedron* **2004**, *60*, 2447. Montalbetti, C.; Falque, V. *Tetrahedron* **2005**, *61*, 10827. Valeur, E.; Bradley, M. *Chem. Soc. Rev.* **2009**, *38*, 606.

levels of epimerization at the α-carbon of the activated carboxylic acid in cases such as disubstituted amines, peptidic amines/carboxylic acids, and acidic amino acids.

Scheme 1. Amide Bond Formation: Examples of Coupling Reagents

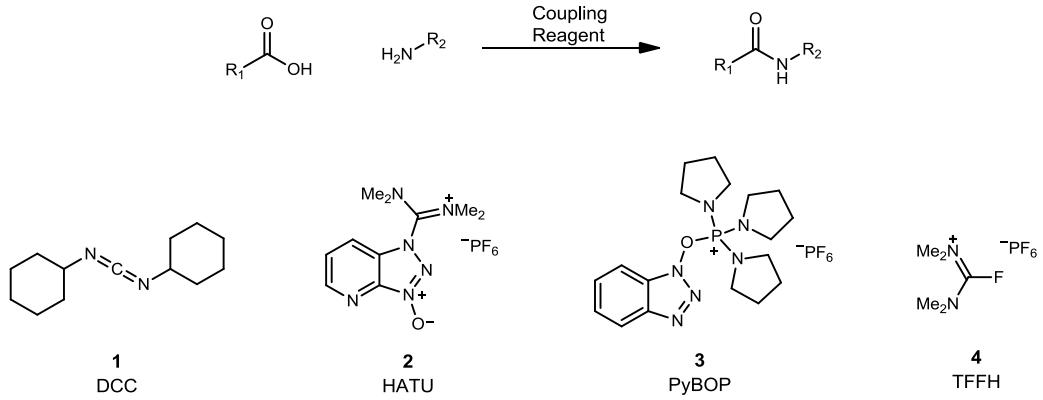

In order to overcome this limitation, additives that can act as rate enhancers (e.g. DMAP) and racemization suppressants (e.g. HOBT) have often been added (Figure 1).

Figure 1. Rate-Enhancers and Racemization Suppressants

While these additives can lower the amount of racemization seen, the problem cannot be completely eliminated.[3] An additional concern when working with coupling reagents is that they are generally expensive, toxic, and used in large excess.

Several alternatives for the formation of amides have also been developed. Solid phase peptide synthesis, a variation of traditional peptide synthesis, relies on large excesses of coupling reagents to drive the amide bond formation to completion. This method is often used due to the easy separation of reactants and the peptide bound to

solid phase (Scheme 2);[4] however, this method also relies on large excesses of reagents (often expensive) and results in a lot of waste. Additional alternatives to traditional amide

Scheme 2. Solid Phase Peptide Synthesis

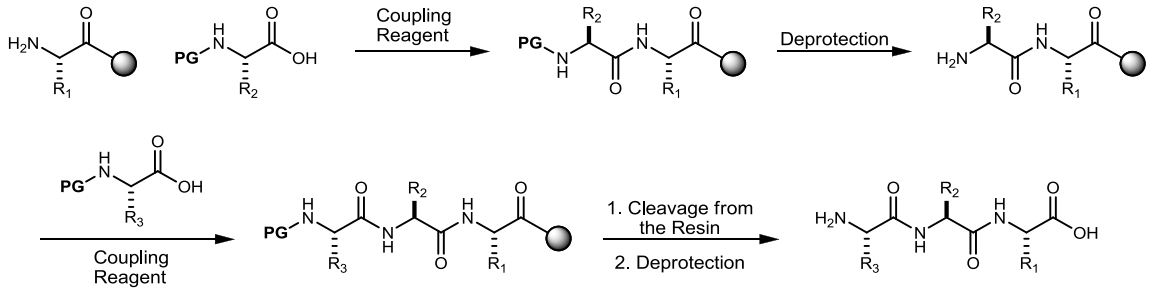

bond synthesis have been developed in order to counteract some of these problems (Scheme 3). These methods include Staudinger ligation,[5] native chemical ligation,[6] oxidative amidation of alcohols,[7] aldehydes,[8] or alkynes,[9] and ketoacid-hydroxylamine ligation,[10] among others.[11]

While there are a variety of methods for amide bond formation, the same problems predominate across most of the available methods. The high cost of coupling reagents and the need to use them in high excess results in an expensive reaction that produces a high volume of chemical waste. Epimerization of the α-carbon of the carboxylic acid remains an obstacle as well due to the majority of amide bond formation

[4] Atherton, E.; Sheppard, R.C. *Solid Phase Peptide Synthesis: A Practical Approach*; Oxford University Press: New York, 1989.
[5]Saxon, E.; Armstrong, J. I.; Bertozzi, C. R. *Org. Lett.* **2000**, *2*, 2141-2143. Saxon, E.; Bertozzi, C. R. *Science* **2000**, *287*, 2007-2010. Nilsson, B. L.; Kiessling, L. L.; Raines, R. T. *Org. Lett.* **2000**, *2*, 1939-1941. For a recent review, see: Kohn, M.; Breinbauer, R. *Angew. Chem., Int. Ed.* **2004**, *43*, 3106-3116.
[6]Dawson, P. E.; Muir, T. W.; Clarklewis, I.; Kent, S. B. H. *Science* **1994**, *266*, 776-779.
[7]Gunanathan, C.; Ben-David, Y.; Milstein, D. *Science* **2007**, *317*, 790-792. Nordstrøm, L. U.; Vogt, H.; Madsen, R. *J. Am. Chem. Soc.* **2008**, *130*, 17672-17673.
[8]Yoo, W. J.; Li, C. J. *J. Am. Chem. Soc.* **2006**, *128*, 13064-13065. Gao, J.; Wang, G. W. *J. Org. Chem.* **2008**, *73*, 2955-2958.
[9]Chan, W. K.; Ho, C. M.; Wong, M. K.; Che, C. M. *J. Am. Chem. Soc.* **2006**, *128*, 14796-14797.
[10]Bode, J. W.; Fox, R. M.; Baucom, K. D. *Angew. Chem., Int. Ed.* **2006**, *45*, 1248-1252.
[11]Li, X.; Danishefsky, S. J. *J. Am. Chem. Soc.* **2008**, *130*, 5446-5448. Li, X.; Yuan, Y.; Kan, C.; Danishefsky, S. J. *J. Am. Chem. Soc.* **2008**, *130*, 13225-13227.

methods requiring an activated ester-type intermediate. This intermediate results in the amide bond carbonyl carbon being electrophilic in nature allowing for racemization of the α-stereocenter to be a viable pathway.

Scheme 3. Novel Methods for Amide Bond Synthesis

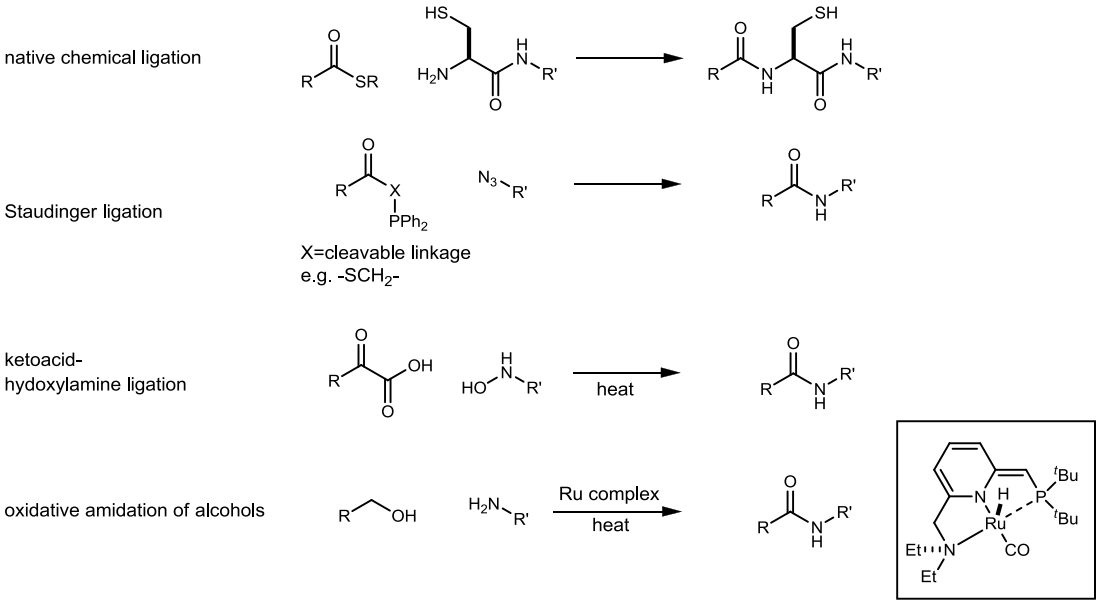

1.1.2. Syntheses of ^{18}O-Labeled Peptides and Their Use

^{18}O-Labeled peptides are commonly used in conjunction with 2D-IR studies to determine protein movements and interactions that are essential to their function. Vibrational spectroscopy studies tend to probe the picosecond time domain, which allows for the large structural dynamics to appear static (inhomogeneous) and fast structural dynamics (such as solvent and hydrogen bonding dynamics) appear dynamic (homogeneous). Effectively, this type of study allows you to take a series of snapshots of the large structural dynamic changes the protein is undergoing over a period of time. Incorporation of an ^{18}O-label at a single point in a protein allows for the resolution of that particular carbonyl peak without perturbing the overall protein structure. ^{18}O-Labeling of a specific amide is normally done in conjunction with ^{13}C labeling of the carbonyl to

further shift the signal to be studied apart. This allows for the systematic study of the large structural dynamics occurring in each region of the protein through the synthesis of a series of identical proteins with the single $^{18}O/^{13}C$ label placed in various regions of the protein.[12]

^{18}O-Labeled proteins have been used in a variety of studies evaluating protein environment and interactions. They have been used in the evaluation of the environmental interactions between a human transmembrane protein and its surroundings to further demonstrate that line width in the 2D-IR spectrum is markedly different for residues lining the interior of a membrane versus its exterior.[12] ^{18}O-Labeled proteins have also been used to evaluate the interactions between a transmembrane dimer of intertwined helices. By selectively labeling one helix with a single ^{13}C-labeled carbonyl and the other with an $^{18}O/^{13}C$-labeled carbonyl at the same residue in both cases, the structural dynamics at the point where the two helices intertwined were probed by observing the resulting signal cross-peaks.[13] $^{18}O/^{13}C$-labeling of a carbonyl at various residues of a photo-switchable protein was used to evaluate potential mechanisms of α-helix folding.[14] By $^{18}O/^{13}C$-labeling an identical series of hIAPP (polypeptide hormone used for storing insulin) proteins at different residues, the aggregation pathway through which amyloid fibril formation occurs was evaluated. This fibril formation in the islets of Langerhans of the pancreas is a common symptom observed in type 2 diabetes patients.[15] $^{18}O/^{13}C$-Labeling of an identical series of Trpzip2 (a 12-residue β-hairpin peptide) at various

[12]Mukherjee, P.; Kass, I.; Arkin, I.; Zanni, M. T. *Proc. Natl. Acad. Sci. U. S. A.* **2006**, *103*, 3528-3533.
[13]Fang, C.; Senes, A.; Cristian, L.; DeGrado, W. F.; Hochstrasser, R. M. *Proc. Natl. Acad. Sci. U. S. A.* **2006**, *103*, 16740-16745.
[14]Ihalainen, J. A.; Paoli, B.; Muff, S.; Backus, E. H. G.; Bredenbeck, J.; Woolley, G. A.; Caflisch, A.; Hamm, P. *Proc. Natl. Acad. Sci. U. S. A.* **2008**, *105*, 9588-9593.
[15]Shim, S. H.; Gupta, R.; Ling, Y. L.; Strasfeld, D. B.; Raleigh, D. P.; Zanni, M. T. *Proc. Natl. Acad. Sci. U. S. A.* **2009**, *106*, 6614-6619.

residues was used to evaluate the conformational changes occurring between its folded and unfolded states.[16] As ^{18}O-labeled peptides become increasingly more valuable as probes of structural dynamics, several methods have been developed for the synthesis of protein backbones with only a single isotopically-labeled residue.

Traditionally, ^{18}O-labeled peptides have been made through acid hydrolysis of amino acids in $H_2{}^{18}O$, followed by iterative solid phase peptide synthesis to produce the desired ^{18}O-labeled peptide (Scheme 4).[17] This method remains in widespread use and

Scheme 4. Traditional Preparation of ^{18}O-Labeled Peptides

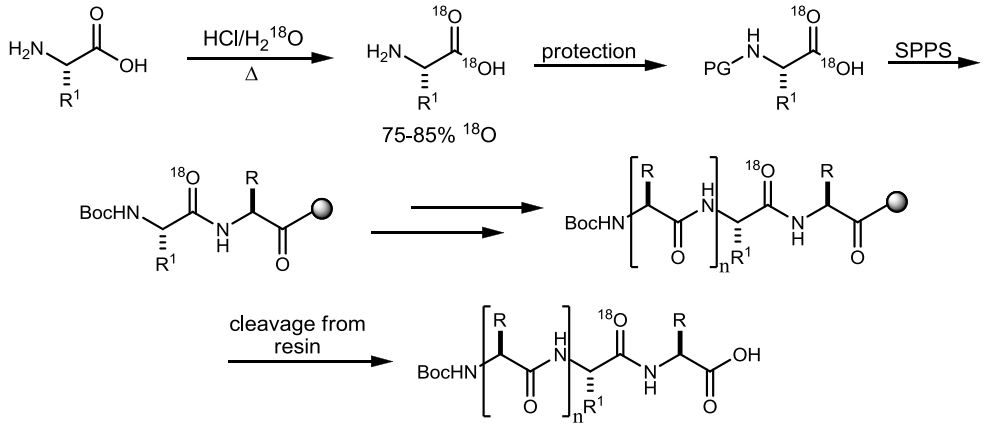

commonly results in 75-85% ^{18}O enrichment of the amino acid.[18] However, this method also requires a large excess of $H_2{}^{18}O$ and elevated temperatures over a 24-hour period just to form the ^{18}O-labeled amino acid prior to the further manipulations necessary to form the ^{18}O-labeled amide.[19] This method also requires one of the two labeled oxygen atoms to be sacrificed since it is removed during the coupling. Another potential pitfall is the

[16]Smith, A. W.; Lessing, J.; Ganim, Z.; Peng, C. S.; Tokmakoff, A.; Roy, S.; Jansen, T. L. C.; Knoester, J. *J. Phys. Chem. B* **2010**, *114*, 10913-10924.
[17]Ponnusamy, E.; Jones, C. R.; Fiat, D. *J. Labelled Compd. Radiopharm.* **1987**, *24*, 773-778.
[18]Seyfried, M. S.; Lauber, B. S.; Luedtke, N. W. *Org. Lett.* **2010**, *12*, 104-106.
[19]Marecek, J.; Song, B.; Brewer, S.; Belyea, J.; Dyer, R. B.; Raleigh, D. P. *Org. Lett.* **2007**, *9*, 4935-4937.

possibility of back exchange between the ^{18}O-labeled carboxylic acid and $H_2{}^{16}O$ water being produced as a side product (Scheme 5).[18]

Scheme 5. Potential Back-Exchange Using $H_2{}^{18}O$/Acid Hydrolysis

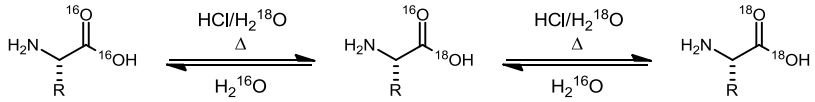

The drawbacks to traditional ^{18}O-labeling method have led to additional studies seeking to improve it. As Fmoc protected amino acids usually result in lower yields and ^{18}O enrichment levels than their Boc protected counterparts, a method was developed specifically for using Fmoc protecting groups (Scheme 6). This method began with protection of the amino acid (usually ^{13}C-labeled) with the Fmoc group prior to $H_2{}^{18}O$/acid hydrolysis. An in situ solution of 0.25 M HCl (in 90% $H_2{}^{18}O$) was prepared from acetyl chloride reacting with $H_2{}^{18}O$ to maintain the acid concentration more precisely.[19]

Scheme 6. Method for ^{18}O Enrichment of FMOC Protected Amino Acids

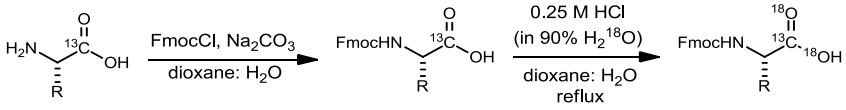

The ^{13}C-enriched Fmoc L-amino acid was then refluxed in a 3:2 dioxane/0.25 M HCl (in 90% $H_2{}^{18}O$) until the ^{18}O enrichment level remained constant by mass spectrometry analysis. The mixture was then concentrated and re-subjected to the reaction conditions to further improve the ^{18}O enrichment level. This method commonly produced Fmoc protected amino acids with ^{18}O enrichment levels ranging from 87 to 96%. This procedure also allowed for the conservation of $H_2{}^{18}O$ by preventing the need

to use it as an excess reagent, as well as recycling the reaction medium after the exchange was complete.[19]

Although the above method prevents the need for an excess of $H_2{}^{18}O$ and results in higher ^{18}O enrichment levels than the standard protocol, its highly acidic conditions prevent its use when dealing with compounds containing acid sensitive protecting groups. This led to the development of another novel protocol that produced the same high levels of ^{18}O enrichment but proved compatible with a variety of acid-sensitive protecting groups (Scheme 7). This protocol functioned through the elimination of potential back-exchange during $H_2{}^{18}O$/acid hydrolysis to enhance ^{18}O enrichment levels. This was done through the addition of a large excess of carbodiimide, which reacted with the $H_2{}^{16}O$ being produced as a byproduct of the exchange to prevent it from reacting with the now ^{18}O-labeled carboxylic acid. Overall, this method resulted in high yields and consistent ^{18}O enrichment levels in the 90s, as well as proving highly compatible with a variety of acid-sensitive protecting groups on both the amine and R side chain. However, the major drawback of this method is that it requires a large excess of both the carbodiimide (30 equivalents) and $H_2{}^{18}O$ (50 equivalents).[18]

Scheme 7. Method for ^{18}O Enrichment Preventing Back-Exchange

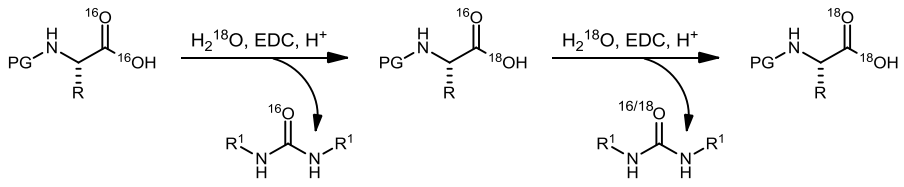

PG= Fmoc, Boc, Trityl

While $H_2{}^{18}O$/acid hydrolysis remains the most common method for ^{18}O enrichment, alternative methods for the production of ^{18}O-labeled amides have been

developed (Scheme 8). One such method allows for the formation of the ^{18}O-labeled amide directly from the ^{16}O-labeled amide using $H_2{}^{18}O$, although this method has not yet been proven to result in high levels of incorporation.[20] A second method allows for formation of the ^{18}O-labeled amide from the corresponding thioamide using 20 mol% CuCl and $^{18}O_2$ gas, although it generally requires elevated reaction temperatures and formation of the unlabeled amide first followed by conversion to the thioamide.[21] It is interesting to note that neither of these methods allows for direct formation of the amide as an ^{18}O-enriched species.

Scheme 8. Alternative Methods for the Preparation of ^{18}O-Labeled Amides

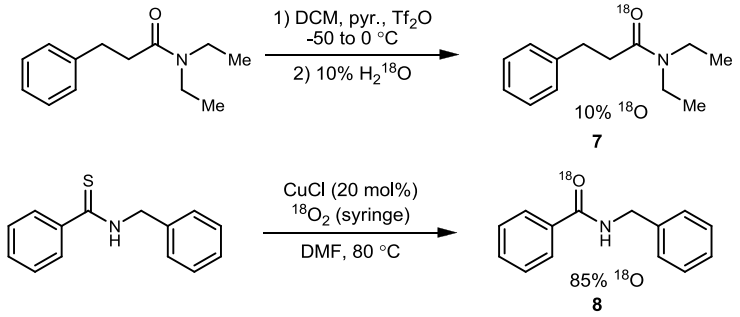

Given the elevated temperatures and large excesses of expensive reagents used throughout these methods, the development of new protocols for the formation of ^{18}O-labeled amides remains a necessity. The ideal methodology should prove cost-effective and allow for direct formation of ^{18}O-enriched amides under mild reaction conditions.

[20]Shibahara, F.; Suenami, A.; Yoshida, A.; Murai, T. *Chem. Commun.* **2007**, 2354-2356.

[21]Charette, A. B.; Chua, P. *Tetrahedron Lett.* **1998**, *39*, 245-248.

1.2 Umpolung Amide Bond Synthesis Mechanistic Study

Previously in the Johnston Group, a novel amide bond forming reaction was developed wherein an amine could be coupled to an α-bromo nitroalkane to form an amide in the presence of an electrophilic halonium source (NIS, Scheme 9).[22] This

Scheme 9. Umpolung Amide Synthesis Using NIS

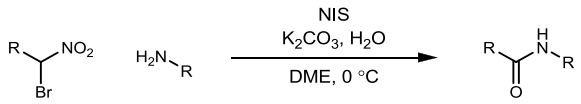

methodology was applied to the formation of a variety of amides (featuring both sterically bulky and peptidic substrates) with promising results (isolated yields of 48-81%). Currently, the only major limitation appears to be in using aromatic amines, as the use of aniline resulted in no amide product formation. Overall, this new methodology represents a novel amide bond formation mechanism that occurs through a reversal of the normal polarities seen in amide bond coupling partners as the amine acts as the electrophile and the α-bromo nitroalkane (a carbonyl surrogate) acts as the nucleophile (Figure 2). This pathway effectively mechanistically prohibits racemization of the α-carbon of the carboxylic acid, which is a common problem in conventional amide bond synthesis, due to the acyl donor carbon now acting as a nucleophile.

While the amide synthesis has been successfully optimized and applied, the mechanism of the reaction remained to be carefully studied, particularly the sequence of events between the tetrahedral intermediate and the amide product. This led to a mechanistic study of the reaction to determine the oxygen donor responsible for the

[22]Shen, B.; Makley, D. M.; Johnston, J. N. *Nature* **2010**, *465*, 1027-1032.

formation of the amide carbonyl and to evaluate its potential for the formation of isotopically labeled peptides.

Figure 2. Umpolung Amide Bond Synthesis

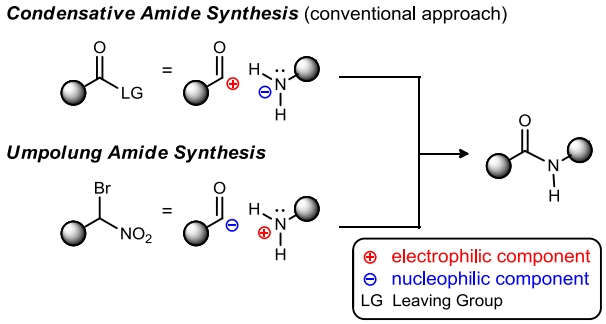

1.2.1 Initial Determination of Oxygen Donor

As shown in Scheme 10, the α-halo nitroalkane is deprotonated by K_2CO_3 and the electron withdrawing effect of the nitro group coupled with the shown resonance structure allows it to act as a carbon nucleophile (**11**). The halonium ion source (NIS) activates the amine through formation of a *N*-haloamine to allow it to act as the electrophile (**12**) resulting in a tetrahedral intermediate (**13**), which exists in the same oxidation state as the desired amide.

Scheme 10. Proposed Mechanism Featuring H_2O as the Amide Carbonyl Oxygen Donor

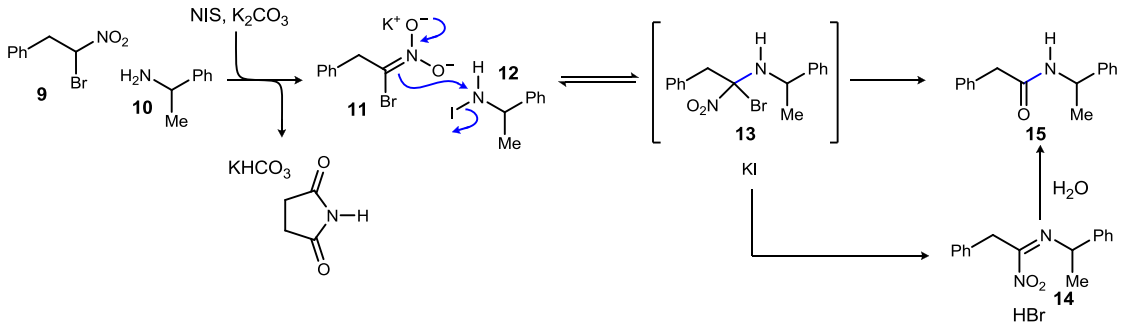

Although the exact source of the amide oxygen is not known, the amide (**15**) could potentially be formed through a hydrolysis-based process. This theory was tested by performing the standard amide synthesis in >99% ^{18}O-labeled-H_2O (Scheme 11).

Scheme 11. ^{18}O-Labeled H_2O Amide Bond Synthesis

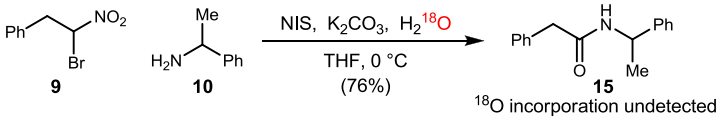

Mass spectrometric analysis of the final amide product revealed less than 1% ^{18}O incorporation indicating that amide bond formation was not occurring through conventional hydrolysis.

Next, we hypothesized that the amide could potentially be formed through an unconventional hydrolysis involving the nitro group. There are several examples of nitro group based hydrolysis available in the literature. In the first example in Scheme 12, **16** is heated allowing the nitro group to rearrange to nitrite **17**. This allows an oxygen from the nitro group to participate in the formation of the carbonyl in **18,** thus acting as proof that a nitro group can participate in the formation of a carbonyl.[23] In the second example, heating of **19** homolytically cleaves the carbon-nitrogen bond, providing a pathway to nitrite and racemized α-nitro/nitrite ester (**21/22**).[24] These examples offer proof that the N to O rearrangement of the nitro group can actually occur in specific circumstances. It is important to note that in both cases listed so far, the nitro group is tertiary and there is a radical stabilizing group present (-CO_2Et). The last example offers further support of the need for of a tertiary nitro group for the rearrangement to nitrite to occur. When

[23]Wilstatter, R; Hottenroth, V. *V. Chem. Ber.***1904**, *37*, 1775.
[24]Hochstein, W; Schoelkopf, U.*U. Justus Liebigs Ann. Chem.* **1978**, 1823.

Scheme 12. Nitro Group Based Hydrolysis

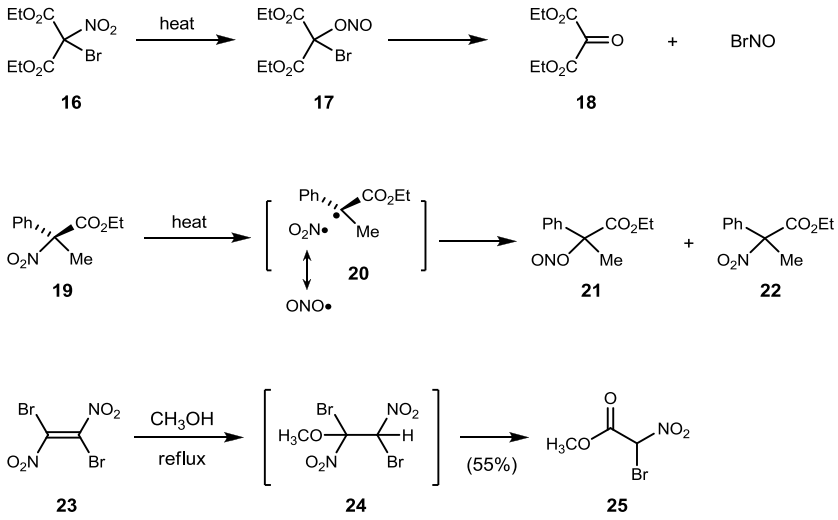

nitro-olefin **23** is refluxed in methanol, it produces a tertiary intermediate (**24**) containing both a nitro group and a halide, which is similar to the putative tertiary intermediate in the umpolung amide synthesis. In this case, the tertiary nitro group rearranges to the nitrite and is hydrolyzed to produce the desired carbonyl.[25] It is important to note that the secondary nitro group remains unaffected by this reaction. In each of these examples, the amide oxygen originates from the nitro group indicating it is a likely source for the amide carbonyl (Scheme 13).

Scheme 13. Proposed Mechanism Featuring the Nitro Group as the Amide Carbonyl Oxygen Donor

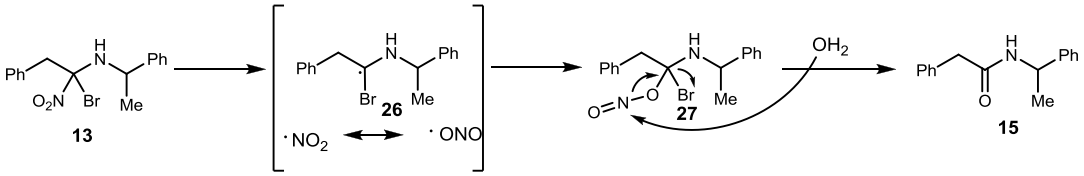

This theory was tested by the formation of doubly ^{18}O-labeled α-bromo nitroalkane (Scheme 14). Doubly ^{18}O-labeled sodium nitrite (**30**) was prepared by

[25]Nguyen, N.V.; Baum, K. *Tetrahedron Lett.* **1992**, *33*, 2949.

Scheme 14. Formation of ^{18}O-Labeled α-Bromo Nitroalkane

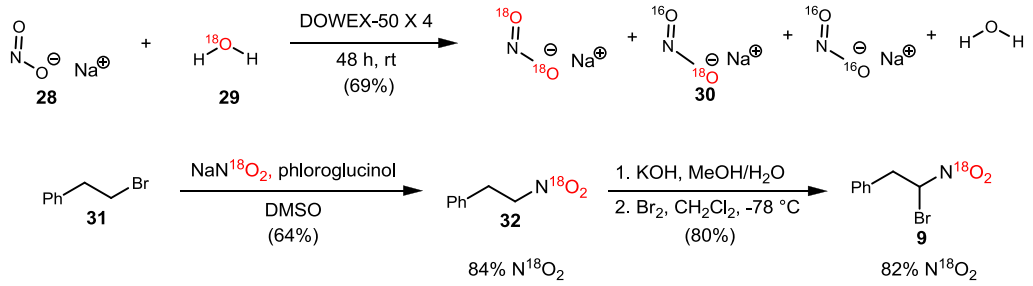

treating sodium nitrite (**28**) with ^{18}O-labeled water (**29**) in acidic conditions generated by the acidic resin Dowex-50X4. The acidic conditions allowed for the generation of nitrous acid, at which point the oxygen atoms of nitrous acid could exchange with the oxygen atoms of the labeled water. The reaction was then treated with sodium hydroxide to reform doubly labeled sodium nitrite (**30**) in 69% yield. It was crucial when performing this reaction that the Dowex-50X4 be freshly regenerated and completely dry. The reaction flask must also be sealed as the nitrous acid can escape as a gas. This exchange occurs through an equilibrium between nitrous acid forms where both oxygen atoms are labeled, one oxygen atom is labeled, and neither oxygen is labeled. Attempts to quantify the ratio of labeled nitrite by mass spectrometry ultimately failed, so the ^{18}O-labeled $NaNO_2$ was used directly in the next reaction where the amount of ^{18}O label could be quantified by mass spectrometry.

^{18}O-Labeled nitroalkane **32** was then formed by reacting the labeled sodium nitrite (**30**) with (2-bromoethyl)benzene (**31**). Since either the nitrogen or oxygen atom in sodium nitrite could act as a nucleophile, phloroglucinol was added to trap any alkyl nitrite that may have formed by converting it to an alcohol.[26] This allowed for straightforward purification by flash column chromatography to obtain the desired ^{18}O-

[26]Procedure adapted from Erickson, A. S.; Kornblum, N. *J. Org. Chem.* **1977**, *42*, 3764.

labeled nitroalkane (**32**) in 64% yield. Analysis of **32** by mass spectrometry showed 84% $^{18}O_2$-incorporation. ^{18}O-Labeled α-bromo nitroalkane (**9**) was generated by deprotonation of the ^{18}O-labeled nitroalkane **(32**) with potassium hydroxide, followed by bromination of the nitronate salt to generate a mixture of monobrominated and dibrominated product. Purification via flash column chromatography gave the ^{18}O-labeled α-bromo nitroalkane (**9)** in 80% yield. Analysis of **9** by mass spectrometry showed 82% incorporation of doubly labeled ^{18}O in the nitro group.

The 82% ^{18}O-labeled-α-bromo nitroalkane was used in the standard amide synthesis reaction, which resulted in only 17% ^{18}O-incorporation (Scheme 15). This clearly indicates that although the nitro group can serve as a carbonyl oxygen donor, there is another source within the reaction that can contribute the oxygen. To evaluate the role of other potential oxygen donors in the reaction, the K_2CO_3 was removed from the reaction and replaced with an excess of amine. This allowed for the elimination of one potential oxygen source and resulted in an increase in ^{18}O-retention at 49%. Removal of the K_2CO_3 in conjunction with the use of both ^{18}O-labeled α-bromo nitroalkane and $H_2{}^{18}O$ also resulted in 49% ^{18}O-incorporation (Scheme 15). This clearly indicates that K_2CO_3 can act as a potential oxygen donor, but there must be another source of oxygen within the reaction that is the primary contributor. Considering the possibility that adventitious oxygen might be involved in the amide formation, the reaction was degassed along with removal of K_2CO_3, which resulted in an increase in ^{18}O-incorporation to 66% (Scheme 15).

Scheme 15. Evaluation of Potential Oxygen Sources

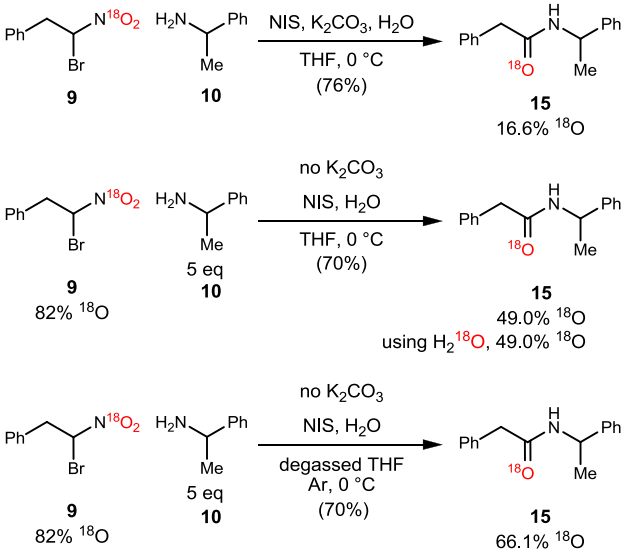

The increase to 66% ^{18}O-incorporation using degassed THF led to the hypothesis that since the reaction of oxygen with carbon radicals is often near the rate of diffusion,[27] oxygen in the air might be capable of intercepting the putative radical intermediate after heterolytic cleavage of the carbon-nitro bond. This theory was tested by running the standard amide synthesis reaction under $^{18}O_2$ gas with no other source of ^{18}O in the reaction. This resulted in 72% ^{18}O-incorporation, establishing that oxygen in the air could serve as the primary oxygen donor for the amide carbonyl (Scheme 16).

Scheme 16. $^{18}O_2$ Gas Amide Bond Synthesis

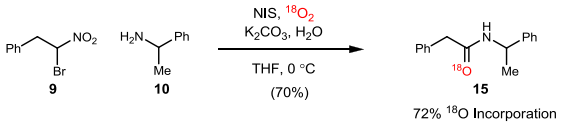

This mechanistic data led to the revised hypothesis that the amide product of this reaction was actually forming through two distinct pathways: an aerobic pathway where

[27]Maillard, B.; Ingold, K. U.; Scaiano, J. C. *J. Am. Chem. Soc.* **1983**, *105*, 5095-5099. Pratt, D. A.; Mills, J. H.; Porter, N. A. *J. Am. Chem. Soc.* **2003**, *125*, 5801-5810.; α-Aminomethyl radical reactions with oxygen: Lalevee, J.; Graff, B.; Allonas, X.; Fouassier, J. P. *J. Phys. Chem. A* **2007**, *111*, 6991-6998.

oxygen serves as the oxygen donor and an anaerobic pathway where the nitro group serves as the oxygen donor (Scheme 17). The results also clearly indicate that the aerobic pathway is much faster than the anaerobic pathway due to the fact that when both ^{18}O-labeled α-bromo nitroalkane and unlabeled oxygen from the air are present in the reaction, the levels of ^{18}O-incorporation are very low.

Scheme 17. Proposed Aerobic and Anaerobic Pathways of Amide Bond Synthesis

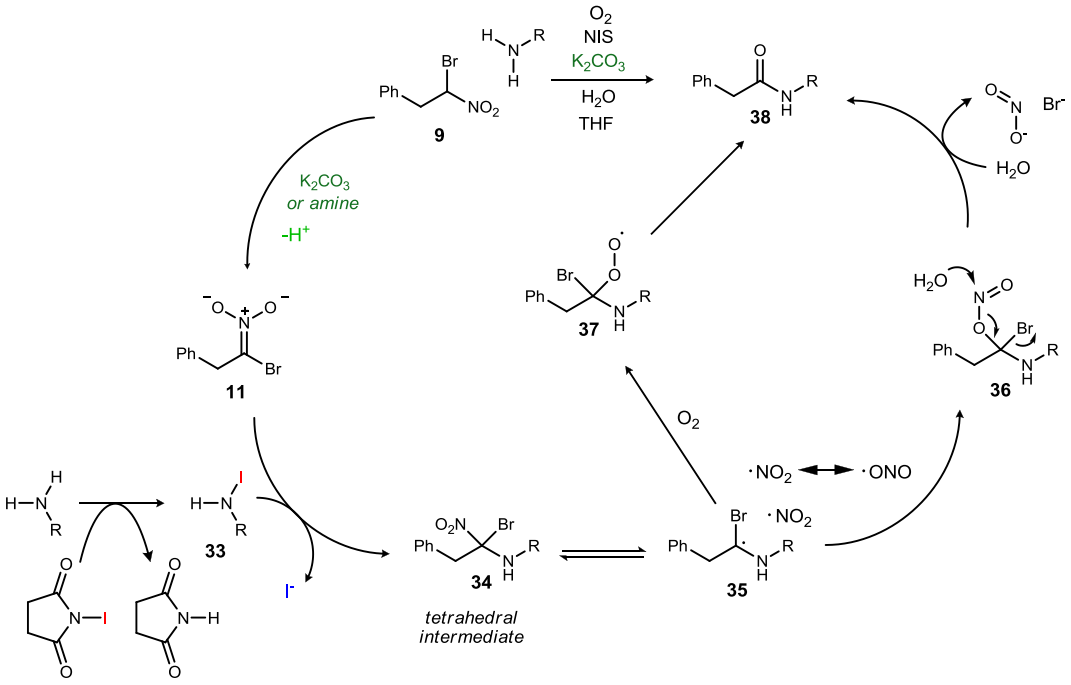

1.2.2 Optimization of ^{18}O-Labeling Method

Once the oxygen source was successfully identified, methods to improve the ^{18}O incorporation into the amide through a more controlled addition of the $^{18}O_2$ gas were investigated. A variety of methods were evaluated, and a comparison is shown in Table 1. In Method 1 all reagents except NIS were added to a 15-mL round bottomed flask to prevent the reaction from starting prior to degassing. The flask was more thoroughly degassed than the previous $^{18}O_2$ gas experiment (undergoing three 45 minute freeze-

pump-thaw cycles through a vacuum line adapter vs. three 10-minute cycles) in order to remove more unlabeled oxygen from the reaction than earlier reaction attempts. Once the degassing was complete, the vacuum line adapter was removed, and NIS was added to the reaction before quickly resealing the flask with a septum. The $^{18}O_2$ gas line (directly attached to the tank with no regulator) and a balloon (flushed with N_2 three times) were inserted through the septum, and $^{18}O_2$ gas was directly added to the flask until the balloon was fully inflated. The reaction was cooled to 0 °C and allowed to proceed as normal. Method 1 resulted in a 66% yield and only a 63% ^{18}O-incorporation by mass spectrometry (Scheme 18).

Since Method 1 showed no improvement in ^{18}O incorporation despite a much more thorough degassing process, it appeared that exposing the reaction to the air for even the shortest amount of time resulted in a higher level of unlabeled oxygen incorporation in the final amide product. This seems even more likely when considering that oxygen reacts with carbon radicals near the rate of diffusion,[27] and this reaction pathway is driven by radical intermediates. This led to the development of Method 2 to prevent the reaction from coming into any unnecessary contact with the air.

In Method 2 all reagents were added to a 15 mL round bottomed flask (RB1) except the α-bromo nitroalkane and amine which were added to a second 10 mL round bottomed flask (RB2). Both flasks were sealed with a septum and parafilmed shut before being thoroughly degassed by undergoing three one-hour freeze-pump-thaw cycles through a vacuum line needle adapter. Once the degassing was complete, the vacuum line needle adapters were removed. The $^{18}O_2$ gas line (directly attached to the tank with no regulator) and a balloon (flushed with N_2 three times) were inserted through the septum

of RB1, and $^{18}O_2$ gas was directly added to the flask until the balloon was fully inflated. A dry syringe was used to transfer the contents of RB2 to RB1. The reaction was cooled to 0 °C and allowed to proceed as normal. Method 2 resulted in a 68% yield and an 83% ^{18}O-incorporation by mass spectrometry (Scheme 18). This supports the hypothesis that any contact with air during the reaction is detrimental to the overall ^{18}O-incorporation levels of the reaction.

Scheme 18. $^{18}O_2$ Gas Addition Methods Comparison

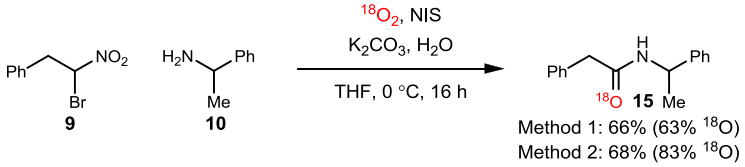

While Method 2 worked well, ensuring high levels of ^{18}O incorporation, it also proved to be quite expensive due to the need to fully inflate the balloon with $^{18}O_2$ gas. This led to the development of a more cost-effective method for achieving high levels of ^{18}O-incorporation. The first step toward developing a more cost-effective method for ^{18}O-incorporation was to make delivery of the $^{18}O_2$ gas more efficient. This was done by attaching a regulator to the $^{18}O_2$ tank for better monitoring of the gas addition, along with a short copper wire attached to a needle to simplify the gas delivery process. The final $^{18}O_2$ gas tank setup is shown in Figure 3. The next stage of improvement involved limiting the surface area of the reaction vessel. Toward this goal, the reaction flask was switched from a 15 mL round bottom flask to a 1 mL reaction vial. This allowed for a smaller amount of $^{18}O_2$ gas to be necessary to fill the available head space of the reaction vessel. Once the basic system was established, attempts to further refine the protocol began.

Figure 3. $^{18}O_2$ Gas Delivery System

In Method 3 all reagents were added to a 1 mL reaction vial (Vial 1) except the NIS which was added as a solution in THF to a second 1 mL reaction vial (Vial 2). K_2CO_3 was removed from the reaction conditions and replaced with excess amine in order to prevent potential stirring problems. Both vials were sealed with a tight fitting septum and parafilmed shut before being thoroughly degassed (undergoing three one hour freeze-pump-thaw cycles through a vacuum line needle adapter). Once the degassing was complete, the reaction vial was refrozen in liquid N_2, and a dry syringe was used to transfer the contents of Vial 2 to Vial 1. The $^{18}O_2$ gas line was inserted through the septum of Vial 1, and the entire system was placed back under vacuum. The vacuum was turned off, and a single charge of $^{18}O_2$ gas was directly added to the vial and the vacuum line was removed. The reaction was cooled to 0 °C and allowed to proceed as normal.

Unfortunately, Method 3 resulted in a 58% yield and only 14% ^{18}O-incorporation into the amide.

Assuming the low incorporation was a result of the vacuum line being removed after $^{18}O_2$ addition (resulting in the loss of any $^{18}O_2$ gas that was in the line), the experiment was repeated with the removal of the vacuum line prior to $^{18}O_2$ gas addition (Method 4). While this modification did result in an increase to 54% ^{18}O-incorporation from Method 3, the incorporation level was still lower than what was seen using the more expensive route. The next modification involved changing three components: 1) the reaction vial was changed to a 1-mL glass vial with a screw cap containing a silicone septum, 2) the vacuum line was left in during the course of the reaction to prevent potential loss of the vacuum prior to $^{18}O_2$ gas addition, as well as to prevent leaving an open hole in the septum, and 3) an extra charge of $^{18}O_2$ gas was added. Unfortunately, Method 5 resulted in a similar 54% ^{18}O-incorporation into the amide.

Since the addition of extra $^{18}O_2$ gas appeared not to improve the overall incorporation of the reaction, it was hypothesized that the absence of K_2CO_3 sufficiently slowed down the reaction to the point that the product was not forming fast enough to interact with the bulk of the $^{18}O_2$ gas before it was lost from the system. This hypothesis was tested by running the same modification as above using K_2CO_3 instead of excess amine (Method 6), which resulted in an increase to 60% ^{18}O-incorporation but only a 37% yield due to poor stirring. Method 7 was the final modification, and it was modified in two key ways: 1) rate of stirring was increased dramatically to help improve the overall yield and 2) $^{18}O_2$ gas was added to the system until the regulator needle remained steady indicating the system was at equilibrium (Figure 4).

Figure 4. Optimized $^{18}O_2$ Gas Amide Synthesis Set Up

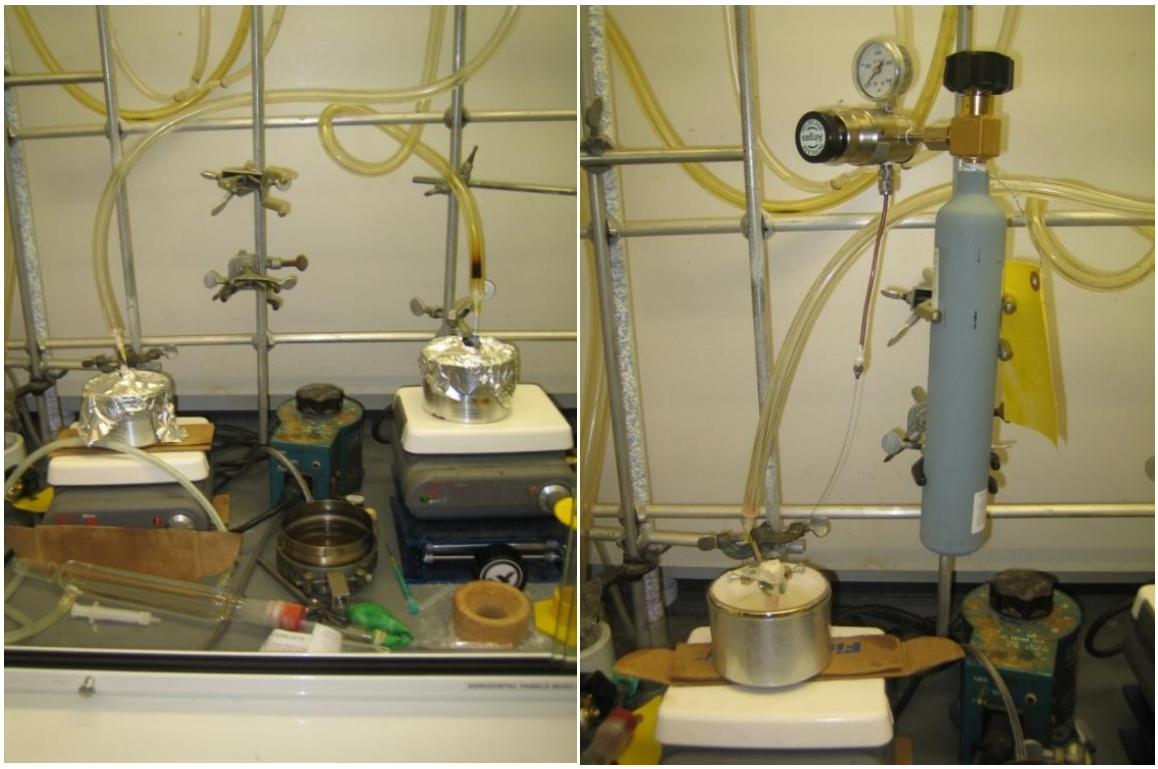

Gratifyingly, this method resulted in a 79% yield and a 79% ^{18}O incorporation. This method achieves a comparable result to the more expensive method which consumes more $^{18}O_2$ gas and still remains more cost-effective despite the additional $^{18}O_2$ gas required to achieve the desired results. With the optimal reaction conditions established, they were applied to a series of substrates to show the general versatility of the method in forming various ^{18}O-labeled amides, including peptides (Table 2).

Table 1. Method Comparison for $^{18}O_2$ Gas Amide Synthesis

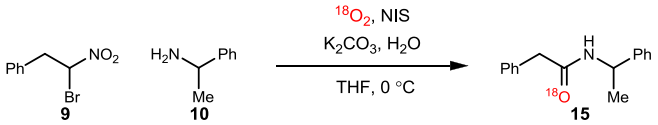

method	% yield	% ^{18}O
1	66	63
2	68	83
3	58	14
4	68	54
5	62	54
6	37	60
7	79	79

Table 2. Substrate Scope for $^{18}O_2$ Gas Amide Bond Formation

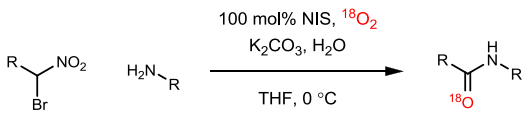

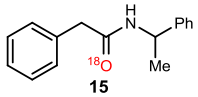

15
79% yield
79% ^{18}O incorporation[a]

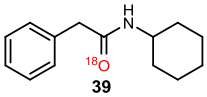

39
78% yield
79% ^{18}O incorporation[b]

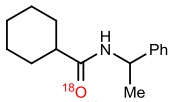

40
81% yield
65% ^{18}O incorporation[c]

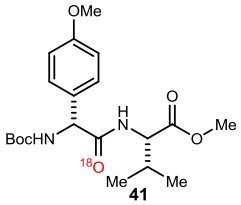

41
65% yield
76% ^{18}O incorporation[d]

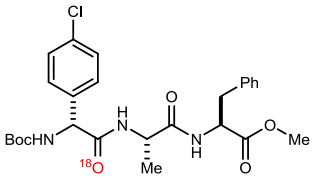

42
58% yield
93% ^{18}O incorporation[d]

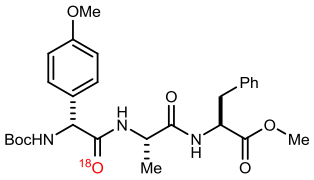

43
49% yield
88% ^{18}O incorporation[d]

[a] ^{13}C NMR indicated approximately 71% ^{18}O incorporation. [b] ^{13}C NMR indicated approximately 72% ^{18}O incorporation. [c] ^{13}C NMR indicated approximately 75% ^{18}O incorporation. [d] ^{18}O incorporation could not be determined by ^{13}C NMR due to overlapping peaks.

Since our previous peptidic substrates resulted in such high ^{18}O-incorporations, an additional substrate scope was undertaken to show the full applicability of this method for ^{18}O-labeleing peptides (Table 3). Since these substrates were prepared on a larger scale than the previous examples, all of these reactions were run slightly more concentrated (0.3M instead of 0.2M) in order to maintain use of the same setup. The reaction solvent was also switched to DME, since it had been noticed that THF was prone to oxidation under UmAS reaction conditions resulting in a slightly lowered yield.

Table 3. Peptidic Substrate Scope of ^{18}O-Labeled Peptides

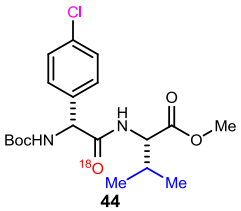

44
60% yield
86% ^{18}O incorporation

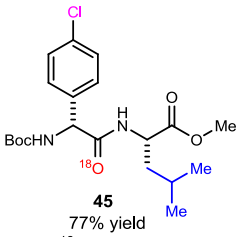

45
77% yield
92% ^{18}O incorporation

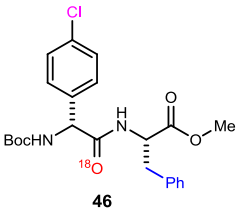

46
45% yield
90% ^{18}O incorporation

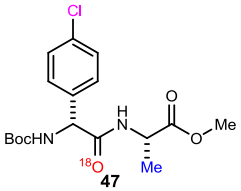

47
71% yield
91% ^{18}O incorporation

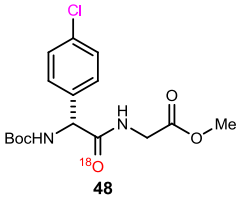

48
62% yield
91% ^{18}O incorporation

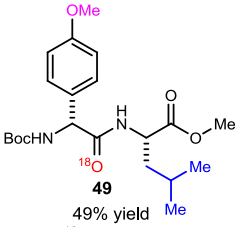

49
49% yield
85% ^{18}O incorporation

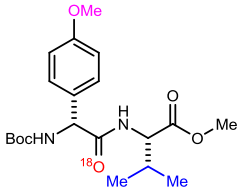

41
53% yield
84% ^{18}O incorporation

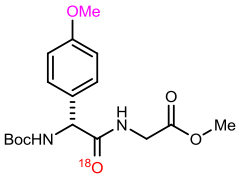

50
41% yield
90% ^{18}O incorporation

1.2.3 NMR, IR, and Mass Spectrometric Analysis of Compounds

There are three primary methods than can be used to evaluate the presence of an ^{18}O-labeled-carbonyl in a compound. These methods are IR, ^{13}C NMR, and mass spectrometry. Due to Hooke's law,[28] a higher weight isotope attached to a carbonyl in the IR will result in a lower frequency shift than what is seen for the lower weight isotope carbonyl peak.[19] Unfortunately, this method can only confirm the presence of an ^{18}O label without providing means of quantitation. The heavy isotope effect states that in ^{13}C NMR, the presence of a higher weight isotope attached to the carbon will result in a slight upfield shift of that carbon peak in the spectrum.[17] If the shift is significant, the approximate amount of ^{18}O-incorporation can be determined based on integration. Unfortunately, the shifts we observed, coupled with broadening of the amide carbonyl carbons, allowed approximation only in the case of simple amides.

Mass spectrometry is by far the most quantitative method for determining the amount of ^{18}O-incorporation in a compound. This is done by using the relative intensities of both the ^{18}O-labeled and ^{18}O-unlabeled fragments to calculate the exact amount of ^{18}O-incorporation present in the sample. The incorporation value is also corrected for the amount of the M+2 mass peak that would be present in a non-labeled sample due to naturally occurring isotope configurations to ensure that the incorporation value indicates only what the reaction itself is responsible for incorporating. For a more direct comparison, the ^{18}O-labeled sample can be directly compared to the authentic ^{16}O-sample. The effectiveness of these three methods was evaluated using both a simple amide and a tripeptide.

---

[28] *Advances in Physical Organic Chemistry, Volume 23*; Gold, V.; Bethell, D., Eds.; Academic Press, Inc.: London, 1987.

Example 1: ^{18}O-Labeled-2-Phenyl-*N*-(1-phenylethyl)acetamide

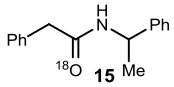

Shown in Figure 5, the IR data for this compound showed a substantial 20 cm^{-1} shift to a lower frequency when compared to data for the standard substrate with no ^{18}O labeling. This is indicative that there is an ^{18}O label present, but this gives us no quantitative data to help determine the amount of incorporation.

Figure 5. IR Data for ^{18}O-Labeled-2-Phenyl-*N*-(1-phenylethyl)acetamide

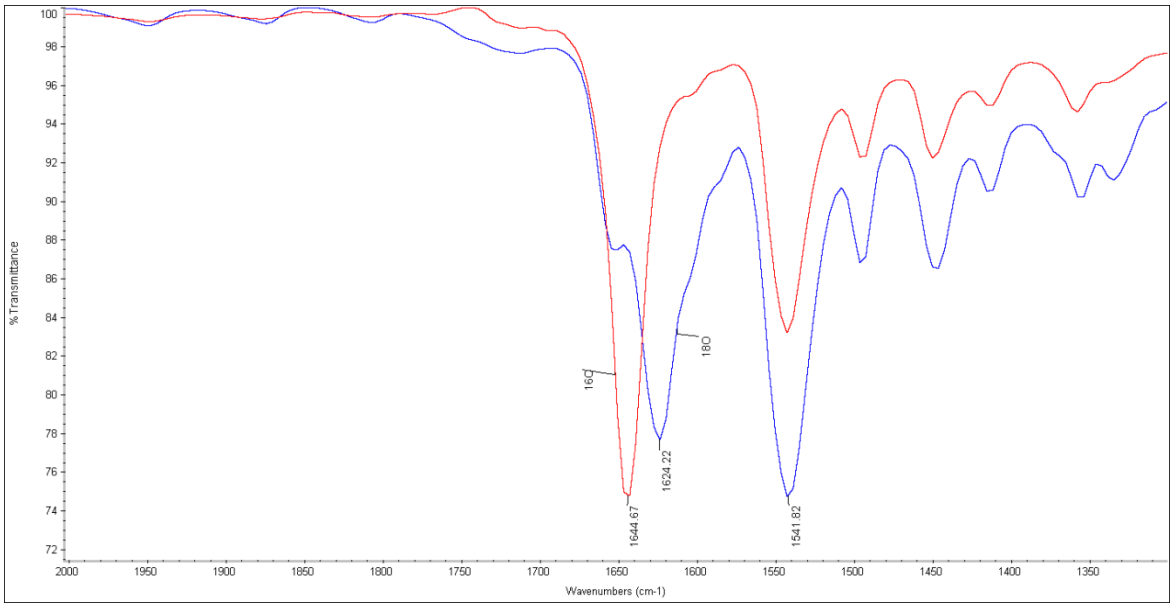

In the case of simple amides such as this one, the ^{13}C NMR data proved useful in approximating the amount of ^{18}O-incorporation present in the compound. As shown in Figure 6, a clear upfield shift of the ^{18}O-labeled carbonyl can be seen. Integration of the two carbonyl peaks indicated an approximate ^{18}O-incorporation of 71%. Mass spectrometry results indicated an exact ^{18}O-incorporation of 79%, indicating that the use of ^{13}C NMR to evaluate the ^{18}O-incorporation of this compound was accurate within 10% of the actual incorporation. This same trend was seen in other examples of simple amides

as well. Thus, ^{13}C NMR is a viable method for experimentaly determining ^{18}O-incorporation of simple amides.

Figure 6. ^{13}C NMR Data (expansion and integration) for ^{18}O-Labeled-2-Phenyl-*N*-(1-phenylethyl)acetamide

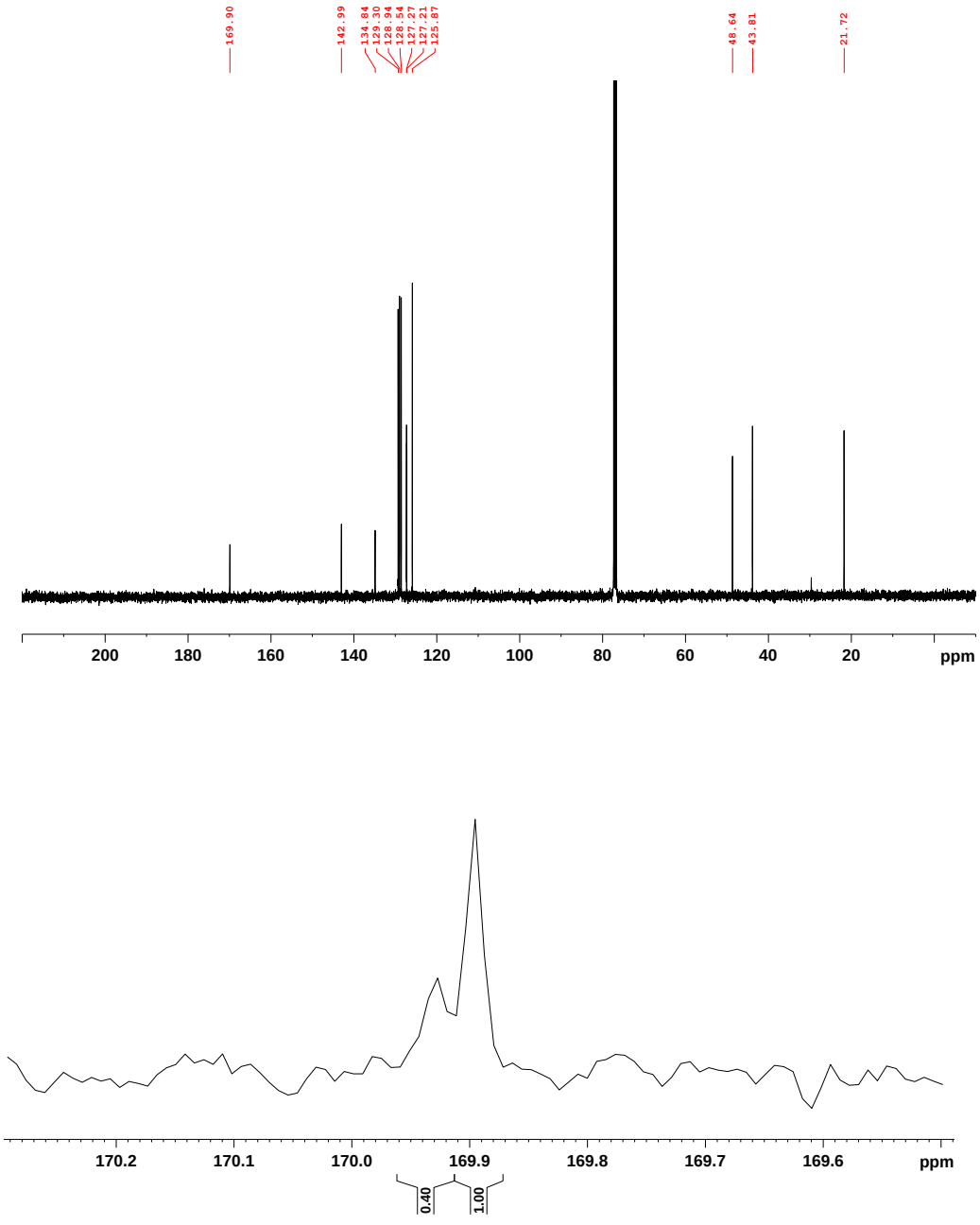

The most quantitative analytical method used was mass spectrometry. In the case of this simple amide, an overall ^{18}O-incorporation of 79% was determined by comparing the intensities of the $[M]^+$ and $[M+2]^+$ mass peaks. Contributors to the $[M+2]^+$ mass peak include M(^{18}O), as well as M($^{13}C_2$) and M($^{15}N_2$). As a result, the natural occurence and intensity expected for the $[M+2]^+$ mass peak in a non-^{18}O-labeled sample must be removed by calculation. An example calculation is shown in Equation 1.

Equation 1. Theoretical ^{18}O Incorporation Mass Spectrometry Calculation

Step 1:(^{16}O ion intensity) x (predicted ^{18}O ion natural abundance in the unlabeled compound)$\diagup$100 = ^{18}O ion intensity expected in the unlabeled compound

Step 2: (^{18}O ion intensity) – (^{18}O ion intensity expected in the unlabeled compound) = corrected ^{18}O ion intensity

Step 3: (Corrected ^{18}O ion intensity) / (Corrected ^{18}O ion intensity + ^{16}O ion intensity) x 100 = % ^{18}O

Equation 2. Mass Spectrometry Calculation for ^{18}O-Labeled-2-Phenyl-*N*-(1-phenylethyl)acetamide

Step 1: (489962 x 1.62) / 100 = 7937

Step 2: 1807239 − 7937 = 1799302

Step 3: 1799302 / (1799302 + 489962) x 100 = 79% ^{18}O

Example 2: ^{18}O-Labeled-*N*-Boc-4-Cl-Phenylglycine-Ala-Phe-OMe

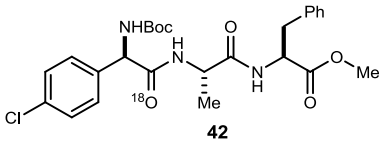

42

Shown in Figure 7, the IR data for this compound showed a substantial 20 cm^{-1} shift to a lower frequency when compared to data for the standard substrate with no ^{18}O

labeling. This is indicative that there is an ^{18}O label present, but this gives us no quantitative data to help determine the amount of incorporation. It is also interesting to note that a separate carbonyl peak is present in the ^{18}O-labeled IR that is not present in the broad carbonyl peak of the standard. This is not a wholly unexpected observation as the presence of an ^{18}O-label at one carbonyl could conceivably cause the entire molecule (and its additional carbonyls) to undergo vibrational changes.

Figure 7. IR Data for ^{18}O-Labeled-*N*-Boc-4-Cl-Phenylglycine-Ala-Phe-OMe

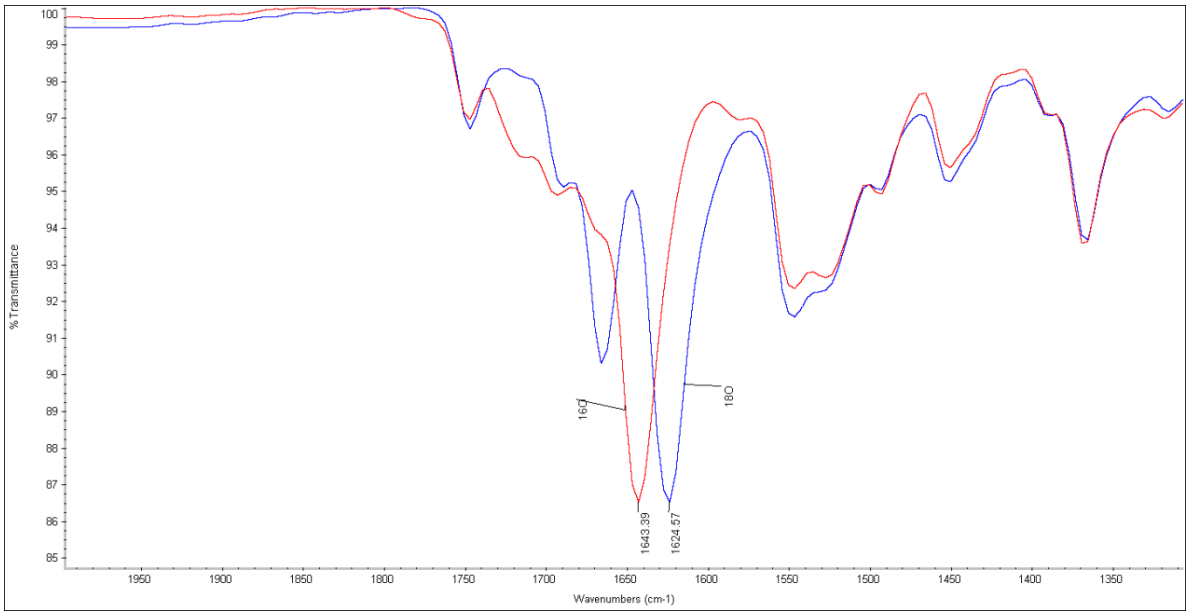

In the case of dipeptides and tripeptides, the ^{13}C NMR data proved a bit complicated to analyze. The identity of the^{18}O-labeled carbonyl was confirmed via process of elimination using HMBC analysis. Shown in Figure 8, C8 correlates to H6 and H9 indicating it is the ester carbonyl. C5 correlates to H3 and H4 indicating it is likely the unlabeled amide carbonyl, as the labeled amide carbonyl should not correlate to H4. C2 is likely to be the labeled-carbonyl amide peak as it weakly correlates to H3 but not H4. The carbamate carbonyl of the Boc group is not shown because it occurs much

Figure 8. HMBC Data Expansion of the Carbonyl Region of ^{18}O-Labeled-*N*-Boc-4-Cl-Phenylglycine-Ala-Phe-OMe

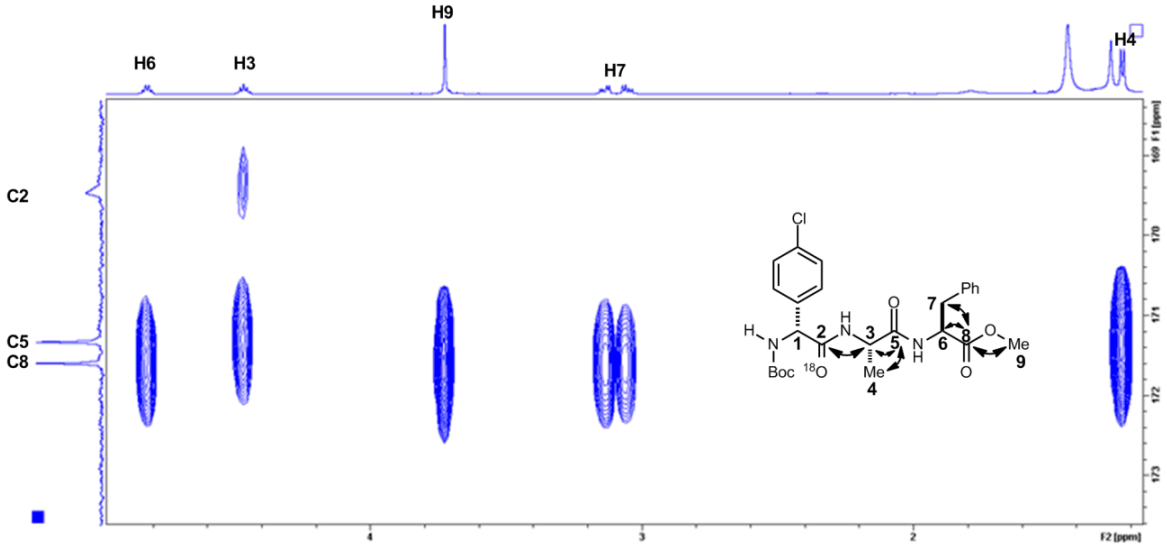

more upfield than the other carbonyl peaks (at 154 ppm), which is to be expected. As shown in Figure 9, the carbamate carbonyl of the Boc group shows only one weak correlation to H1 when the spectrum is highly magnified. This is likely due to the broad nature of both the carbon and proton peak.

Figure 9. HMBC Data Expansion Featuring the Carbamate Carbonyl of the Boc Group

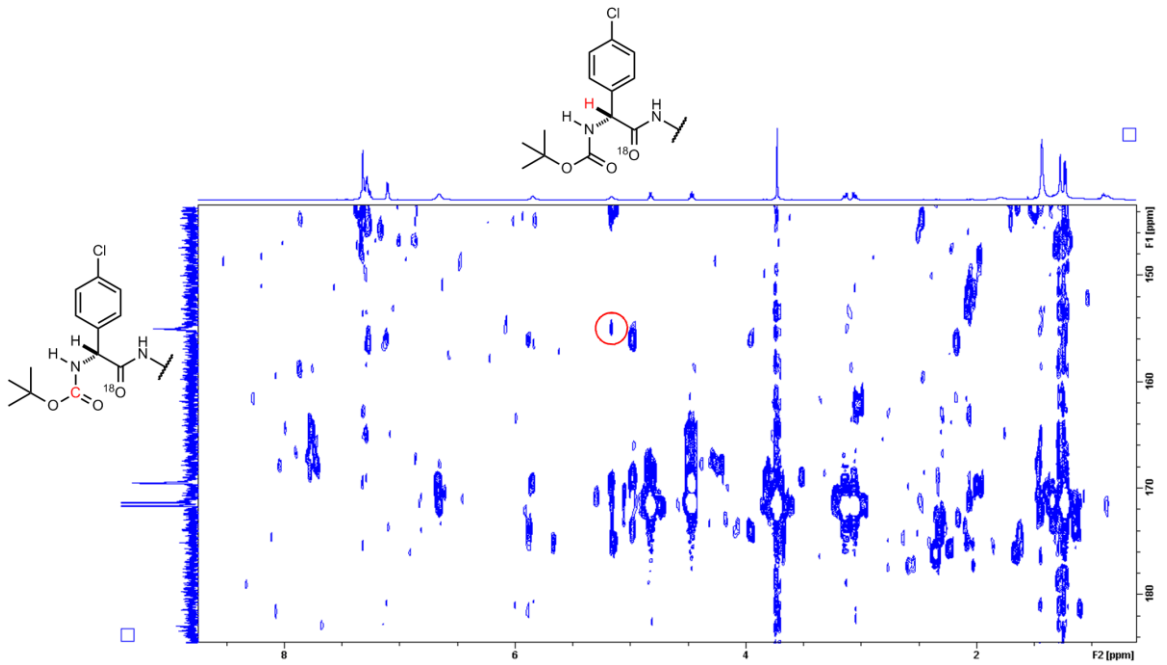

As shown in Figure 10, the upfield shift is not clear and results in a broad carbonyl peak that is impossible to integrate successfully. This led to additional ^{13}C

Figure 10. ^{13}C NMR data (expansion) for ^{18}O-Labeled-*N*-Boc-4-Cl-Phenylglycine-Ala-Phe-OMe

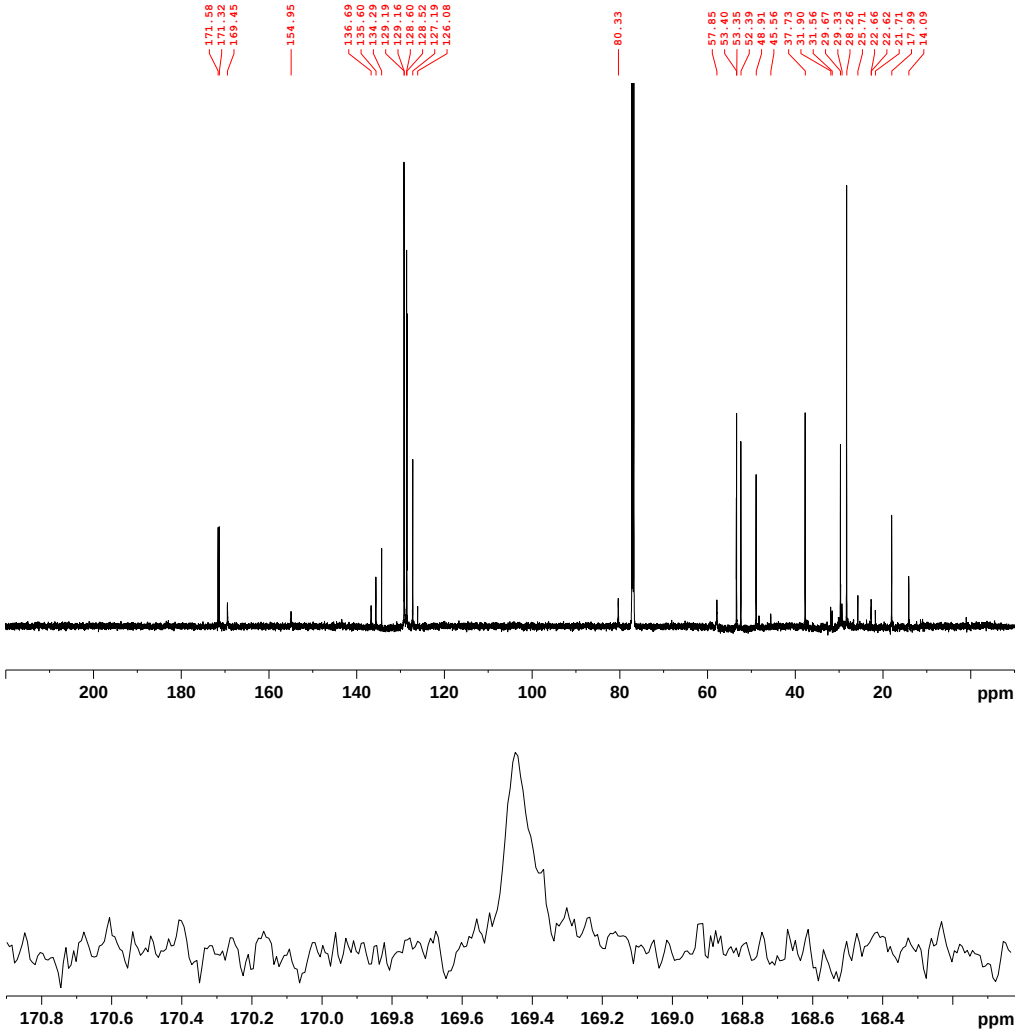

NMR studies with the substrate by comparing the carbonyl shift at various amounts of ^{18}O incorporation. Figure 11 shows the spectra for the substrate at 0% and 93% ^{18}O-incorporation, while Figure 12 shows the spectra for the substrate at 27% and 93% ^{18}O-incorporation. In both cases, a slight upfield shift of the broad carbonyl peak is apparent

depending on the amount of incorporation. Interestingly, slight upfield shifts of the other two carbonyl peaks (the second amide and the ester) are detectable as well.

Figure 11. ^{13}C NMR for ^{18}O-Labeled-*N*-Boc-4-Cl-Phenylglycine-Ala-Phe-OMe at 0% and 93% Incorporation

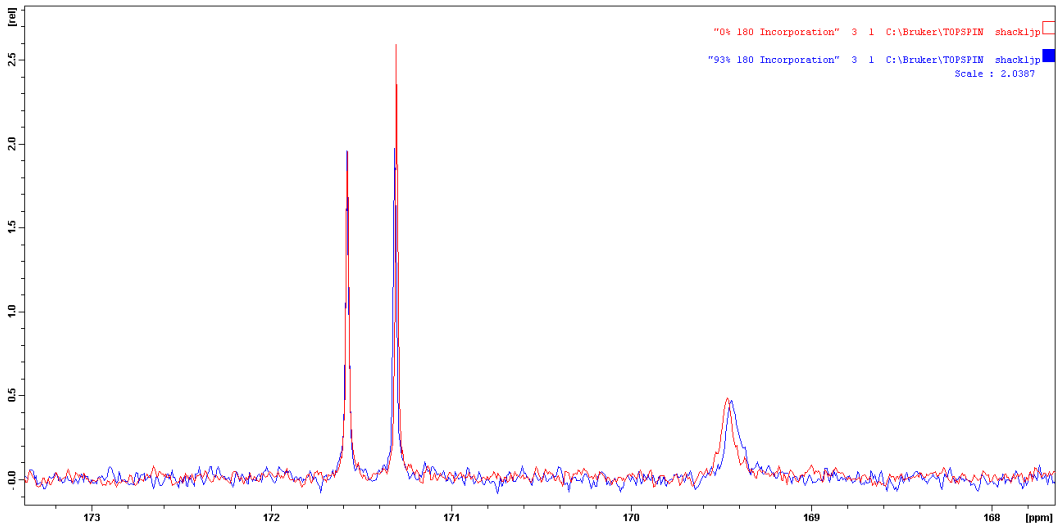

Figure 12. ^{13}C NMR for ^{18}O-Labeled-*N*-Boc-4-Cl-Phenylglycine-Ala-Phe-OMe at 27% and 93% Incorporation

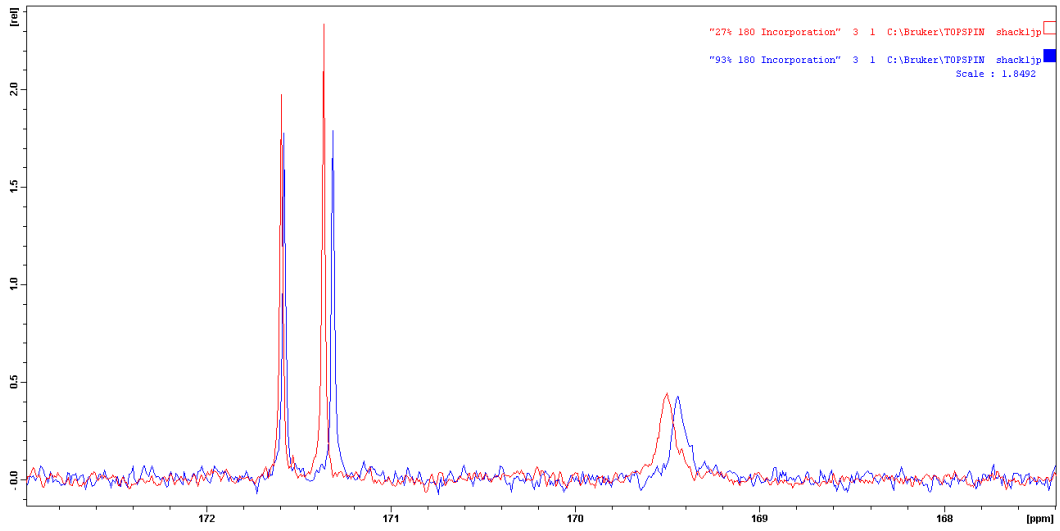

While signs of ^{18}O-incorporation can be observed in the ^{13}C NMR spectra, it requires additional data to be obtained and a much more complicated evaluation process. Furthermore, it still lacks the ability to serve as a viable method for approximating the

amount of ^{18}O-incorporation and serves only to confirm the presence and location of the ^{18}O-label. In this case, IR would clearly establish the presence of the ^{18}O-label. Thus, qualitative analysis by IR followed by direct submission for mass spectrometry analysis is the more effective method for determining the presence of ^{18}O and its resulting incorporation in dipeptides and tripeptides.

Using mass spectrometry, an overall ^{18}O-incorporation of 93% was determined for the tripeptide by comparing the intensities of the $[M]^+$ and $[M+2]^+$ mass peaks and performing the same calculation shown in Equation 1.

Equation 3. Mass Spectrometry Calculation for ^{18}O-Labeled-*N*-Boc-4-Cl-Phenylglycine-Ala-Phe-OMe

Step 1: (12293 x 32.27) / 100 = 3967

Step 2: 156806 − 3967 = 152839

Step 3: 152839 / (152839 + 12293) x 100 = 93% ^{18}O

1.2.4 Formation of Doubly Labeled ^{18}O Peptides Through Standard Coupling

Since many protein studies feature doubly labeled ^{18}O peptides, it was hypothesized that a straightforward method for formation of these doubly labeled ^{18}O peptides could be developed through the use of our ^{18}O-labeling method, followed by a standard coupling of two ^{18}O-labeled peptide fragments after deprotection/hydrolysis. With this hypothesis in mind, formation of the following pentapeptide was attempted using an ^{18}O-labeled dipeptide and ^{18}O-labeled tripeptide (Figure 13). Unfortunately, only trace amounts of the desired pentapeptide could be isolated (1.5 mg, ~5% yield). Analysis of the pure pentapeptide by mass spectrometry resulted in 63% doubly ^{18}O-labeled pentapeptide, 30% singly ^{18}O-labeled pentapeptide, and 7% unlabeled pentapeptide.

Since the yield of the coupling proved to be so low, unlabeled versions of the dipeptide and tripeptide were prepared in order to further evaluate coupling conditions.

Figure 13. Hydrolysis, Deprotection, and Formation of a Doubly-^{18}O-Labeled Pentapeptide

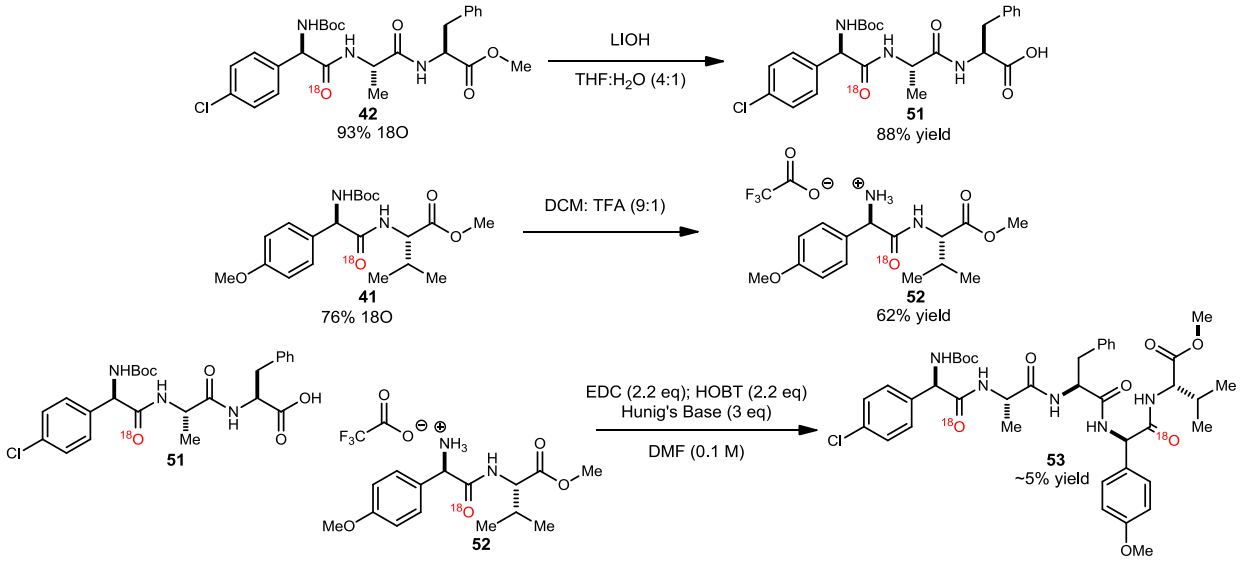

The initial coupling conditions were retried on a larger scale using the unlabeled dipeptide and tripeptide; however, they still resulted in only trace amounts of the desired pentapeptide. Next, the coupling was tried using the variety of different coupling reagents shown in Figure 14. However, all coupling attempts resulted in what appeared to be either trace amounts of the desired pentapeptide or no formation of the pentapeptide. Large excesses of amine (5 equivalents) and coupling reagent (PyBOP, 5 equivalents) were also used in an attempt to increase conversion to the desired pentapeptide; however, no improvements in yield were seen. Although the yield could not be optimized further, the coupling was repeated using ^{18}O-labeled coupling partners, and trace amounts of the desired doubly ^{18}O-labeled pentapeptide were isolated via PrepLC (Scheme 19). The structure of the product was verified by NMR, and mass spectrometric analysis of the doubly ^{18}O-labeled pentapeptide resulted in 57% doubly ^{18}O-labeled pentapeptide, 36% singly ^{18}O-labeled pentapeptide, and 8% unlabeled pentapeptide.

Figure 14. Coupling Reagents Used in the Standard Coupling

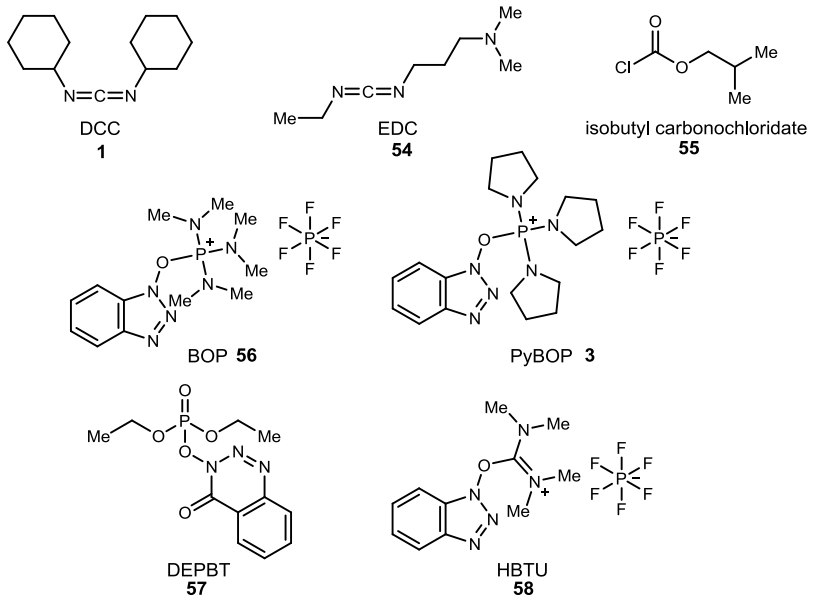

Scheme 19. Formation of the Doubly ^{18}O-Labeled Pentapeptide

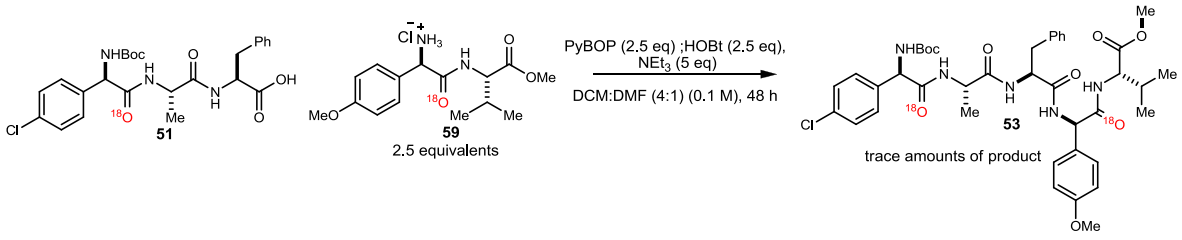

Since all attempts to form the desired pentapeptide had resulted in trace amounts of product or no product formation, it was hypothesized that the coupling might be struggling under a combination of the steric bulk of the carboxylic acid fragment and a sterically hindered amine (due to the arylglycine ring). This hypothesis was tested by running two additional PyBOP mediated couplings: 1) coupling boc-protected phenyl alanine and a dipeptide without an arylglycine by the amine and 2) coupling boc-protected phenyl alanine and a dipeptide featuring an arylglycine by the amine (Scheme 20). This allowed for a direct comparison between the effectiveness of the coupling reagent when coupling a less bulky carboxylic acid to an amine without an arylglycine,

coupling a less bulky carboxylic acid to an amine containing an arylglycine, and coupling a bulky carboxylic acid to an amine by an arylglycine. As shown in Scheme 20, a clear trend can be observed in that as the steric bulk near the reaction site of the coupling partners increase, the yield decreases to the point that only trace amounts of product can be isolated. This suggests that the steric bulk of the coupling partners is playing a role in the low amount of product formation being observed.

Scheme 20. Comparison of Coupling Reagent Effectiveness

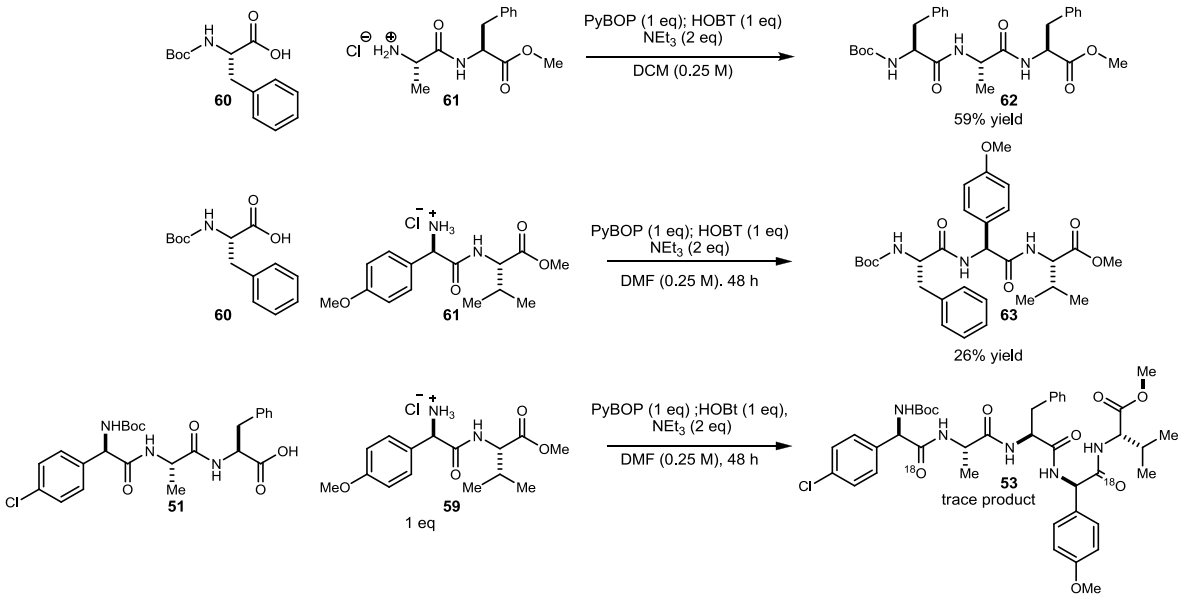

While evaluating the potential role of the steric bulk of the coupling partners, it was hypothesized that the formation of a doubly ^{18}O-labeled peptide might proceed more smoothly featuring coupling partners with minimal steric bulk near the reaction site. Since our available library of ^{18}O-labeled peptides all featured an arylglycine group near the amine reaction site, steric bulk was minimized on the acid coupling partner by featuring a glycine residue rather than a phenylalanine residue near the reaction site. Gratifyingly, this coupling resulted in a 38% yield (Scheme 21), and the product structure

was verified by NMR. Mass spectrometric analysis resulted in 76% doubly ^{18}O-labeled tetrapeptide, 21% singly ^{18}O labeled tetrapeptide, and 3% unlabeled tetrapeptide.

Scheme 21. Formation of a Doubly ^{18}O-Labeled Tetrapeptide

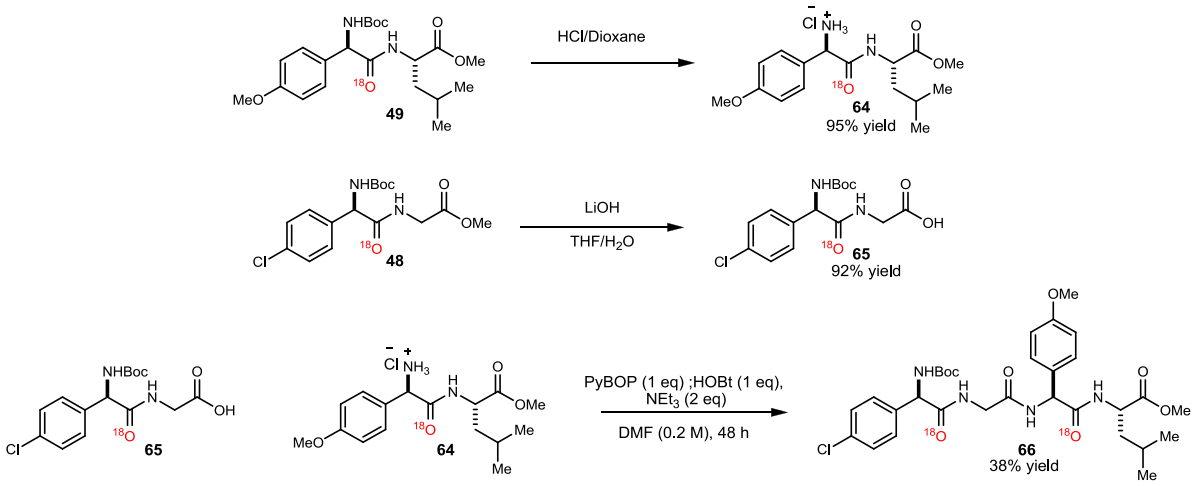

Chapter 2

Catalytic Umpolung Amide Synthesis

2.1 Introduction

The novel protocol for umpolung amide synthesis developed by Johnston, Shen, and Makley[22] resulted in good yields for a variety of amide substrates. However, the success of this reaction depends on the use of stoichiometric amounts of NIS, which is quite expensive ($1032 per mole, Sigma Aldrich) compared to iodine ($142 per mole, Sigma Aldrich). This stimulated a desire to develop a more cost-effective version of this reaction.

2.1.1 Alternatives to NIS

Early attempts to improve the cost-efficiency of this reaction focused on finding a less expensive, but equally effective halogenating agent to replace NIS.[29] The first alternative halogenating agents tried were NBS and NCS in order to directly compare the three *N*-halosuccinimide halogen sources (Table 4). Unfortunately, both NBS and NCS resulted in much lower yields of the desired amide product. The NBS reaction appeared to suffer from slow conversion resulting in the formation of dibrominated nitroalkane as a major byproduct, but full conversion to the desired amide product could be obtained if 5 equivalents of amine were used and the reaction was run at room temperature. Formation of the dibrominated nitroalkane could also be minimized by pre-mixing the NBS and amine prior to addition of the α-bromo nitroalkane or base. Unfortunately, the NBS

[29]Makley, D. M.; Johnston, J. N. *Unpublished Results.*

reaction still resulted in a lower yield than the optimized NIS reaction. The NCS reaction appeared to undergo full conversion, but the crude ^{1}H NMR showed a large excess of amine and the presence of multiple co-products. This likely indicates that the presence of NCS is encouraging decomposition of the α-bromo nitroalkane.

Table 4. Comparison of N-Halosuccinimide Halonium Sources[a]

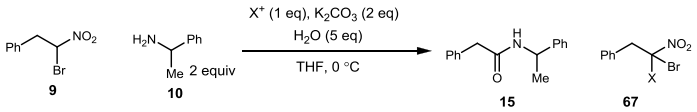

entry	X^+ source	cost/mole (%)	conversion (%)	19:50	% yield
1	NIS	1032	100	1 : 0	72
2	NBS	58	50	3 : 4	25
3[b]	NBS	58	71	1 : 0	56
4[c]	NBS	58	100	1 : 0	68
5	NCS	27	100	1 : 0	21

[a] Work performed by Dawn Makley, [b] NBS and amine were pre-mixed before adding α-bromo nitroalkane or base, [b] 5 equivalents amine were used, and the reaction was run at room temperature.

Next, a more extensive screen of potential halogenating reagents was performed (Table 5).[29] In each example, the *N*-halo amine was preformed followed by addition of K_2CO_3 and H_2O before being cooled to 0 °C prior to α-bromo nitroalkane addition. Despite extended reaction times, the majority of the tested halogenating reagents produced low yields. TCCA appeared promising with a 55% yield; unfortunately, it proved inconsistent on attempts to replicate it. *N*-Bromophthalimide resulted in a higher yield than NBS, which makes it likely that extra equivalents of amine could further improve this yield. Iodine, a much cheaper source of iodonium, resulted in a comparable yield to that obtained with NIS; unfortunately, iodine resulted in inconsistent yields when tested on different reaction substrates.

Table 5. Full Halogenating Reagent Screen[a]

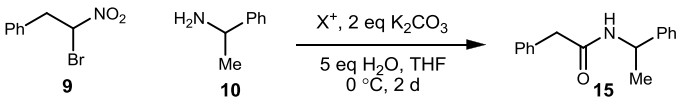

	entry	X^+ source	equiv	% yield	cost/mol ($)
	1	none	--	3	–
Cl^+	2[c,d]	$Ca(ClO)_2$[e]	1.5	22	7
Cl^+	3[c,d]	NCS	1.0	40	27
Cl^+	4[c]	TCCA	0.33	55	4
Cl^+	5[c]	DCDMH	0.5	53	10
Br^+	6[f]	Br_2	1.0	40	25
Br^+	7[f]	NBS	1.0	56	58
Br^+	8[f]	NBP	1.0	54	585
Br^+	9[f]	DBDMH	0.5	28	10
I^+	10	I_2	1.0	70	60
I^+	11	ICl	1.0	43	97
I^+	12	NIS	1.0	72	1032

[a] Work performed by Dawn Makley, [b] order of addition: amine, X^+ source, K_2CO_3 and H_2O added; brought to 0 °C; α-BN added, [c] reaction done in DME, [d] reaction let stir 3 d, [e] 65% available Cl^+, [f] reaction let stir 4 d.

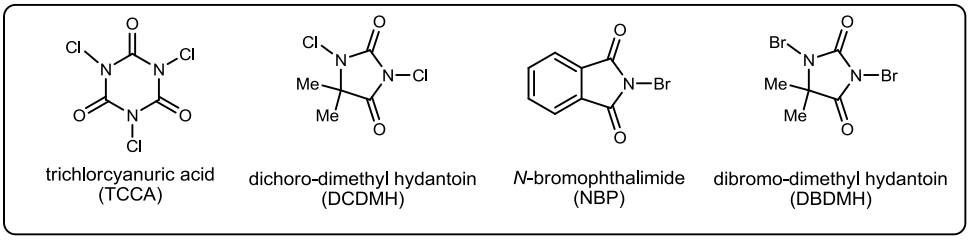

2.1.2 Oxygen-Catalyzed Turnover of NIS

While attempting to establish the primary oxygen donor of the amide carbonyl, it was observed that the reaction proceeded much faster under an oxygen atmosphere. In particular, the aerobic pathway to amide formation was proceeding much faster than the anaerobic pathway to amide formation. One hypothesis to explain why the aerobic pathway was proving to be faster than the anaerobic pathway was that molecular oxygen was somehow aiding in the conversion of iodine back to iodonium, maintaining a constant concentration of iodonium available throughout the course of the reaction. If

molecular oxygen could be proved to catalyze the turnover of iodide to iodonium, this would allow for a cost-effective improvement to the umpolung amide synthesis by allowing NIS to be used in catalytic amounts instead of stoichiometric amounts.

Scheme 22. Proposed Aerobic Pathway Featuring Turnover of Iodide to Iodonium

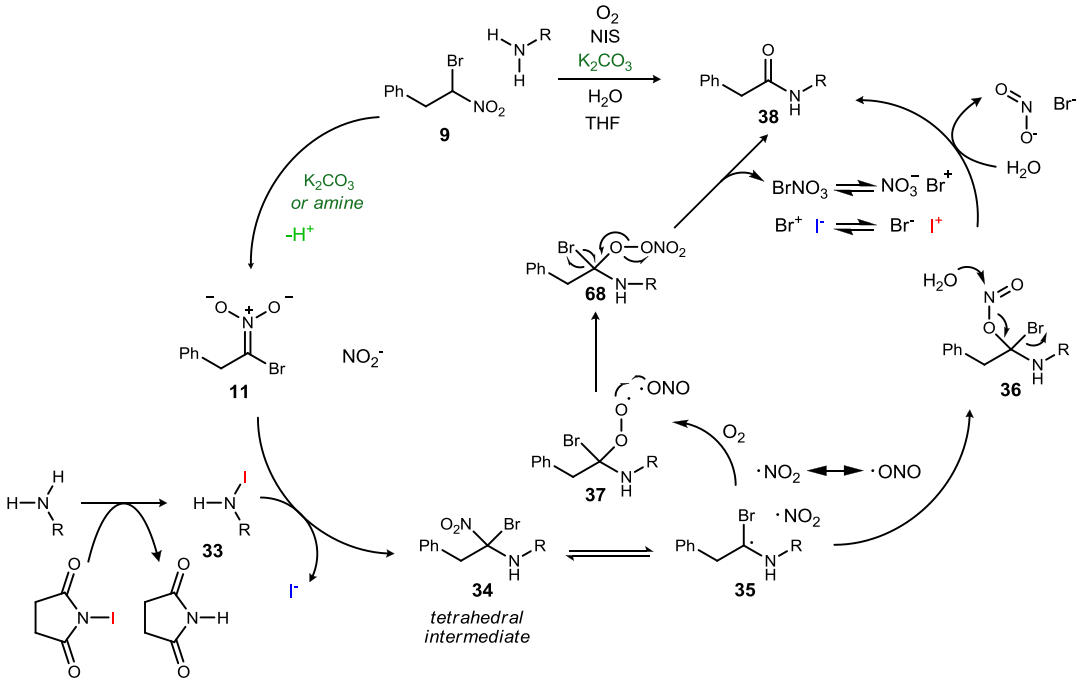

As a result of the mechanistic study, **37** is considered a likely intermediate along the aerobic pathway; however, subsequent breakdown to form the amide product and the mechanism for turnover of iodide to iodonium remains unknown. One potential mechanism for product formation and reformation of iodonium is shown in Scheme 22. This mechanism is supported by the fact that nitrite radicals have been shown in the literature to react with superoxide[30] and $XONO_2$ (X=Cl, Br, I) compounds are known to

[30]Goldstein, S.; Czapski, G. *J. Am. Chem. Soc.* **1998**, *120*, 3458-3463. Hodges, G. R.; Ingold, K. U. *J. Am. Chem. Soc.* **1999**, *121*, 10695-10701.

form via radical processes.[31] However, the final breakdown to product and conversion of iodide back to iodonium could potentially occur through a number of potential pathways, as radical reactions between oxygen and halogens[32] and nitro radicals and halogens[33] are also well documented in the literature.

2.2 Catalytic Umpolung Amide Bond Synthesis

The possibility of adding NIS in catalytic amounts under an oxygen atmosphere was tested on the standard reaction and resulted in 75% yield after only 2 hours (Scheme 23). This result is indicative of the fact that this amide synthesis can be performed much more cost-effectively through the use of a catalytic amount of expensive halogenating reagent. Since THF oxidation was observed in several crude reaction mixtures, the solvent was switched to DME for all further reactions.

Scheme 23. Umpolung Amide Synthesis Using Catalytic NIS (5 mol %)[34]

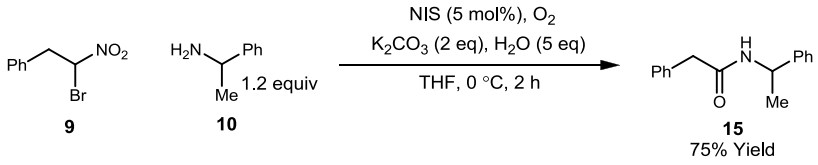

Once the catalytic NIS conditions proved effective, they were tested on a broad variety of amines and α-bromo nitroalkane donors. The yields were compared to those achieved under stoichiometric conditions. Table 6 shows the substrate scope of α-bromo nitroalkane donors tested under the new catalytic conditions. Gratifyingly, the yields

[31]Papayannis, D. K.; Kosmas, A. M. *Chem. Phys.* **2005**, *315*, 251-258.
[32]Kosmas, A. M. *Bioinorg. Chem. Appl.* **2007**, 11/1-11/9; Drougas, E.; Kosmas, A. M. *J. Phys. Chem. A* **2007**, *111*, 3402-3408; Laszlo, B.; Huie, R. E.; Kurylo, M. J.; Miziolek, A. W. *J. Geophys. Res., [Atmos.]* **1997**, *102*, 1523-1532.
[33]Jia, X.-J.; Liu, Y.-J.; Sun, J.-Y.; Sun, H.; Wang, F.; Pan, X.-M.; Wang, R.-S. *Theor. Chem. Acc.* **2010**, *127*, 49-56.
[34]Shen, B.; Johnston, J. N. *Unpublished Results.*

Table 6. Catalytic Umpolung Amide Synthesis: Substrate Scope of α-Bromo Nitroalkane Donors

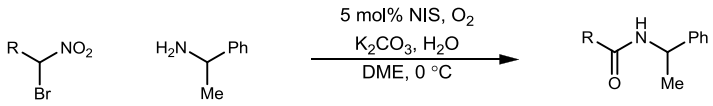

entry[a]	product	equivalents of amine	catalytic % yield	stochiometric % yield
1	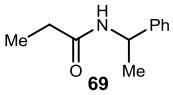 **69**	1.2	72	71
2	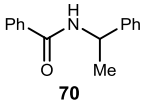 **70**	1.2	84	76
3	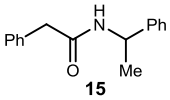 **15**	1.2	73	75
4	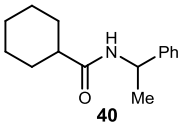 **40**	1.2	81	70
5	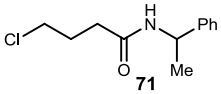 **71**	1.2	72	81
6	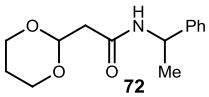 **72**	1.2	74	72
7	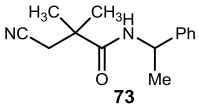 **73**	1.2	53	54
8	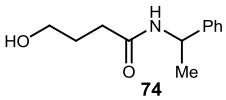 **74**	1.2	41	48
9	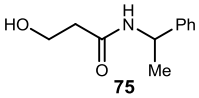 **75**	1.2	71	70
10	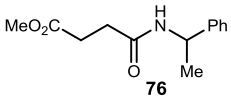 **76**	1.2	76	70

[a] α-BNA was added to a 15 mL rxn flask, followed by H_2O and DME. The reaction was cooled to 0 °C, followed by addition of NIS and K_2CO_3. An oxygen balloon was added, followed by rapid addition of amine. Reaction was allowed to stir for 2-15 hours.

observed using catalytic conditions were consistent or higher than those seen under stoichiometric conditions. The substrate scope of *N*-Boc α-bromo nitroamine donors is shown in Table 7, and the results were more mixed. While couplings between the α-bromo nitroamine (where R^1=Cl) and a single amino acid (entries 1 and 2) produced

Table 7. Catalytic Umpolung Amide Synthesis: Substrate Scope of *N*-Boc α-Bromo Nitroamines

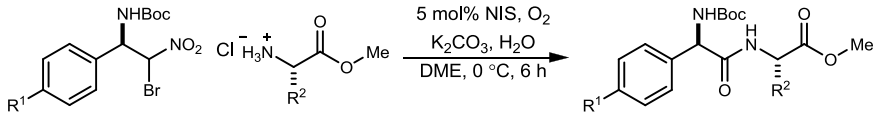

entry[a]	product	equivalents of amine	catalytic % yield	stochiometric % yield
1	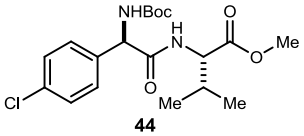 **44**	1.2	73	70
2	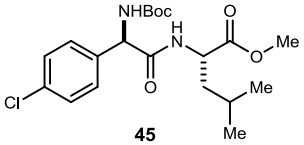 **45**	1.2	77	81
3	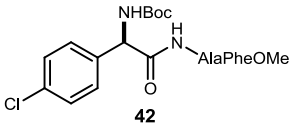 **42**	1.2	51	72
4	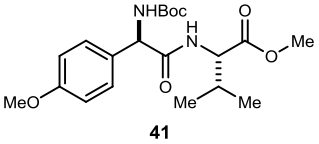 **41**	1.2	59	75
5[b]	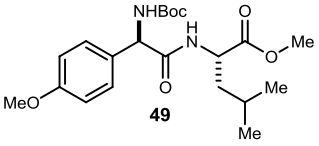 **49**	1.2	50	76
6[b]	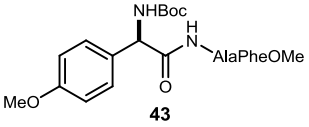 **43**	1.2	34	72

[a] α-BNA was added to a 15 mL rxn flask, followed by H_2O and DME. The reaction was cooled to 0 °C, followed by addition of NIS and K_2CO_3. An oxygen balloon was added, followed by rapid addition of amine. Reaction was allowed to stir for 6 hours, [b] reaction was run for 48 hours.

similar yields under catalytic conditions as seen under stoichiometric conditions, coupling with the dipeptide (entry 3) resulted in a remarkably lower yield than what is seen under stoichiometric conditions. The couplings shown in entries 1-3 also proved incredibly time dependent, as letting the reaction run over 48 hours instead of 6 hours led to a 5-10% decrease in yield. The α-bromo nitroamine (where R^1=OMe) couplings resulted in much lower yields than seen in entries 1-3. While the coupling shown in entry 4 did not suffer from any noticeable time dependency, the couplings depicted in entries 5 and 6 experienced a significant drop in yield (24% and 21% respectively) when the reaction time was lowered to 6 hours.

One potential theory for the lower yields is that the α-bromo nitroamines of entries 4-6 are much more likely to undergo electrophilic aromatic substitution due to the electron donating capabilities of the methoxy group, leading to permanent loss of the iodonium. With that theory in mind, further optimization of these catalytic couplings began through studying the effect of increasing the equivalents of NIS on entry 5 (Table 8). An increase to 10 mol% NIS (instead of 5 mol% NIS) resulted in an increase in yield to 60%; however, further increases to 20 mol% NIS resulted in no improvement to the yield (57%). Interestingly, the increase to 10 mol% NIS also allowed the reaction to be run for a shorter reaction time (6 hours) to achieve a similar yield (63%). However, it was seen that lowering the reaction time even further (to 2 and 4 hours) resulted in significant loss in yield (24% and 52% respectively). The same increase in NIS equivalents (to 10 mol%) was also tried in the couplings depicted in entries 4 and 6; however, no improvement in yield was seen in either case.

Table 8. Optimization of NIS Equivalents for Entry 5

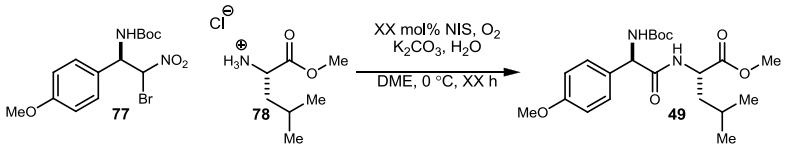

entry	mol% NIS	rxn time	Yield
1	5	48	50
2	10	48	60
3	10	6	63
4	20	48	57

Further optimization of this reaction was attempted by altering the reaction temperature. However, both increasing and decreasing the reaction temperature resulted in a loss in yield (Table 9).

Table 9. Temperature Variation Studies on Entry 5

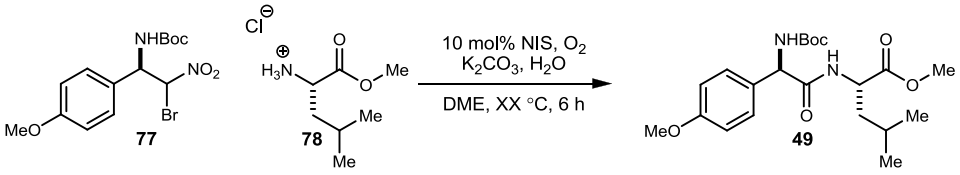

entry	XX ° C	Yield
1	-22	26
2	0	63
3	25	50

It was also hypothesized that the methyl ester could be undergoing hydrolysis under the basic reaction conditions leading to diminished yields. This theory was tested by using leucine *t*-butyl ester instead of leucine methyl ester. Unfortunately, this resulted in an overall lower yield for the coupling than what was seen when using the methyl ester (Figure 15). However, it is important to note that when both the leucine methyl ester

Figure 15. Protecting Group Change

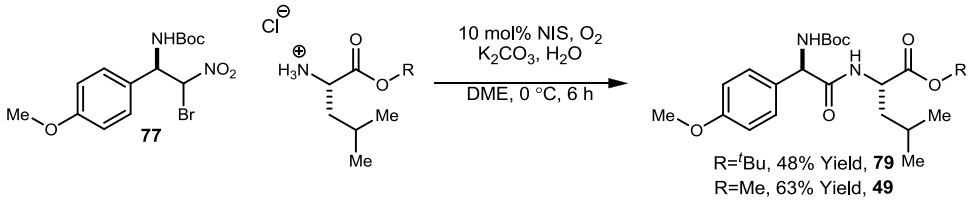

and leucine *t*-butyl ester couplings were allowed to run for 3 days, the yield of the *t*-butyl leucine coupling was comparably higher. This seems to indicate that while the methyl ester peptide is more prone to hydrolysis over longer periods of time than the *t*-butyl ester peptide, the leucine methyl ester coupling produces an overall higher yield at a shorter reaction time than the leucine *t*-butyl ester coupling produces at the longer reaction time (Figure 16).

Figure 16. Protecting Group Change over a Longer Reaction Time

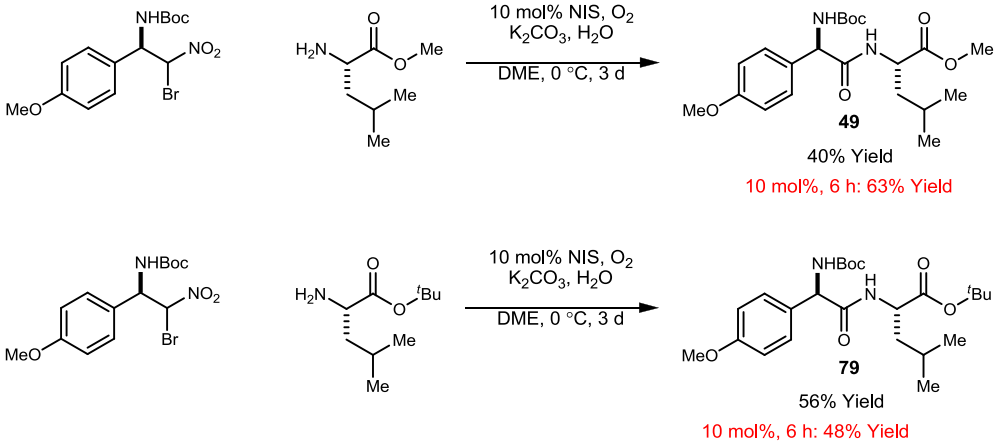

Table **10** shows the substrate scope of various amines coupled under the catalytic conditions. Fortunately, the yields observed using catalytic conditions were consistent for the most part with those seen under stoichiometric conditions. However, entries 9 and 10 resulted in a 20% decrease in yield when compared to the stoichiometric conditions. The

Table 10. Catalytic Umpolung Amide Synthesis: Substrate Scope of Amines

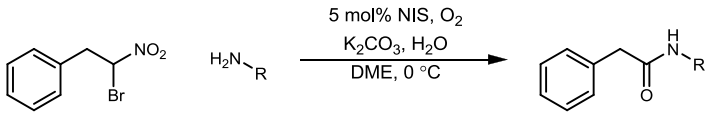

entry[a]	product	equivalents of amine	catalytic % yield	stochiometric % yield
1	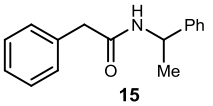 **15**	1.2	73	75
2	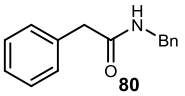 **80**	1.2	76	72
3	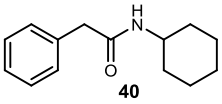 **40**	1.2	73	72
4	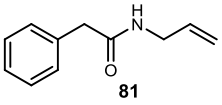 **81**	1.2	76	73
5	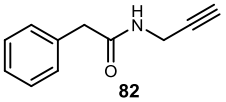 **82**	1.2	62	61
6	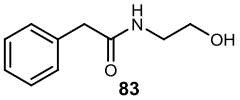 **83**	1.2	86	86
7	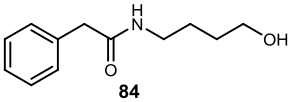 **84**	1.2	69	71
8	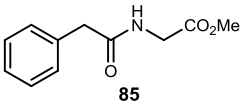 **85**	1.2	74	72
9	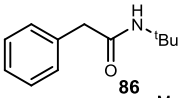 **86**	2	41	60 (1.8 eq)
10	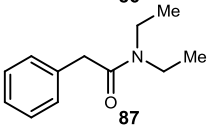 **87**	2	32	50 (1.2 eq)

[a] α-BNA was added to a 15 mL rxn flask, followed by H_2O and DME. The reaction was cooled to 0 °C, followed by addition of NIS and K_2CO_3. An oxygen balloon was added, followed by rapid addition of amine. Reaction was allowed to stir for 2-15 hours.

yield of entry 9 can be improved to 50% when 3 equivalents of amine are used, and the yield of entry 10 can be improved to 40% when 3 equivalents of amine are used. This trend indicates that as the substituents on the amine become more bulky, the catalytic conditions appear to be slightly less effective than the stoichiometric conditions. Further optimization remains necessary to improve the yields of bulky and disubstituted amine couplings under both stoichiometric and catalytic conditions.

2.3 Catalytic Umpolung Amide Coupling Using Disubstituted Amines

Disubstituted amides are found in a variety of natural products, many of which are desirable synthetic targets due to their biological activity. Several examples of biologically active disubstituted amides can be seen in Figure 17.

Figure 17. Natural Product Examples Featuring Disubstituted Amides

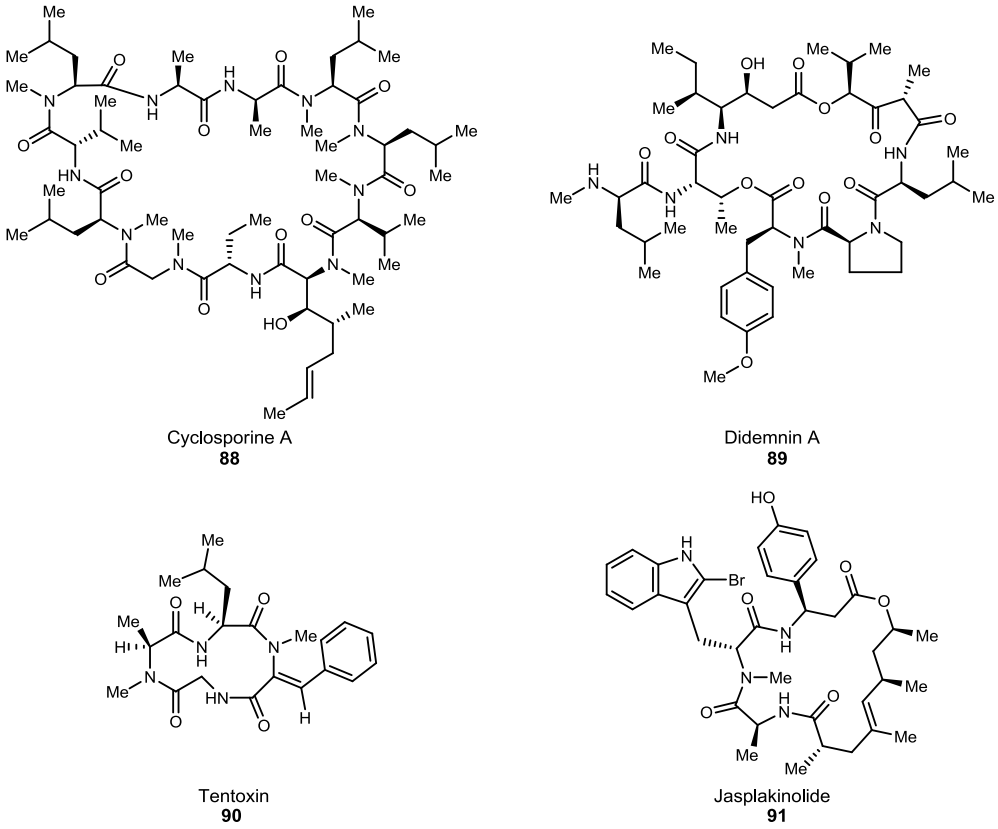

Cyclosporine A (**88**) is a fungal metabolite that acts as a reversible inhibitor of cytokines in T helper cells. It has immunosuppressive properties and has been used in the treatment of Bechet's syndrome, rheumatoid arthritis, and Crohn's disease.[35] The didemnins (**89**) have also been shown to exhibit significant immunosuppressive and antiproliferative activity,[36] while tentoxin (**90**) has been used as a selective weed killer.[37] Jasplakinolide (**91**) has exhibited a broad range of biological activity including antifungal, anthelminthic, insecticidal, and anti-cancer properties.[38]

The increased biological activity of peptides containing *N*-alkyl residues is attributed to a decreased preference for the *trans* conformation, which is normally highly favored by monosubstituted amides. This allows for the formation of more biologically active β-hairpin peptide conformations. Conformational effects on both intra- and intermolecular hydrogen bonding also lead to substantial changes in the secondary and tertiary protein structure, allowing *N*-methylated peptides to be used in conformational structure-activity studies. *N*-Alkylated peptides also tend to enhance hydrophobicity and prove to be more stable in the presence of proteolytic enzymes, which can lead to enhanced bioavailability and medicinal potential.[39]

One of the defining problems in using peptides as therapeutics is that many of the potential drug candidates have a short half-life *in vivo* and poor bioavailability. This has led to the formation of *N*-methylated derivatives of a variety of biologically active peptides, which naturally contain only monosubstituted amides. This has been shown to

[35]Wu, X. Y.; Stockdill, J. L.; Wang, P.; Danishefsky, S. J. *J. Am. Chem. Soc.* **2010**, *132*, 4098-4100.
[36]Jou, G.; Gonzalez, I.; Albericio, F.; Lloyd-Williams, P.; Giralt, E. *J. Org. Chem.* **1997**, *62*, 354-366.
[37]Loiseau, N.; Cavelier, F.; Noel, J.-P.; Gomis, J.-M. *J. Pept. Sci.* **2002**, *8*, 335-346.
[38]Tannert, R.; Hu, T.-S.; Arndt, H.-D.; Waldmann, H. *Chem. Commun.* **2009**, 1493-1495.
[39]Humphrey, J. M.; Chamberlin, A. R. *Chem. Rev.* **1997**, *97*, 2243-2266.

enhance metabolic stability, as well as intestinal permeability, leading to increased oral availability of some peptidic drug candidates. *N*-Methylation has also been shown to enhance the selectivity of some peptidic drug candidates.[40] The potential therapeutic uses of *N*-alkylated peptidic natural products and their derivatives have led to an increased interest in the development of novel synthetic methodologies for the formation of disubstituted amides.

2.3.1 Current Methods and Challenges of Coupling Disubstituted Amines

The synthesis of disubstituted amides has proven quite difficult under classic dehydrative conditions due to the fact that the steric hindrance of the disubstituted amine outweighs its nucleophilicity. This generally results in slow coupling rates, leading to long reaction times, low yields, and undesired side products.[39] This has proven

Scheme 24. Mechanism of Racemization in *N*-Methyl Amino Acid Couplings

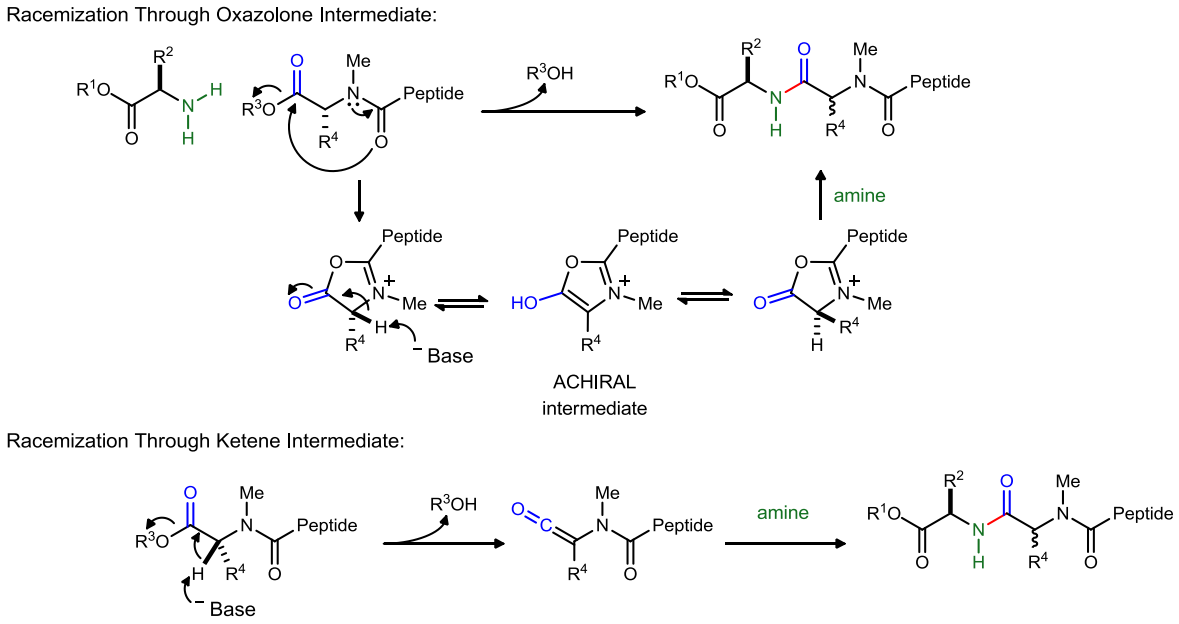

[40]Chatterjee, J.; Gilon, C.; Hoffman, A.; Kessler, H. *Acc. Chem. Res.* **2008**, *41*, 1331-1342.

particularly true for coupling *N*-methyl-amino acids and esters, as they are increasingly prone to slow reaction rates and racemization.[41] The increased racemization rate is likely due to the absence of the acidic amide proton, which would usually ionize first and help suppress α-deprotonation under basic conditions (Scheme 24).[39]

Interestingly, the presence of HOBt (usually a racemization suppressant) has actually been shown to increase racemization when coupling *N*-methyl amino acids. This is likely due to the fact that the intermediate HOBt ester is too sterically bulky to react with the disubstituted amine, leading to a slower reaction rate, and therefore a greater possibility of racemization (Scheme 25).[42]

Scheme 25. HOBt Racemization Suppressant Mechanism

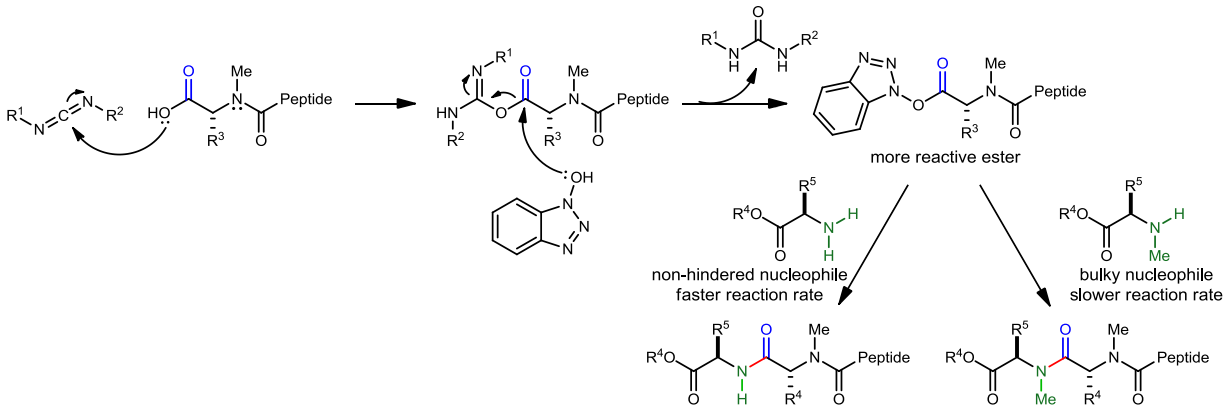

An additional difficulty encountered when coupling *N*-methyl dipeptides is the potential formation of a diketopiperazine side product (Scheme 26). Although this problem can be avoided by extending the chain length of the carboxylic acid coupling partner, racemization through the oxazolone intermediate becomes even more likely.[39]

[41]Fang, J. B.; Sanghi, R.; Kohn, J.; Goldman, A. S. *Inorg. Chim. Acta* **2004**, *357*, 2415-2426.

[42]Montalbetti, C.; Falque, V. *Tetrahedron* **2005**, *61*, 10827-10852.

Scheme 26. Mechanism for Diketopiperazine Formation

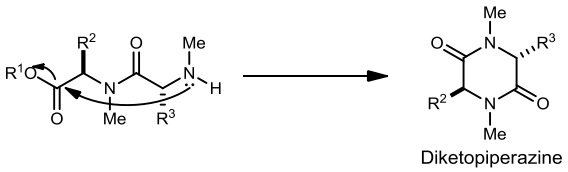

Since the majority of commonly used coupling reagents result in either decreased or inconsistent yields when used to couple disubstituted amines,[43] the development of novel coupling reactions with the potential to avoid these shortcomings has become an increasing area of interest. One of the first novel coupling reactions of disubstituted amines was developed and reported by Wenger, in the first total synthesis of cyclosporine A. This coupling works by activating the carboxylic acid toward substitution via formation of a mixed pivalic anhydride intermediate. This method resulted in fair yields (60-70%) and only moderate racemization (5-20%).[44] Further developments led to the activation of the carboxylic acid by formation of a mixed bis(2-oxo-3-oxazolidinyl)phosphonic (BOP) anhydride, which resulted in higher yields and reduced racemization. This improvement is likely caused by intermolecular hydrogen bonding between the oxazolidinone carbonyl and the amine hydrogen.[45] Since BOPCl will react faster with a carboxylate anion than with a disubstituted amine, this modification can be performed in one pot. However, it is important to note that monosubstituted amines are capable of competing with the carboxylate anion for BOPCl, so this type of coupling should be limited to disubstituted amines (Figure 18).[46]

[43]Valeur, E.; Bradley, M. *Chem. Soc. Rev.* **2009**, *38*, 606-631.
[44]Wenger, R. M. *Helv. Chim. Acta* **1983**, *66*, 2672-2702.
[45]Van Der Auwera, C.; Anteunis, M. J. O. *Int. J. Pept. Protein Res.* **1987**, *29*, 574-588.

[46]Colucci, W. J.; Tung, R. D.; Petri, J. A.; Rich, D. H. *J. Org. Chem.* **1990**, *55*, 2895-2903.

Figure 18. Mixed Pivalic and BOP Anhydride Activated Carboxylic Acids

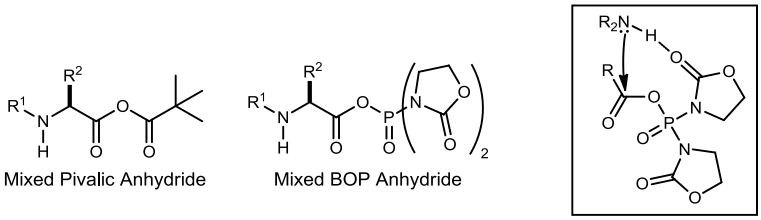

In recent years, there have been several developments in the synthesis of disubstituted amides. In 2003 Batey reported the synthesis of disubstituted amides from carbamoylimidazolium salts in excellent yields (80-100%) with no required purification steps; however, no peptidic coupling examples were given.[47] In 2004 Goldman reported the synthesis of disubstituted amides in moderate to high yields using $TaCl_5$ as a coupling

Scheme 27. Recent Advances in the Synthesis of Disubstituted Amides

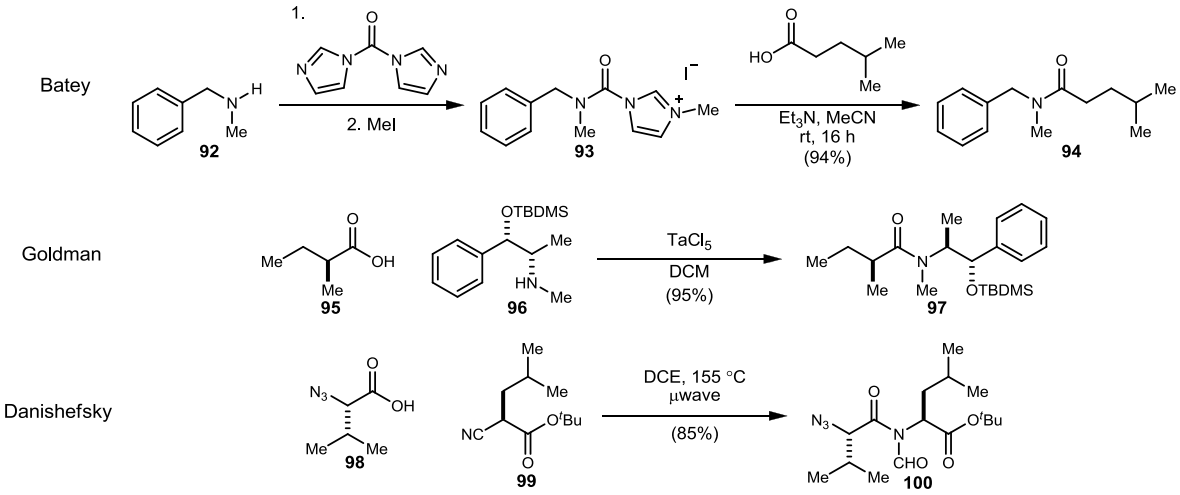

agent, including several peptidic coupling examples (73-95%).[41] In 2009, Danishefsky reported the synthesis of disubstituted amides from isonitriles and gave a handful of examples showing good yields (80-90%).[48] He later showcased this methodology in a

[47]Grzyb, J. A.; Batey, R. A. *Tetrahedron Lett.* **2003**, *44*, 7485-7488.
[48]Rao, Y.; Li, X.; Danishefsky, S. J. *J. Am. Chem. Soc.* **2009**, *131*, 12924-12926.

total synthesis of cyclosporine A resulting in an overall yield of 54% (Scheme 27).[49]

2.3.2 Reaction Optimization of Disubstituted Amine Coupling

To further optimize our catalytic amide bond synthesis for the formation of disubstituted amides, a representative coupling using diethyl amine was chosen for further evaluation (Scheme 28). In each experimental modification, one equivalent of

Scheme 28. Model Reaction for Disubstituted Amide Formation Optimization

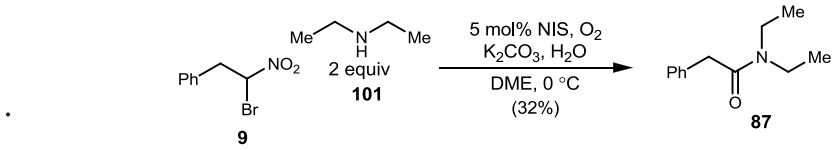

α-bromo nitroalkane and five equivalents of H_2O were added to DME (0.2 M) and cooled to 0 °C. After addition of 2 equivalents of K_2CO_3 and 5 mol% NIS, an O_2 balloon was added, followed by rapid addition of diethyl amine. The reaction was then stirred at 0 °C for the specified reaction time. The reaction mixture was then diluted with DCM, dried over $MgSO_4$, filtered, and concentrated.

In previous experimental results, it was observed that increasing the equivalents of amine often resulted in an increase in yield. This also proved to be the case in this reaction; when three equivalents of amine were used instead of two, the yield increased to 41%. Interestingly, the use of three equivalents of distilled diethyl amine actually resulted in a drop in yield to 28% (Table 11).

[49]Wu, X. Y.; Stockdill, J. L.; Wang, P.; Danishefsky, S. J. *J. Am. Chem. Soc.* **2010**, *132*, 4098-4051.

Table 11. Effect of Amine Equivalents on Disubstituted Amide Synthesis

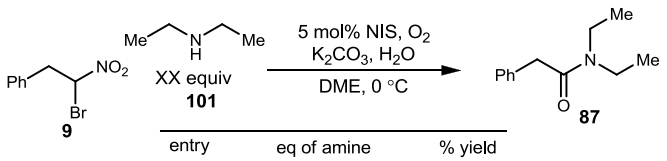

entry	eq of amine	% yield
1	2	32
2	3	40
3[a]	3	28

[a] Amine was distilled

To better observe whether the reaction was reaching full conversion, the reaction was monitored by analyzing aliquots from the reaction at various times by NMR. Based on this analysis, the reaction appeared to be stalling at 65% conversion after 5 to10 hours. This indicated that it was likely that the catalytic iodonium was no longer present in the reaction mixture after 10 hours. This led to the theory that an additional 5 mol% NIS added after 5 hours might result in an improved reaction conversion.

Table 12. Effect of Additional NIS Addition

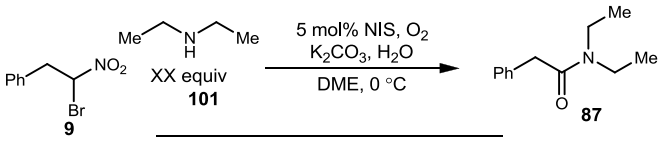

entry	eq of amine	% yield
1[a]	1.2	35
2[a]	3	49

[a] Additional 5 mol% NIS added after 5 hours.

The addition of a second 5 mol% aliquot of NIS to the reaction after 5 hours led to an 8% increase in yield (49%). However, attempting to lower the equivalents of amine from 3 to 1.2 equivalents resulted in a drop in yield to 35% indicating an excess of amine was still necessary (Table 12).

Since addition of a second 5 mol% aliquot of NIS after 5 hours had resulted in a slight improvement in yield, an additional 5 mol% of NIS was added to the reaction every

5 hours until complete conversion was observed by NMR (Table 13). Complete conversion was observed after 29 hours, with the eventual addition of a total of 20 mol% NIS.

Table 13. Reaction Conversion with Additional NIS Monitored by NMR Aliquot

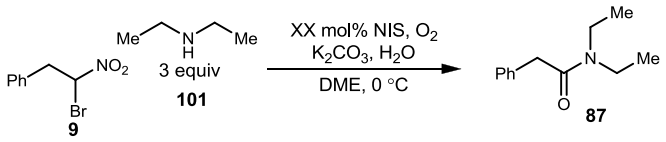

entry	time (h)	mol % NIS[a]	conversion (%)[b]	% yield
1	5	5	52	–
2	10	10	61	–
3	23	15	78	–
4	29	20	100	37

[a] Additional 5 mol% aliquot of NIS was added at each new entry, [b] based on ^{1}H NMR analysis of remaining α-BNA.

Despite what appeared to be complete disappearance of the starting α-bromo nitroalkane, the reaction only resulted in a 37% yield. The reaction was then repeated, adding a full 20 mol% of NIS at the beginning of the reaction instead of in aliquots, but the yield (47%) still remained consistent with the yield observed using 10 mol% NIS, despite the apparent difference in conversion.

Throughout the course of the reaction, it was observed that a yellowish solid was forming in the solution and sticking to the sides of the flask. In the work-up of this reaction, this solid was filtered off as it was assumed to be K_2CO_3, since it is not entirely soluble under the reaction conditions. However, a modification of the reaction work-up conditions to include an acidification and extraction with DCM resulted in a large amount of dinitroalkane being present in the crude ^{1}H NMR (24%), whereas no dinitroalkane had

been seen in the crude ^{1}H NMR previously (Table 14). This suggested the possibility that large amounts of dinitroalkane were forming, but it was either precipitating out as a salt or becoming trapped in the insoluble K_2CO_3. The dinitroalkane most likely formed through the ter Meer reaction pathway (Scheme 29).[50]

Scheme 29. The ter Meer Reaction

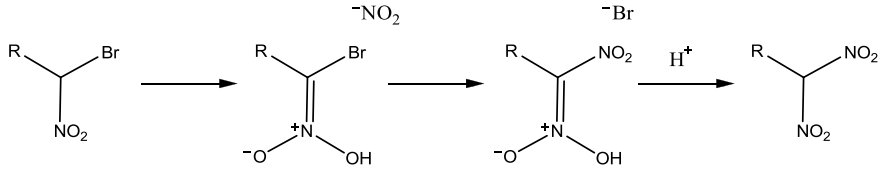

In order to prove that formation of the dinitroalkane was having a significant effect on the yield, the reaction was repeated at –22 °C. This was done because dropping the temperature had previously been shown to decrease dinitroalkane formation. The same acidic workup was performed on the -22 °C reaction and resulted in an improved yield of 52% (up from 41% at 0 °C). A decrease in dinitroalkane formation (13%) was observed; furthermore, 8% of the starting α-bromo nitroalkane remained indicating that the lower temperature was slowing down conversion of the α-bromo nitroalkane to both dinitroalkane and product. This experiment indicated that dinitroalkane formation was having a significant effect on the overall yield of the reaction (Table 14).

Table 14. Acidic Workup and Temperature Effects on the Disubstituted Amide Synthesis

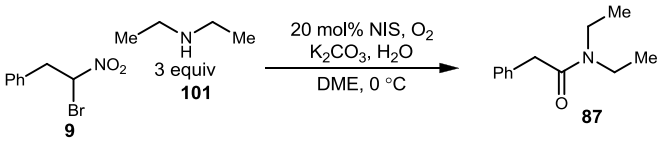

entry	temp (°C)	BNA : dinitro : amide	eq of amine	% yield
1[a,b]	0	0 : 24 : 76	3	41
2[a,c]	-22	8 : 13 : 79	3	52

[a] Reactions were acidified and extracted with DCM, [b] reaction was ran for 2 days, [c] reaction was ran for 3 days.

[50]ter Meer *Ann.* **1876**, *181*, 4; Hawthorne, M. F. *J. Am. Chem. Soc.* **1956**, *78*, 4980-4.

Since the change in workup had such a significant effect on what was seen in the crude ^{1}H NMR of the disubstituted amine coupling, the reaction was repeated using a monosubstituted amine. Interestingly, the crude ^{1}H NMR of the monosubstituted amine coupling revealed 12% of the α-bromo nitroalkane remaining and 2% dinitroalkane, whereas a simple filtration work up showed complete consumption of the α-bromo nitroalkane and 2% dinitroalkane formation (Scheme 30).

Scheme 30. Acidic Workup vs. Filtration Workup for Monosubstituted Amine Coupling

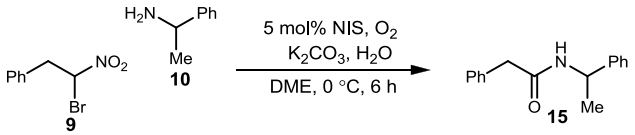

Filtration Workup: 98% Amide, 2% Dinitro (73% Yield)
Acid/Extraction Workup: 86% Amide, 12% BNA, 2% Dinitro (67% Yield)

Since both disubstituted and monosubstituted amine coupling yields seemed to suffer due to the formation of the dinitroalkane side product, it was hypothesized that any modification that resulted in an improved product to dinitroalkane ratio for the monosubstituted coupling would also result in an improved conversion in the disubstituted coupling. Since the monosubstituted amine coupling was known to be complete after only 2 hours, it was used to screen a variety of conditions with the hope that an increase in conversion, as well as an increase in the product to dinitroalkane ratio, would be seen that could translate to better conversions and higher yields in the disubstituted amine couplings.

Since the conversion ratios were changing so drastically upon the use of an acidic workup, it was hypothesized that once the α-bromo nitroalkane was deprotonated some of it could fall out of solution as the potassium salt, as the reaction mixture remains

heterogeneous throughout the entire course of the reaction. This theory was tested by screening various ionic carbonate bases, as well as two hydroxide bases (Table 15).

Table 15. Base Screen for the Monosubstituted Amine Coupling

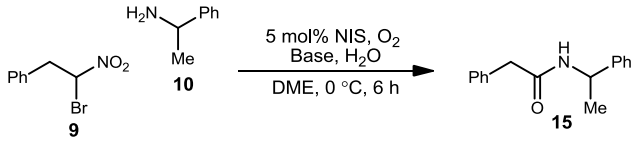

	entry	base	BNA : dinitro : amide[a]	% yield
+1 Cations	1	Li_2CO_3	40 : 15 : 45	39
	2	Na_2CO_3	3 : 23 : 74	55
	3	K_2CO_3	12 : 2 : 86	67
	4[b]	K_2CO_3	0 : 7 : 93	61
	5[c]	K_2CO_3	2 : 9 : 89	61
	6	Cs_2CO_3	0 : 12 : 88	67
	7[c]	Cs_2CO_3	0 : 16 : 84	58
	8	$(NH_4)_2CO_3$	16 : 25 : 59	46
+2 Cations	9	$CaCO_3$	47 : 14 : 39	30
	10	$BaCO_3$	43 : 15 : 41	39
Hydroxide Bases	11	NaOH	2 : 10 : 88	57
	12	KOH	81 : 4 : 15	12

[a] Ratios determined by NMR Analysis, [b] 5 mol % tetra butyl ammonium iodide was added,[c] 5 mol % tetra butyl ammonium bromide was added.

Unfortunately, none of the bases resulted in increased yields. Cs_2CO_3 resulted in a similar yield to K_2CO_3, but further attempts to improve these yields through the addition of phase transfer catalysts (to increase transfer between the organic layer and the small aqueous layer of the reaction) only resulted in lower yields despite appearing to produce higher conversions to product. While the bulk of the +1 cations tested resulted in a

similar yield to K_2CO_3, the +2 cations and the hydroxide bases resulted in significantly lower yields (with the exception of NaOH).

Earlier in this optimization study, it had been found (Table 11) that the use of distilled amine resulted in a lower yield than when the amine was not distilled. Since no impurities were observed in the ^1H NMR of the diethyl amine, it was assumed that the additional water that would be present in the non-distilled amine could potentially be improving the reaction rate through increased solubility of K_2CO_3, as well as any resulting salts. Interestingly, the removal of water from the standard reaction conditions when coupling the disubstituted amine resulted in only trace amounts of the desired amide product indicating water was playing an important role in the reaction. This led to an evaluation of what effect alternating the amount of water present in the reaction had on the overall conversion and yield for the monosubstituted amine coupling (Table 16).

Table 16. Effect of Water on the Monosubstituted Amine Coupling

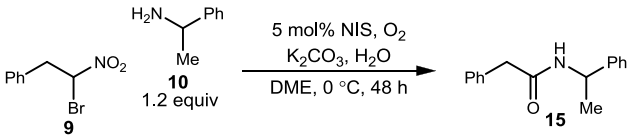

entry	equiv. H_2O	BNA : dinitro : amide	% yield
1	0	0 : 22 : 78	56
2	2	0 : 12 : 88	67
3	5	0 : 13 : 87	67
4	10	0 : 13 : 87	60
5	50	37 : 12 : 51	32
6	200	28 : 12 : 60	39

While completely removing water (to the best of our abilities) from the reaction resulted in a slight drop in yield, 2 to 10 equivalents of water could be added with no variation in yield. An increase to 50 equivalents, or higher, of water resulted in a

significant decrease in yield; this is likely due to the fact that as the amount of water in the reaction increased, two layers were visibly forming in the reaction mixture, resulting in less interaction between the base and any water soluble salts with the organic layer.

The next modification was to evaluate alternatives to water that could potentially help solubilize the K_2CO_3 and improve the homogeneity of the reaction (Table 17). Unfortunately, substitution of an alcohol for water only resulted in a lower yield, indicating it caused decreased solubility of the K_2CO_3.

Table 17. Potential Water Substitutes for the Monosubstituted Amine Coupling

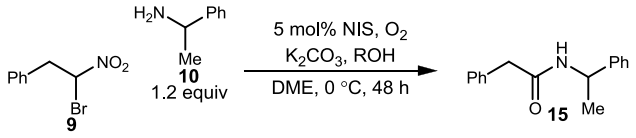

entry	ROH	BNA : dinitro : amide	% yield
1	H_2O	0 : 13 : 87	67
2	MeOH	0 : 28 : 72	57
3	EtOH	4 : 23 : 73	58

Since the reaction mixture was still very heterogeneous, it was hypothesized that decreasing the reaction concentration might increase interactions between the organic phase and small aqueous phase. Unfortunately, changes in the reaction concentration appeared to have no noticeable effect on the reaction yield. Since increasing the homogeneity of the reaction by varying the concentration and amount of water had not worked, it was hypothesized that the use of a more water miscible solvent might have the desired effect. Several solvent systems that are known to be more miscible with water were tested, but only slight decreases in yield were observed (Table 18).

Table 18. Solvent Screen for the Monosubstituted Amine Coupling

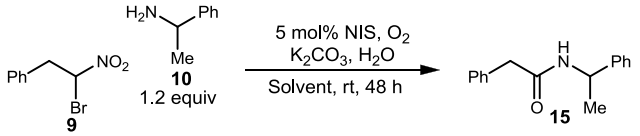

entry	solvent	BNA : dinitro : amide	% yield
1	nitromethane	92 : 0 : 8	–
2	dioxane	6 : 3 : 91	57
3	DME/dioxane	0 : 17 : 83	62

To further investigate the effect of temperature on the coupling, the reaction was both warmed to room temperature after thirty minutes and stirred at room temperature in hopesof a higher rate of conversion (Table 19). Interestingly, the reaction at room temperature resulted in a 10% increase in yield (76%) when compared to the reaction at 0 °C (67%). Gratifyingly, no increase in dinitroalkane formation was observed with the higher temperature. Unfortunately, this same increase in yield was not observed with the disubstituted amine coupling at room temperature. In fact, a significant drop in yield was observed, from 49% to 19%, despite the observed ratio of product to dinitroalkane remaining consistent (100% conversion: 21% dinitroalkane formation). This seemed to indicate that although the α-bromo nitroalkane was being completely consumed, it was not converting to only product and dinitroalkane. This would then result in the ratios between those three components (α-bromo nitroalkane, dinitroalkane, and amide) not accurately reflecting the true amount of product being formed in the reaction. This effect is likely increased for the formation of disubstituted amides due to the disubstituted amine couplings being slower than monosubstituted amine couplings, which would allow the α-bromo nitroalkane more time to undergo alternative mechanistic pathways.

Table 19. Temperature Variations of the Monosubstituted Amine Coupling

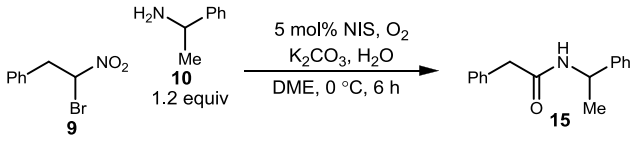

entry	temperature (°C)	BNA : dinitro : amide	% yield
1	0	0 : 13 : 87	67
2[a]	0	0 : 3 : 97	63
3	rt	0 : 6 : 94	76
4[b]	rt	0 : 7 : 93	67

[a] Reaction warmed to rt after 30 minutes, [b] reaction was run for 24 hours.

With the goal in mind being to reach a better understanding of what was actually occurring during the course of the disubstituted amine coupling reaction, the reaction was evaluated over a 48 hour reaction time. Since the conversion ratios were not accurately reflecting the amount of product formed, an individual reaction was set up for each reaction time point, and the product was isolated to achieve an accurate yield (Table 20).

Table 20. Reaction Time Evaluation for Disubstituted Amine Couplings

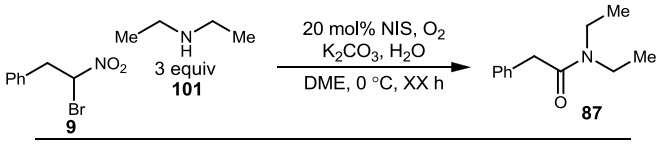

entry	time (h)	BNA : dinitro : amide	% yield
1	1	17 : 14 : 69	36
2	2	4 : 25 : 71	40
3	5	4 : 26 : 69	43
4	14	9 : 14 : 77	43
5	30	2 : 18 : 80	40
6	48	0 : 24 : 76	41

Interestingly, the reaction appeared to reach its optimum yield at 5 hours, revealing that the reaction was occurring much faster than originally thought. The ratio of the α-bromo nitroalkane to product and dinitroalkane also stayed consistent in entries 1-3, proving that the observed ratio is not an accurate depiction of actual product formation.

Entries 4-6 also show a significant trend, as the observed ratio seems to indicate increased product formation, something which is not observed in the isolated yield. This suggests the possibility that both the dinitroalkane and the α-bromo nitroalkane might be undergoing further reactive pathways or decomposition.

The possibility of the α-bromo nitroalkane undergoing some type of alternative mechanistic pathway was investigated by subjecting the α-bromo nitroalkane to the coupling conditions without the amine coupling partner. After 48 hours, no α-bromo nitroalkane remained and the crude ^{1}H NMR appeared very messy with no identifiable products. The amine donor was then added to the same reaction mixture, but no product was observed. This seems to support the theory that the α-bromo nitroalkane is undergoing some type of decomposition or alternative reaction pathway, leading to intermediates that will not convert to the desired amide product. Since these alternative pathways were not easily identifiable, the goal then became to investigate methods for speeding up the desired amide synthesis reaction, rather than preventing the undesired pathways, so that the maximum amount of α-bromo nitroalkane would react before it could be consumed by the alternative pathway.

One possibility for speeding up the desired amide synthesis reaction was to determine whether the reaction was stalling due to one of the necessary reagents becoming unavailable. This was investigated by running a series of disubstituted amine couplings, with each variation having one of the necessary components present in excess (Table 21). In entry 5 it was observed that an increase in the amount of NIS present in the reaction led to a substantial increase in yield (57% up from 43%), which seemed to

indicate that a higher concentration of NIS was necessary to ensure increased amounts of catalytic turnover of iodonium to help speed up the reaction.

Table 21. Excess Reagent Screen for Disubstituted Amine Couplings

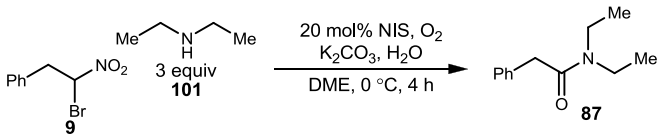

entry	excess reagent[a]	BNA : dinitro : amide	% yield
1	None	4 : 26 : 69	43
2	K_2CO_3 (4 eq)	15 : 12 : 73	36
3	Amine (6 eq)	3 : 17 : 80	37
4	NIS (20 mol%)	6 : 13 : 81	30
5	NIS (40 mol%)	0 : 0 : 100	57

[a] Half the excess reagent was added at the beginning. The second half was added after 1 hour.

The hypothesis that a greater concentration of NIS was necessary to speed up the desired reaction pathway was further tested by evaluating the disubstituted amine coupling reaction at various concentrations of NIS (Table 22). As the amount of NIS was increased over the same time scale, an obvious increase in yield was observed. This is clear evidence that while the catalytic disubstituted amine coupling may currently be too slow to overcome potential degradation pathways of the α-bromo nitroalkane, the stoichiometric disubstituted amine coupling yield can be increased to 61% under an oxygen atmosphere. Interestingly, it was also observed that when the reaction was allowed to run for 48 hours, as opposed to a shorter reaction time, a clear decrease in yield was observed. This could be indicative that the amide product is susceptible to degradation or alternative mechanistic pathways when it remains under the reaction conditions for an extended time.

Table 22. Variations in NIS Equivalents for Disubstituted Amine Couplings

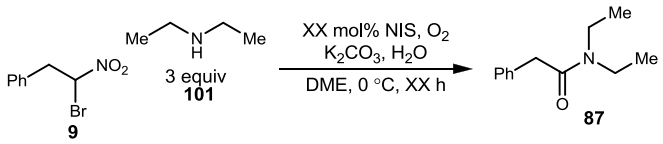

entry	time (h)	mol% NIS	% yield
1	2	5	13
2	2	40	51
3	2	100	51
4	4	40	56
5	4	100	61
6	48	5	40
7	48	40	42
8	48	100	47

Although a halogenating agent screen has been done on the monosubstituted amine coupling, the best performing halogenating agents were tried on the disubstituted amine coupling, in order to see if the same trend would be observed (Table 23). Unfortunately, all alternative halogenating agents proved greatly inferior to NIS for disubstituted amine couplings, even iodine which had performed well in the previous halogenating agent screen.

Table 23. Halogenating Agent Screen for the Disubstituted Amine Couplings

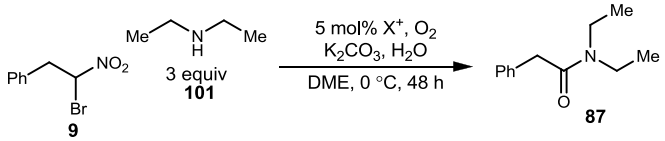

entry	X^+	% yield
1	NIS	39
2	I_2	21
3	NBP	<20
4	$Ca(ClO)_2$	<20

Other attempts to speed up the catalytic disubstituted amide bond formation

include saturating the reaction solution with oxygen and preforming the NIS-amine complex prior to addition, both of which resulted in no improvement in yield. Attempts to stop the possible radical degradation pathway the α-bromo nitroalkane was undergoing, by adding small amounts of radical inhibitor to the reaction, resulted in complete shutdown of the desired and undesired reaction pathways and complete conservation of α-bromo nitroalkane.

2.3.3 Coupling Examples Featuring N-Me Amino Esters

The synthesis of disubstituted amides is an important organic transformation due to the increasing number of biologically active *N*-alkylated peptidic natural products. These natural products are also proving to have increased biological activity and metabolic stability when compared to their non-*N*-alkylated counterparts. Currently, the majority of current methods for synthesizing disubstituted amides go through an activated carboxylic acid intermediate, leading to the potential for epimerization, whereas our novel amide bond formation chemistry eliminates that possibility. However, attempts to apply umpolung amide synthesis to the formation of *N*-methyl peptides have met with some resistance. Initial reactions focused on the coupling of *N*-methyl phenylalanine methyl ester and *N*-methyl alanine methyl ester to an arylglycine bromo nitroalkane donor. The syntheses of these amino ester derivatives are shown in Scheme 31.

Scheme 31. Synthesis of *N*-Methyl Amino Ester Derivatives

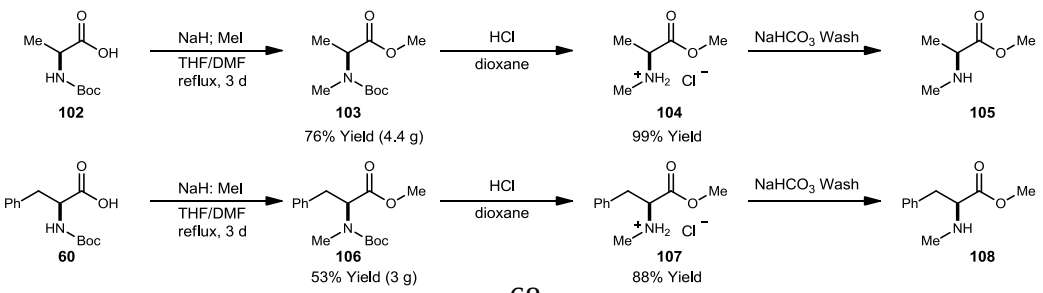

Initial attempts focused on the coupling of the *N*-methyl phenylalanine methyl ester salt and the arylglycine bromo nitroalkane donor. However, the reaction mixture appeared complicated by ^{1}H NMR and proved difficult to purify. Furthermore, large amounts of the starting arylglycine bromo nitroalkane were isolated from the reaction mixture indicating a potential low conversion to product. Hypothesizing that the low conversion might be due to the large excess of K_2CO_3 required due to the use of the amino ester salt, the coupling was next attempted using the free base amino ester. While reaction stirring was much improved, the crude ^{1}H NMR remained messy and only slight amounts of potential product were seen (Scheme 32).

Scheme 32. UmAS Couplings Featuring *N*-Methyl Phenylalanine Methyl Ester

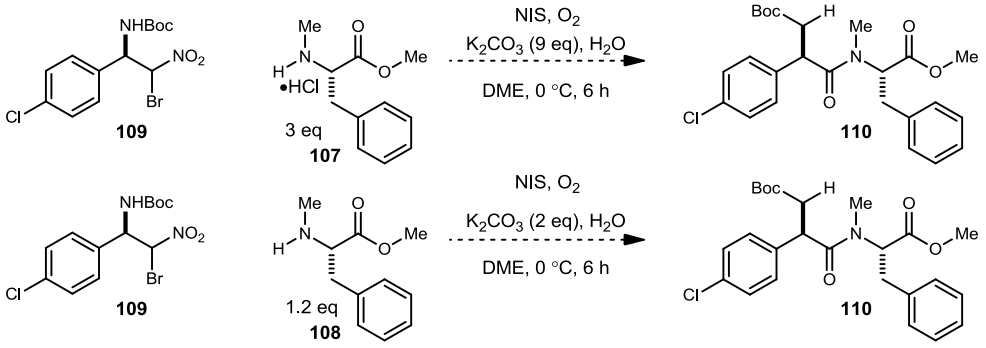

Even more surprisingly, it was revealed upon careful purification that the desired amide product was not formed. Instead, the isolated products proved to be the starting bromo nitroalkane and an altered form of the *N*-methyl phenylalanine methyl ester (Scheme 33).

Scheme 33. Purification Results for the *N*-Methyl Phenylalanine Methyl Ester

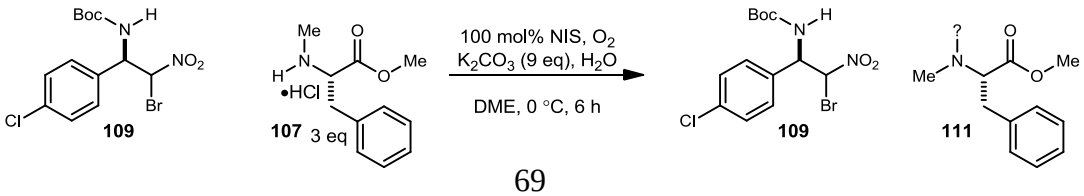

As shown in Figure 19, the ^{1}H NMR of the isolated altered *N*-methylphenylalanine methyl ester appears similar to the starting ^{1}H NMR of phenylalanine methyl ester with two noticeable exceptions: 1) two rotamers are now visible in the spectrum and 2) the majority of protons have shifted downfield with the most noticeable shift belonging to the α-proton.

Figure 19. NMR Comparison of *N*-Methylphenylalanine Methyl Ester to its Altered Derivative

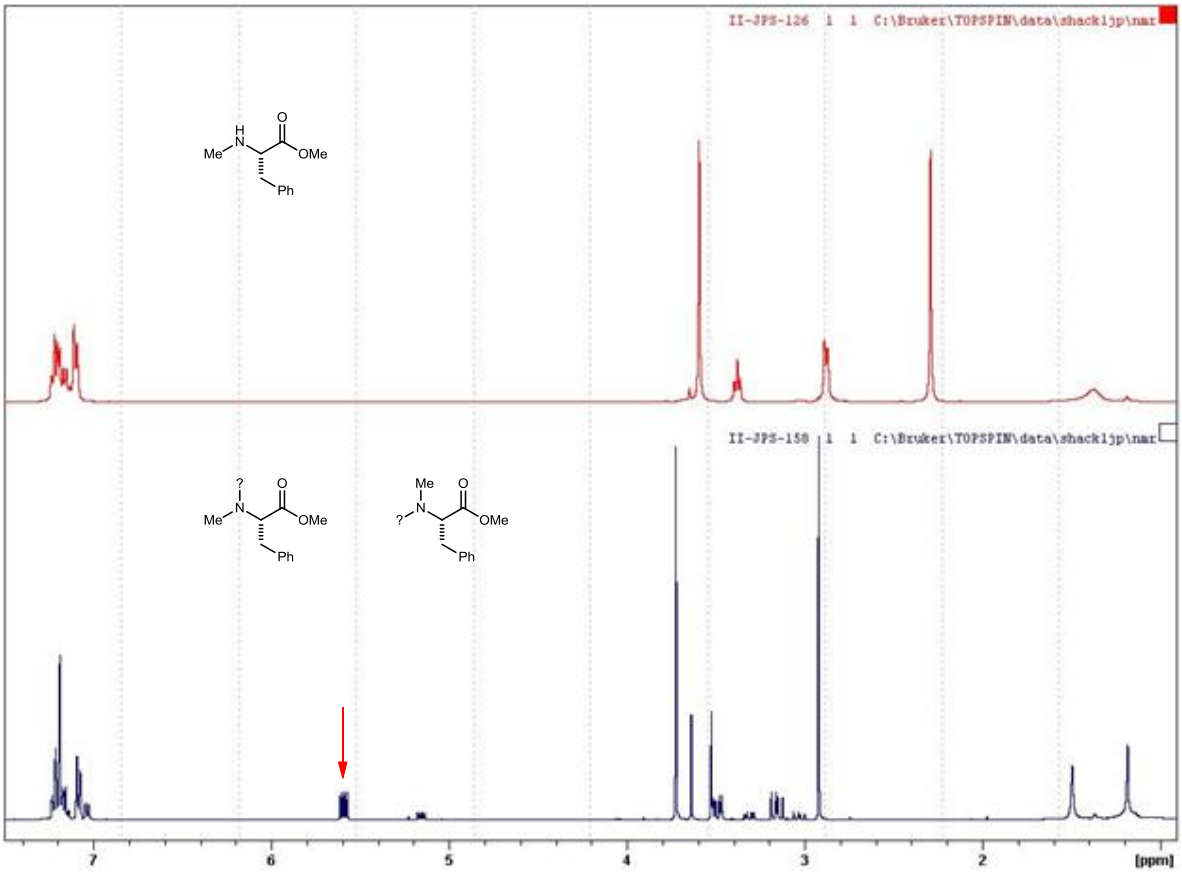

Since the most noticeable shifts appear to be the N-Me peak and the α-proton, it is likely that the nitrogen atom now bears an additional substituent that contains no carbons or protons and is causing the downfield shift. This hypothesis is further supported by the presence of no –NH stretches in the IR and the presence of two rotamers in the ^{1}H NMR.

Based on this evidence, it was hypothesized that the isolated *N*-methylphenylalanine methyl ester derivative was actually the iodinated form of the *N*-methylphenylalanine methyl ester. However, this product could not be confirmed by mass spectrometry analysis.

Once it was established that the desired amide product was not forming when coupling *N*-methyl phenylalanine methyl ester, our focus shifted toward the coupling of the *N*-methyl alanine methyl ester. Since the free base form of the *N*-methyl alanine methyl ester proved quite volatile, all coupling attempts used the amino ester salt. Gratifyingly, this resulted in the isolation of pure *N*-methyl alanine methyl ester amide in 33% yield (Scheme 34). Increasing the amount of H_2O to 15 equivalents instead of 5 equivalents to help solubilize the additional K_2CO_3 resulted in a substantial loss in yield (13%). This is likely due to the excess water allowing the mixture to become too biphasic. Increasing the reaction time to 3 days instead of 6 hours also resulted in no improvement in the yield (34%).

Scheme 34. Formation of the *N*-Methyl Alanine Methyl Ester Amide

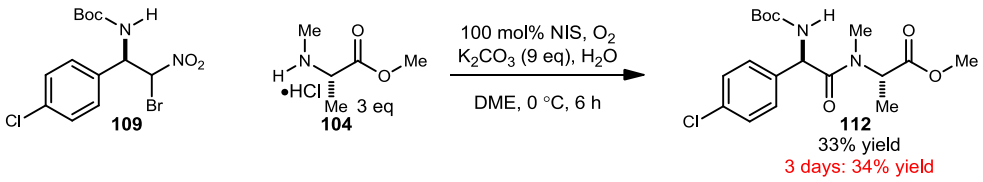

Further optimization of this coupling was attempted by increasing the equivalents of amine salt and K_2CO_3. An increase to 4 equivalents of amine salt and 9 equivalents of K_2CO_3 was tried over reaction times ranging from 6 to 48 hours (Table 24, entries 1-3). The best yield for this coupling was consistently obtained using 4 equivalents of amine salt, 9 equivalents of K_2CO_3, and a 21 hour reaction time (41%, averaged over 2 runs).

Table 24. Optimization of *N*-Methylalanine Methyl Ester Coupling

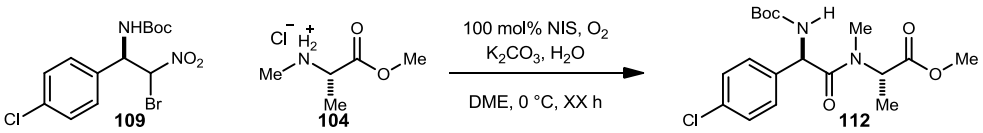

entry	eq amine	eq K_2CO_3	rxn time	yield (%)
1	4	9	6 h	25
2	4	9	21 h	41
3	4	9	48 h	25
4	6	12	6 h	23
5	6	12	18 h	25
6	6	18	18 h	9

Unfortunately, further increasing the equivalents of the amine salt and K_2CO_3 to 6 and 12 equivalents respectively resulted in a loss in yield (Table 24, entries 4 and 5). Increasing the amount of K_2CO_3 to 18 equivalents in the hope that it would increase the amount of the amine salt being deprotonated resulted in a significant loss in yield due to the reaction mixture becoming too heterogeneous (Table 24, entry 6).

Considering that amide product could be obtained from the *N*-methyl alanine methyl ester coupling and not from the *N*-methyl phenylalanine methyl coupling, it was hypothesized that the side chain of the *N*-methyl amino methyl esters was significantly affecting the yield of the reaction. This was a likely possibility as the reaction mechanism is dependent on the ability of the nitronate to perform a substitution on a disubstituted nitrogen atom (Scheme 35). Since that would be a difficult substitution to begin with, it would be unsurprising that as the substituents on the nitrogen atom become more bulky the yield of the reaction would lower.

Scheme 35. Potential Intermediates in Disubstituted UmAS

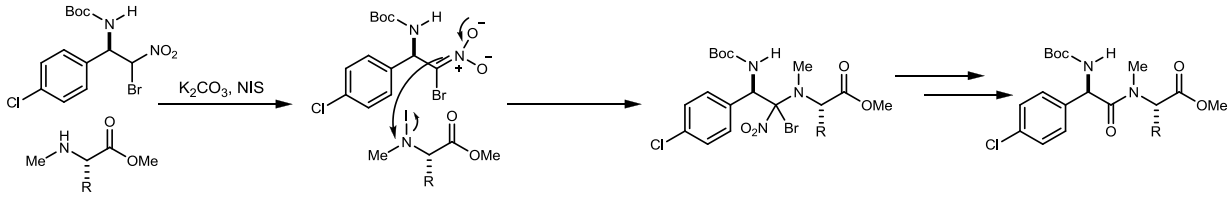

This hypothesis was tested through the use of *N*-methyl glycine methyl ester in the coupling to allow for the complete elimination of the side chain. *N*-methyl glycine methyl ester was synthesized as shown in Scheme 36. The stoichiometric coupling of the

Scheme 36. Synthesis of *N*-Methyl Glycine Methyl Ester

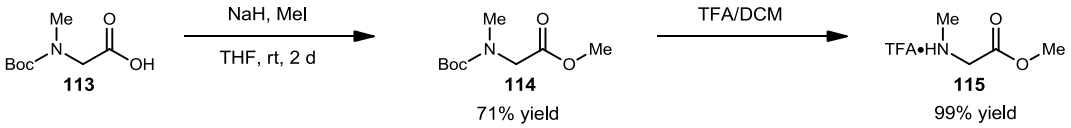

p-ClAryl bromo nitroalkane and *N*-methyl glycine methyl ester resulted in a 56% yield under oxygen (Scheme 37). Attempts to further optimize this reaction through increased reaction times or increased equivalents of amine salt resulted in a loss in yield. Since the amine salt proved highly hygroscopic, the coupling was attempted with H_2O as the solvent in the hopes that once the nitronate was generated it would prove soluble in H_2O. Unfortunately, this resulted in no product formation and the isolation of the starting bromo nitroalkane.

Scheme 37. Formation of the *N*-Methyl Glycine Methyl Ester Amide

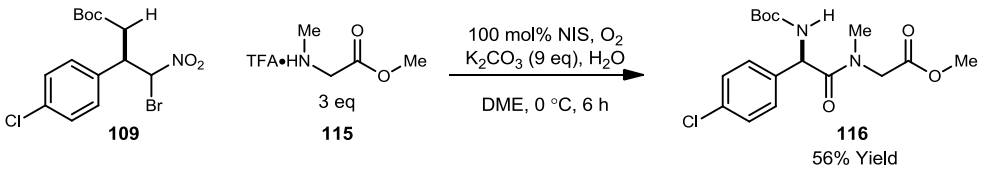

Overall, a clear trend can be observed that as the side chain of the *N*-methyl amino ester increases in bulk, the yield of UmAS decreases significantly to the point where the desired amide product can no longer be formed (Table 25). Even in the cases shown where product can be formed, the yield is moderate to low even when stoichiometric amounts of NIS are employed. This seems to indicate that *N*-methyl amino esters are not currently ideal candidates for UmAS under catalytic conditions. Unfortunately, attempts to form the desired *N*-methyl amino ester amides under standard UmAS stoichiometric conditions resulted in even lower yields than those seen under catalytic conditions.

Table 25. The Effect of the Side Chain on Coupling *N*-Methylamino Esters

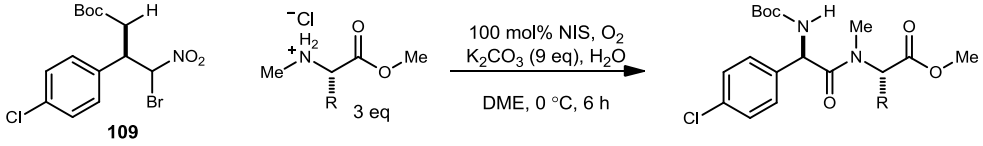

entry	**R**	yield (%)
1	-H	56
2	-Me	33
3	-CH_2Ph	0

Chapter 3

Experimental

All reagents and solvents were commercial grade and purified prior to use when necessary. Tetrahydrofuran (THF) was dried by passage through a column of activated alumina as described by Grubbs.[51] This was done to accurately quantitate the amount of water in each reaction. NIS was recrystallized from dioxane/CCl_4.

Thin layer chromatography (TLC) was performed using glass-backed silica gel (250 μm) plates, and flash chromatography utilized 230-400 mesh silica gel from Scientific Adsorbents. Products were visualized by UV light, iodine, and/or the use of ninhydrin solution.

IR spectra were recorded on a Thermo Nicolet IR100 spectrophotometer and are reported in wavenumbers (cm^{-1}). Compounds were analyzed as neat films on a NaCl plate (transmission). Nuclear magnetic resonance spectra (NMR) were acquired on a Bruker DRX-400 (400 MHz) or a Bruker AVIII-600 (600 MHz) spectrometer. Chemical shifts are measured relative to residual solvent peaks as an internal standard set to 7.26 and 77.1 for $CDCl_3$. Mass spectra were recorded on a Thermo Electron Corporation MAT 95XP-Trap mass spectrometer by use of chemical ionization (CI), electron impact ionization (EI) or electrospray ionization (ESI) by the Indiana University Mass Spectrometry Facility, or on a Synapt hybrid quadrupole/oa-TOF mass spectrometer equipped with a

[51]Pangborn, A. B.; Giardello, M. A.; Grubbs, R. H.; Rosen, R. K.; Timmers, F. J. *Organometallics* **1996**, *15*, 1518-1520.

dual chemical ionization/electrospray (ESCI) source by Vanderbilt University Mass Spectrometry Facility. A post-acquisition gain correction was applied using sodium formate or sodium iodide as the lock mass.

^{18}O Percentage Mass Spectrometry Calculation

Contributions to the [M+2] mass peak include M(^{18}O)and the natural abundance of M($^{13}C_2$) and 2(^{15}N). Their contribution is removed from the final ^{18}O percentage by the following calculation:

(^{16}O ion intensity)x(predicted ^{18}O ion natural abundance in the unlabeled compound)/100 = ^{18}O ion intensity expected in the unlabeled compound

(^{18}O ion intensity)– (^{18}O ion intensity expected in the unlabeled compound) = corrected ^{18}O ion intensity

(Corrected ^{18}O ion intensity) / (Corrected ^{18}O ion intensity + ^{16}O ion intensity)x100 = XX% ^{18}O

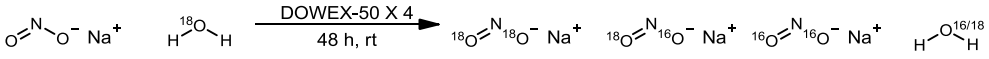

Preparation of $^{18}O_2$-Labeled Sodium Nitrite (30)

Following the procedure developed by Yang and Goldberg,[17] a round-bottomed flask was charged with $H_2{}^{18}O$ (0.5 mL, 27.8 mmol) via syringe and cooled to 0 °C. Sodium nitrite (109 mg, 1.58 mmol) and dry, activated Dowex-50X4 (30 mg) were added, and the flask was sealed with a glass stopper and parafilm. The reaction mixture was allowed to stir at room temperature for 48 h, using pH paper to confirm reaction completion (pH less than

4). The reaction mixture was filtered to remove Dowex-50X4 and brought to pH 11.8 with NaOH powder. H_2O was removed via short path distillation under reduced pressure to give $^{18}O_2$-labeled sodium nitrite as a solid (79.5 mg, 69%). The ^{18}O enrichment in $NaN^{18}O_2$ was not determined.

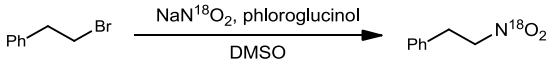

^{18}O-(2-Nitroethyl)benzene (^{18}O-Labeled 32)

$NaN^{18}O_2$ (110 mg, 1.51 mmol) was added to a solution of the bromide (155 mg, 837 µmol) in DMSO (2.8 ml, 0.3 M), followed by phloroglucinol (116 mg, 921 µmol). The mixture was stirred at room temperature for 2 d. The resulting solution was poured into ice water and extracted with Et_2O. The organic layer was dried, filtered, and concentrated. The residue was purified by flash column chromatography on silica gel (5% ethyl acetate in hexanes) to give the nitroalkane as a colorless oil (82.7mg, 64%).R_f= 0.40 (20% EtOAc/hexanes); IR (neat) 3065, 3032, 2920, 1527, 1340 cm^{-1}; ^{1}H NMR (400 MHz, $CDCl_3$)δ 7.35-7.31 (m, 2H), 7.30-7.27 (m, 1H), 7.22-7.20 (m, 2H), 4.62 (t, *J* = 7.6 Hz, 2H), 3.33 (t, *J* = 7.6 Hz, 2H); ^{13}C NMR (100 MHz, $CDCl_3$) ppm 135.7, 128.9, 128.6, 127.4, 76.2, 33.4; HRMS (CI): Exact mass calcd for $C_8H_{13}N_2{}^{16}O_2[M+NH_4]^+$169.0976, found 169.0964:3.1%; $C_8H_{13}N_2{}^{16}O^{18}O[M+NH_4]^+$171.1014, found 171.1017:26.9%; $C_8H_{13}N_2{}^{18}O_2[M+NH_4]^+$173.1056, found 173.1051:70.1%. Overall 83.6% ^{18}O incorporation (=1/2(26.9)+70.1).

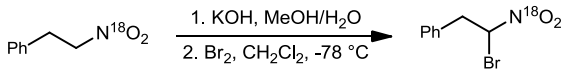

^{18}O-(2-Bromo-2-nitroethyl)benzene (^{18}O-Labeled 9)

The nitroalkane (78.8 mg, 508µmol) was added to a solution of KOH (28.5 mg, 508 µmol) in 25% MeOH:H_2O (1.2 mL) and allowed to stir until the nitroalkane completely dissolved. The reaction was cooled to -22 °C and transferred to a separatory funnel. A solution of bromine (81.1 mg, 508 µmol) in DCM (2.5 mL) was cooled to -78 °C and quickly added to the separatory funnel, which was shaken vigorously until the orange color disappeared. The reaction mixture was extracted with DCM, dried over $MgSO_4$, filtered, and concentrated.[26] The residue was purified via flash column chromatography (2-3% ethyl acetate in hexanes) to afford the α-bromo nitroalkane as a colorless oil (95.0mg, 80%). IR (neat) 3066, 3032, 2927, 1538, 1323 cm^{-1}; ^{1}H NMR (400 MHz, $CDCl_3$) δ 7.37-7.32 (m, 3H), 7.22-7.19 (m, 2H), 6.04 (dd, *J* = 8.2, 6.1 Hz, 1H), 3.76 (dd, *J* = 14.6, 8.2 Hz, 1H), 3.51 (dd, *J* = 14.6, 6.1 Hz, 1H); ^{13}C NMR (100 MHz, $CDCl_3$) ppm 133.3, 129.2, 129.1, 128.4, 79.2, 43.5; HRMS (CI): Exact mass calcd for $C_8H_{12}BrN_2{}^{16}O_2[M+NH_4]^+$247.0322, 3.3%; $C_8H_{12}BrN_2{}^{16}O^{18}O[M+NH_4]^+$249.0195, 29.1%; $C_8H_{12}BrN_2{}^{18}O_2[M+NH_4]^+$251.0220, 67.7%. Overall 82.2% ^{18}O incorporation (=1/2(29.1)+67.7).[52]

[52]Only the nominal masses match with the calculated values. The NH_3 data are good for the relatives ratios. They are not internally calibrated since NH_3 gas will not ionize perfluorokerosene. CH_4 is too aggressive to make a stable M^+ ion for nitro compounds. HNO_2 comes off as a neutral loss easily.

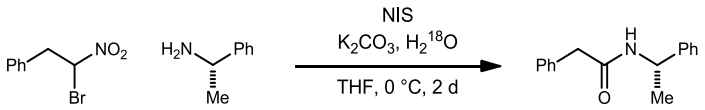

Amide 15 Prepared Using >99% $H_2{}^{18}O$

A 15 mL round-bottom was charged with a solution of α-bromo nitroalkane (30.8 mg, 134 µmol) dissolved in THF (0.67 mL). (*S*)-α-Methylbenzylamine (20.7 µL, 161 µmol) was added via microsyringe, and the reaction was cooled to 0°C. Solid potassium carbonate (37.0 mg, 267 µmol) and NIS (30.1 mg, 134 µmol) were added, followed by $H_2{}^{18}O$ (13.4 µL, 669 µmol). The reaction mixture was allowed to stir for 48 h at 0°C.Anhydrous $MgSO_4$ was added, and the reaction mixture was diluted with dichloromethane, filtered, and concentrated. The residue was purified via flash column chromatography (20% ethyl acetate in hexanes) to afford the amide as a yellow solid (24.5 mg, 76%). R_f=0.35 (40% EtOAc/hexanes); spectroscopic data (IR, ^{1}H NMR and ^{13}C NMR) was in complete accord with that previously reported.[53] HRMS (ES): Exact mass calcd for $C_{16}H_{18}NO[M+H]^+$ 240.1388, found 240.1389. The labeled product was not observed by mass spectrometry, indicating <1% ^{18}O incorporation.

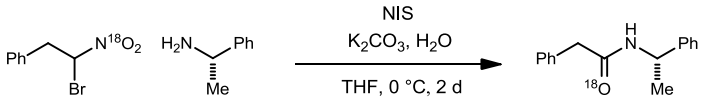

Amide 15 Prepared Using 82% ^{18}O-Labeled α-bromo nitroalkane

A 15 mL round bottom was charged with a solution of ^{18}O-labeled α-bromo nitroalkane (20.0 mg, 85 µmol) dissolved in THF (430 µL). (*S*)-α-Methylbenzylamine (13.2 µL, 103 µmol) was added via microsyringe, and the reaction was cooled to 0°C. Solid potassium carbonate (23.6 mg, 171 µmol) and NIS (19.2 mg, 85 µmol) were added, followed by

[53]Nordstrøm, L. U.; Vogt, H.; Madsen, R. *J. Am. Chem. Soc.* **2008**, *130*, 17672-17673.

distilled H_2O (7.7 µL, 427 µmol). The reaction mixture was allowed to stir for 48 h at 0°C.Anhydrous $MgSO_4$ was added, and the reaction mixture was diluted with dichloromethane, filtered, and concentrated. The residue was purified via flash column chromatography (20% ethyl acetate in hexanes) to afford the amide as a yellow solid (15.8 mg, 76%). R_f=0.35 (40% EtOAc/hexanes); spectroscopic data (IR, ^{1}H NMR and ^{13}C NMR) was in complete accord with that previously reported for ^{16}O-amide,[53] but two IR carbonyl peaks are present at 1644 and 1629 cm^{-1}. The ^{13}C NMR also showed the presence of ^{16}O and ^{18}O carbonyl peaks with the ^{18}O peak shifted upfield approximately 0.03 ppm. Integration of these two peaks indicated around a 22% ^{18}O incorporation. HRMS (CI): Exact mass calcd for $C_{16}H_{18}NO[M+H]^+$240.1383 and $C_{16}H_{18}N^{18}O[M+H]^+$242.1425, found 240.1605 and 242.1664. The relative intensities of these two peaks and their natural abundances were used to determine a 17% ^{18}O incorporation.

^{18}O Percentage Mass Spectrometry Calculation:

(834168 X 1.62) / 100 = 13514

179346 − 13514 = 165832

(165832/(165832 + 834168)) X 100 = 17% ^{18}O

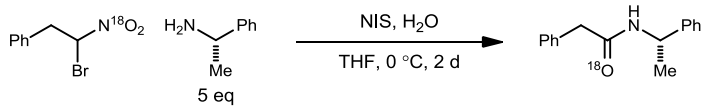

Amide 15 Prepared Using ^{18}O-Labeled α-bromo nitroalkane and Excess Amine

A 15 mL round bottomed flask was charged with a solution of ^{18}O-labeled α-bromo nitroalkane (20 mg, 85 µmol) dissolved in THF (430 µL). (*S*)-α-Methylbenzylamine (55 µL, 427 µmol) was added via microsyringe, and the reaction was cooled to 0°C.NIS (19.2 mg, 85 µmol) was added, followed by distilled H_2O (7.7 µL, 427 µmol). The reaction mixture was allowed to stir for 48 h at 0°C. Anhydrous $MgSO_4$ was added, and the reaction mixture was diluted with dichloromethane, filtered, and concentrated. The residue was purified via flash column chromatography (20% ethyl acetate in hexanes) to afford the amide as a yellow solid (14.2 mg, 70%). R_f=0.35 (40% EtOAc/hexanes); spectroscopic data (IR, ^{1}H NMR and ^{13}C NMR) was in complete accord with that previously reported,[53] but two IR carbonyl peaks are present at 1648 and 1627 cm^{-1}. The ^{13}C NMR also showed the presence of ^{16}O and ^{18}O carbonyl peaks with the ^{18}O peak shifted upfield approximately 0.03 ppm. Integration of these two peaks indicated a 49% ^{18}O incorporation. HRMS (CI): Exact mass calcd for $C_{16}H_{18}NO$ $[M+H]^+$ 240.1383 and $C_{16}H_{18}N^{18}O$ $[M+H]^+$ 242.1425, found 240.1592 and 242.1637. The relative intensities of these two peaks and their natural abundances were used to determine a 49% ^{18}O incorporation.

^{18}O Percentage Mass Spectrometry Calculation:

(510360 X 1.62) / 100 = 8268

497908 − 8268 = 489640

(489640/ (489640 + 510360)) X 100 = 49% ^{18}O

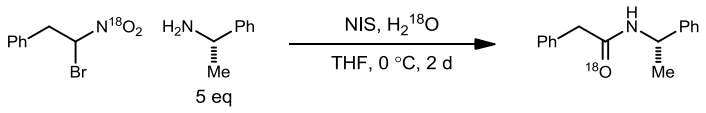

Amide 15 Prepared Using ^{18}O-Labeled α-bromo nitroalkane/$H_2{}^{18}O$ and Excess Amine

A 15 mL round bottom was charged with a solution of ^{18}O-labeled α-bromo nitroalkane (20 mg, 85 µmol) dissolved in THF (430 µL). (*S*)-α-Methylbenzylamine (55 µL, 427 µmol) was added via microsyringe, and the reaction was cooled to 0°C. NIS (19.2 mg, 85 µmol) was added, followed by $H_2{}^{18}O$ (7.7 µL, 427 µmol). The reaction mixture was allowed to stir for 48 h at 0°C.Anhydrous $MgSO_4$ was added, and the reaction mixture was diluted with dichloromethane, filtered, and concentrated. The residue was purified via flash column chromatography (20% ethyl acetate in hexanes) to afford the amide as a yellow solid (14.2 mg, 70%). R_f=0.35 (40% EtOAc/hexanes); spectroscopic data (IR, ^1H NMR and ^{13}C NMR) was in complete accord with that previously reported,[53] but two IR carbonyl peaks are present at 1649 and 1629 cm^{-1}. The ^{13}C NMR also showed the presence of ^{16}O and ^{18}O carbonyl peaks with the ^{18}O peak shifted upfield approximately 0.03 of these two peaks indicated around a 46% ^{18}O incorporation. HRMS (CI): Exact mass calcd for $C_{16}H_{18}NO$ $[M+H]^+$ 240.1383 and $C_{16}H_{18}N^{18}O$ $[M+H]^+$ 242.1425, found 240.1592 and 242.1637. The relative intensities of these two peaks and their natural abundances were used to determine a 49% ^{18}O incorporation.

^{18}O Percentage Mass Spectrometry Calculation:

(510334 X 1.62) / 100 = 8267

497933 − 8267 = 489666

(489666/ (489666 + 510334)) X 100 = 49% ^{18}O

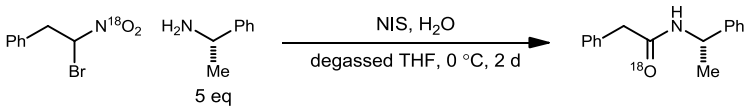

Amide 15 Prepared Using^{18}O-Labeled α-bromo nitroalkane, Excess Amine, and Degassed Solvent

A 15 mL round bottom was charged with a solution of ^{18}O-labeled α-bromo nitroalkane (9 mg, 39 μmol) dissolved in degassed THF (190 μL). (*S*)-α-Methylbenzylamine (24.8 μL, 192 μmol) was added via microsyringe, and the reaction was cooled to 0°C.NIS (8.7 mg, 39 μmol) was added, followed by distilled H_2O (3.5 μL, 192 μmol). The reaction mixture was allowed to stir under argon for 48 h at 0°C.Anhydrous $MgSO_4$ was added, and the reaction mixture was diluted with dichloromethane, filtered, and concentrated. The residue was purified via flash column chromatography (20% ethyl acetate in hexanes) to afford the amide as a yellow solid (6.5mg, 70%). R_f=0.35 (40% EtOAc/hexanes); spectroscopic data (IR, ^1H NMR and ^{13}C NMR) was in complete accord with that previously reported,[53] but two IR carbonyl peaks are present at 1654 and 1629 cm^{-1}. The ^{13}C NMR also showed the presence of ^{16}O and ^{18}O carbonyl peaks with the ^{18}O peak shifted upfield approximately 0.03 ppm. Integration of these two peaks indicated around a 58% ^{18}O incorporation. HRMS (EI): Exact mass calcd for $C_{16}H_{17}NO$ $[M]^+$ 239.1310 and $C_{16}H_{17}N^{18}O$ $[M]^+$ 241.1353, found 239.1287 and 241.1328. The relative intensities of these two peaks and their natural abundances were used to determine a 66% ^{18}O incorporation.

^{18}O Percentage Mass Spectrometry Calculation:

(10660544 X 1.62) / 100 = 172701

20970944 − 172701 = 20798243

(20798243/ (20798243 + 10660544)) X 100 = 66% ^{18}O

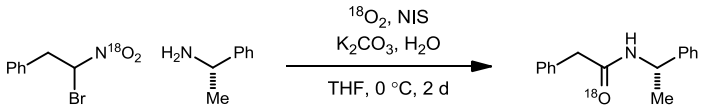

Amide 15 Prepared Using Degassing and $^{18}O_2$ Gas

The α-bromo nitroalkane (28.5 mg, 124 µmol) and amine (19 µl, 149 µmol) were added to a 10 mL round-bottomed flask (flask A) and sealed with a septum wrapped with parafilm. K_2CO_3 (34.3 mg, 124 µmol), NIS (27.9 mg, 124 µmol), and H_2O (11.2 µl, 620 µmol) were added to a second 10 mL round-bottomed flask (flask B) in a solution of THF (620 µL), which was subsequently sealed with a septum and wrapped with parafilm. Both flasks were degassed using three 80 minute freeze-pump-thaw cycles. A balloon (that had been evacuated and purged 3 times with nitrogen) was added to flask B, and $^{18}O_2$ gas was added directly to flask B through the septum until the balloon was fully inflated. The contents of flask A were transferred to flask B via dry microsyringe in one portion. The reaction was allowed to stir at 0 °C for 16 h. Anhydrous $MgSO_4$ was added, and the reaction mixture was diluted with dichloromethane, filtered, and concentrated. The residue was purified via flash column chromatography (20% ethyl acetate in hexanes) to afford the amide as a yellow solid (20.1 mg, 68%). R_f=0.35 (40% EtOAc/hexanes); spectroscopic data (IR, ^{1}H NMR and ^{13}C NMR) was in complete accord with that previously reported,[53] but two IR carbonyl peaks are present at 1654 and 1624

cm^{-1}. The ^{13}C NMR also showed the presence of ^{16}O and ^{18}O carbonyl peaks with the ^{18}O peak shifted upfield approximately 0.03 of these two peaks indicated around a 79% ^{18}O incorporation. LRMS (EI): Exact mass calcd for $C_{16}H_{17}NO[M]^+$ 239.1305 and $C_{16}H_{17}N^{18}O[M]^+$ 241.1347, found 239.20 and 241.20. The relative intensities of these two peaks and their natural abundances were used to determine a 83% ^{18}O incorporation.

^{18}O Percentage Mass Spectrometry Calculation:

(180492 X 1.62) / 100 = 2924

904618 − 2924 = 901694

(901694/ (901694 + 180492)) X 100 = 83% ^{18}O

General Procedure A: Amide Synthesis Using an Ammonium Salt

K_2CO_3 (3.2 equiv) was added to the suspension of the ammonium salt (1.2 equiv) and the α-bromo nitroalkane (1.0 equiv, 0.2 M) in THF and H_2O (5.0 equiv) at 0 °C, followed by NIS (1.0 equiv). The reaction mixture was stirred at 0 °C for 2 d. The resulting mixture was diluted with dichloromethane and filtered to remove K_2CO_3. The filtrate was concentrated and subjected to purification by flash column chromatography on silica gel.

General Procedure B: Optimized Amide ^{18}O-Labeling using a 1 mL-Dram Vial

The α-bromo nitroalkane (1 equiv) and amine (1.2 equiv) were added to a 1 mL glass screw cap vial (vial A), followed by addition of H_2O (5 equiv) and K_2CO_3 (2.0 equiv with free amines and 3.2 equiv with ammonium salts). THF (200 μL) was added to the vial, which was subsequently sealed with the screw cap (containing a silicone septum) and parafilmed. NIS (1 equiv) in THF (200 μL) was added to a second 1 mL glass screw cap vial (vial B) and sealed with the silicone septum screw cap and parafilmed. Both flasks

were degassed using three 80 minute freeze-pump-thaw cycles. Once degassing was complete, vial A was refrozen in liquid nitrogen. The NIS solution in vial B was transferred to vial A via dry micro-syringe in one portion. Once the transferred solution had frozen, the $^{18}O_2$ regulator needle was inserted through the septum, and the entire system was placed under high vacuum (0.05 Torr). The vacuum was turned off, and the $^{18}O_2$ gas regulator was opened to allow its entry to the system under static vacuum, and until the regulator pressure gauge remained steady. The reaction was warmed to 0 °C and allowed to stir overnight. If the pressure gauge needle dropped while the reaction was warming, additional $^{18}O_2$ gas was added to allow the needle to return to its previously stable state. Following a 16 to 44 h reaction time, anhydrous $MgSO_4$ was added. The reaction mixture was diluted with dichloromethane, filtered, and concentrated. The residue was purified via flash column chromatography.

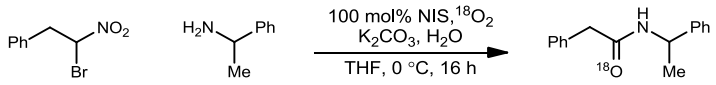

^{18}O-Labeled 2-Phenyl-*N*-(1-phenylethyl)acetamide (^{18}O-Labeled 15)

Following General Procedure B, the α-bromo nitroalkane (26.1 mg, 113 μmol) and amine (17.3 μl, 136 μmol) provided the amide after flash column chromatography (20% ethyl acetate in hexanes) as a white solid (21.7 mg, 79%). R_f=0.35 (40% EtOAc/hexanes); spectroscopic data (IR, ^{1}H NMR and ^{13}C NMR) was in complete accord with that previously reported,[53] but a shift in the IR carbonyl peak from 1645to 1624 cm^{-1} was observed. The ^{13}C NMR also showed the presence of ^{16}O and ^{18}O carbonyl peak with the ^{18}O peak shifted upfield approximately 0.03 of these two peaks indicated around a 71% ^{18}O incorporation. LRMS (EI): Exact mass calcd for $C_{16}H_{17}NO[M]^+$ 239.13 and

$C_{16}H_{17}N^{18}O[M]^+$ 241.13, found 239.20 and 241.20. The relative intensities of these two peaks and their natural abundances were used to determine a 79% ^{18}Oincorporation.

^{18}O Percentage Mass Spectrometry Calculation:

(489962 X 1.62) / 100 = 7937

1807239 − 7937 = 1799302

(1799302/ (1799302 + 489962)) X 100 = 79% ^{18}O

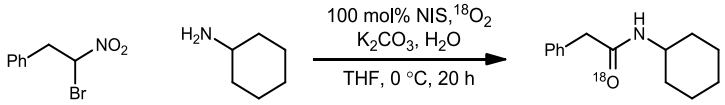

^{18}O-Labeled *N*-Cyclohexyl-2-phenylacetamide (^{18}O-Labeled 39)

Following General Procedure B, the α-bromo nitroalkane (30.1 mg, 131 μmol) and amine (18 μl, 157 μmol) provided the amide after flash column chromatography (20% ethyl acetate in hexanes) as a white solid (22.5 mg, 78%). R_f= 0.11 (20% EtOAc/hexanes); spectroscopic data (^1H NMR) was in complete accord with that previously reported.[54] A shift in the IR carbonyl peak from 1638 cm^{-1} to 1620 cm^{-1} was observed. The ^{13}C NMR also showed the presence of ^{16}O and ^{18}O carbonyl peaks with the ^{18}O peak shifted upfield approximately 0.03 of these two peaks indicated approximately 72% ^{18}O incorporation. LRMS (EI): Exact mass calcd for $C_{16}H_{18}NO[M]^+$ 217.15 and $C_{16}H_{18}N^{18}O[M]^+$ 219.15, found 217.20 and 219.20. The relative intensities of these two peaks and their natural abundances were used to determine a 79% ^{18}O incorporation.

[54]Chan, W. K.; Ho, C. M.; Wong, M. K.; Che, C. M. *J. Am. Chem. Soc.* **2006**, *128*, 14796-14797.

^{18}O Percentage Mass Spectrometry Calculation:

(163531 X 1.28) / 100 = 2093

601428 − 2093 = 599335

(599335/ (599335 + 163531)) X 100 = 79% ^{18}O

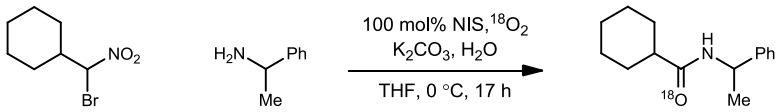

^{18}O-Labeled*N*-(1-Phenylethyl)cyclohexanecarboxamide (^{18}O-Labeled 40)

Following General Procedure B, the α-bromo nitroalkane (28.7 mg, 129 µmol) and amine (19.7 µl, 155 µmol) provided the amide after flash column chromatography (10% ethyl acetate in hexanes) as an off-white solid (24.5 mg, 81%). R_f=0.25 (20% EtOAc/hexanes);spectroscopic data (^{1}H NMR) was in complete accord with that previously reported.[55] A shift in the IR carbonyl peak from 1644 cm^{-1} to 1623 cm^{-1} was observed. The ^{13}C NMR also showed the presence of ^{16}O and ^{18}O carbonyl peak with the ^{18}O peak shifted upfield approximately 0.03 of these two peaks indicated around a 75% ^{18}O incorporation. LRMS (EI): Exact mass calcd for $C_{16}H_{18}NO[M]^+$ 231.16 and $C_{16}H_{18}N^{18}O[M]^+$ 233.17, found 231.25 and 233.30. The relative intensities of these two peaks and their natural abundances were used to determine a 65% ^{18}O incorporation.

^{18}O Percentage Mass Spectrometry Calculation:

(95132 X 1.44) / 100 = 1370

180814 − 1370 = 179444

[55] Vora, H. U.; Rovis, T. *J. Am. Chem. Soc.* **2007**, *129*, 13796-13797.

(179444/ (179444 + 95132)) X 100 = 65% ^{18}O

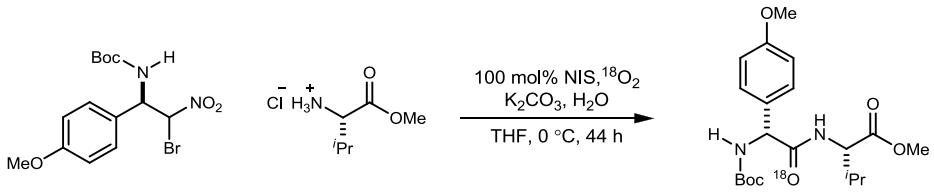

^{18}O-Labeled-*N*-Boc-4-OMe-Phenylglycine-Val-OMe (^{18}O-Labeled 41)

Following General Procedure B, the α-bromo nitroalkane (40.6 mg, 108μmol) and ammonium salt of valine (21.7 mg, 130μmol) provided the dipeptide (single diastereomer) after flash column chromatography (20% ethyl acetate in hexanes) as a viscous oil (27.6 mg, 65%). R_f=0.32 (30% EtOAc/hexanes). A shift in the IR carbonyl peak from 1664 cm^{-1} to 1645 cm^{-1} was observed. The ^{13}C NMR ^{16}O and ^{18}O carbonyl peaks were too close to approximate the ^{18}O incorporation. HRMS (ESI): Exact mass calcd for $C_{20}H_{30}N_2NaO_6$ $[M+Na]^+$417.2002 and $C_{20}H_{30}N_2NaO_5{}^{18}O$ $[M+Na]^+$ 419.2059, found 417.1995and 419.2036. The relative intensities of these two peaks and their natural abundances were used to determine a 76% ^{18}O incorporation.

^{18}O Percentage Mass Spectrometry Calculation:

(46161 X 3.62) / 100 = 1671.03

145922 − 1671 = 144251

(144251/ (144251 + 46161)) X 100 = 76% ^{18}O

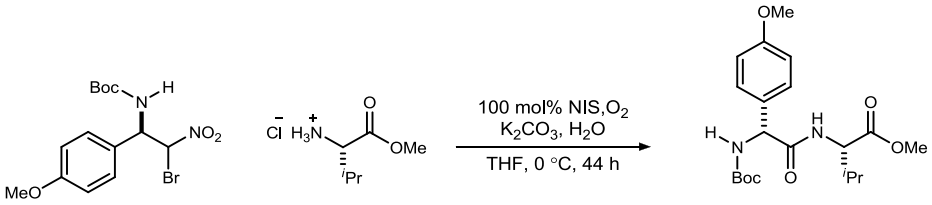

***N*-Boc-4-OMe-Phenylglycine-Val-OMe (41)**

Following General Procedure A, the α-bromo nitroalkane (23 mg, 61μmol) and the ammonium salt of valine (12.3 mg, 73.2μmol) provided the dipeptide (single diastereomer) after flash column chromatography (20% ethyl acetate in hexanes) as a viscous oil (17.8 mg, 74%). $[\alpha]_D^{20}$ -37 (*c* 1.0, $CHCl_3$); R_f=0.32 (30% EtOAc/hexanes); IR (film) 3321, 2965, 2930, 2362, 1740, 1664, 1612, 1511 cm^{-1}; ^1H NMR (400 MHz, $CDCl_3$) δ 7.30 (d, *J* = 8.0 Hz, 2H), 6.87 (d, *J* = 8.4 Hz, 2H), 6.30 (br s, 1H), 5.67 (br s, 1H),5.13 (br s, 1H), 4.54 (dd, *J* = 8.8, 4.8 Hz, 1H), 3.79 (s, 3H), 3.73 (s, 3H), 2.06 (qqd, *J* = 6.8, 6.8, 5.0 Hz,1H), 1.41 (s, 9H), 0.76 (d, *J* = 6.8 Hz, 3H), 0.71 (d, *J* = 6.8 Hz, 3H); ^{13}C NMR (150 MHz, $CDCl_3$) ppm 172.1, 170.2, 159.5, 128.4, 114.3, 58.0, 56.93, 55.2, 52.2, 31.3, 31.1, 29.6, 28.2, 18.7, 17.3; HRMS (ESI): Exact mass calcd for $C_{20}H_{30}N_2NaO_6$ $[M+Na]^+$ 417.2002, found 417.2001.

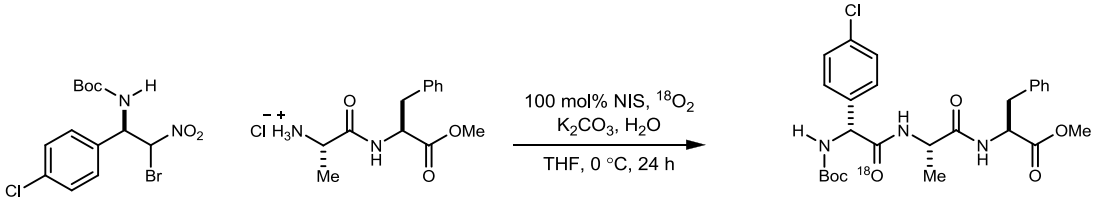

^{18}O-Labeled-*N*-Boc-4-Cl-Phenylglycine-Ala-Phe-OMe (^{18}O-Labeled 42)

Following General Procedure B, with an additional base wash (satd. aqueous K_2CO_3) after chromatography, the α-bromo nitroalkane (39.9 mg, 105 μmol) and ammonium salt (36.2 mg, 126 μmol) provided the amide after flash column chromatography (30-40% ethyl acetate in hexanes) as a white solid (31.4 mg, 58%); spectroscopic data (^1H NMR,

^{13}C NMR, and IR) was in complete accord with that previously reported.[22] A shift in the IR carbonyl peak from 1643 cm^{-1} to 1625 cm^{-1} was observed. The ^{13}C NMR ^{16}O and ^{18}O carbonyl peaks were too close together to approximate the ^{18}O incorporation. HMBC NMR analysis confirmed the identity of the ^{18}O-labeled carbonyl at 169.5 ppm. HRMS (ESI): Exact mass calcd for $C_{26}H_{32}ClN_3NaO_6$[M+Na]$^+$540.1877 and $C_{26}H_{32}ClN_3NaO_5{}^{18}O$[M+Na]$^+$542.1862, found 540.1837 and 542.1928. The relative intensities of these two peaks and their natural abundances were used to determine a 93% ^{18}O incorporation.

^{18}O Percentage Mass Spectrometry Calculation:

(12293 X 32.27) / 100 = 3967

156806 − 3967 = 152839

(152839/ (152839 + 12293)) X 100 = 93% ^{18}O

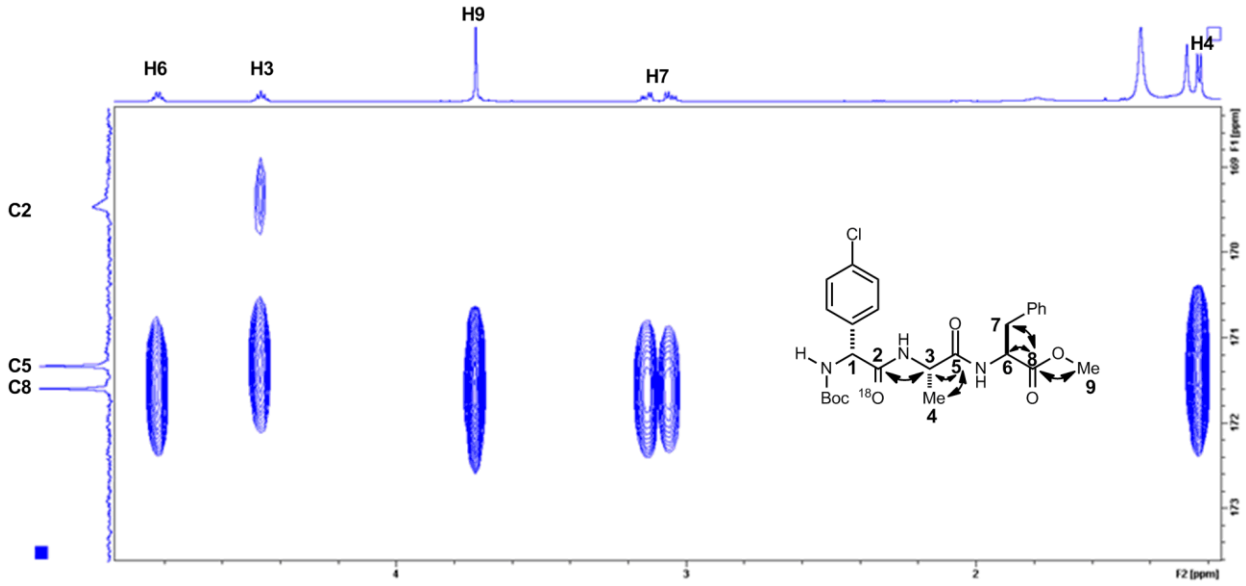

HMBC Analysis (Carbonyl Assignments):

C8 correlates to H6 and H9 indicating it is the ester carbonyl. C5 correlates to H3 and H4 indicating it is likely the unlabeled amide carbonyl, as the labeled amide carbonyl should not correlate to H4. C2 is likely to be the labeled amide carbonyl peak as it weakly correlates to H3 but not H4. The carbamate carbonyl of the Boc group only shows one potential correlation to H1 when the spetrum is highly magnified. This weak signal is likely due to the broad nature of both the carbon and proton shifts. A correlation between the labeled amide carbonyl (C2) and H1 cannot be clearly identified, which is also likely due to the broad nature of both the carbon and proton shifts. The shift of the carbamate carbonyl of the Boc group is also much further upfield than the ester and amide carbonyl peaks, which is to be expected.

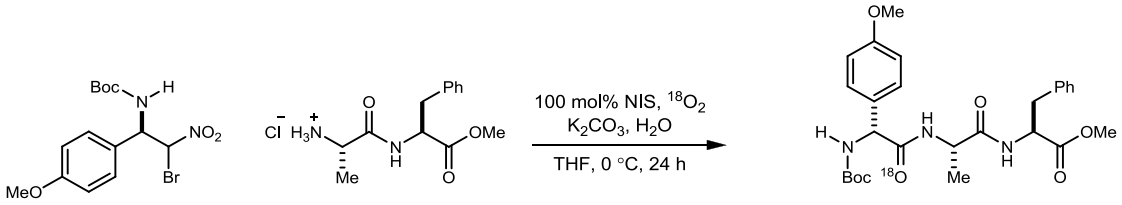

^{18}O-Labeled-*N*-Boc-4-OMe-Phenylglycine-Ala-Phe-OMe (^{18}O-Labeled 43)

Following General Procedure B, with an additional base wash (satd. aq. K_2CO_3) after chromatography, the α-bromo nitroalkane (41.6 mg, 111 μmol) and ammonium salt (38.2 mg, 133 μmol) provided the amide after flash column chromatography (40% ethyl acetate in hexanes) as a white solid (27.7 mg, 49%); spectroscopic data (^{1}H NMR, ^{13}C NMR, and IR) was in complete accord with that previously reported. A shift in the IR carbonyl peak from 1647 cm^{-1} to 1630 cm^{-1} was observed. The ^{13}C NMR ^{16}O and ^{18}O carbonyl peaks were too close to approximate the ^{18}O incorporation. HMBC NMR analysis confirmed the identity of the ^{18}O-labeled carbonyl at 170.2 ppm. HRMS (ESI): Exact mass calcd for

$C_{27}H_{35}N_3NaO_7$ $[M+Na]^+$536.2372 and $C_{27}H_{35}N_3NaO_6{}^{18}O$ $[M+Na]^+$ 538.2432, found 536.2352 and 538.2407. The relative intensities of these two peaks and their natural abundances were used to determine a 88% ^{18}O incorporation.

^{18}O Percentage Mass Spectrometry Calculation:

(6168 X 5.99) / 100 = 370

45097 − 370 = 44728

(44728/ (44728 + 6168)) X 100 = 88% ^{18}O

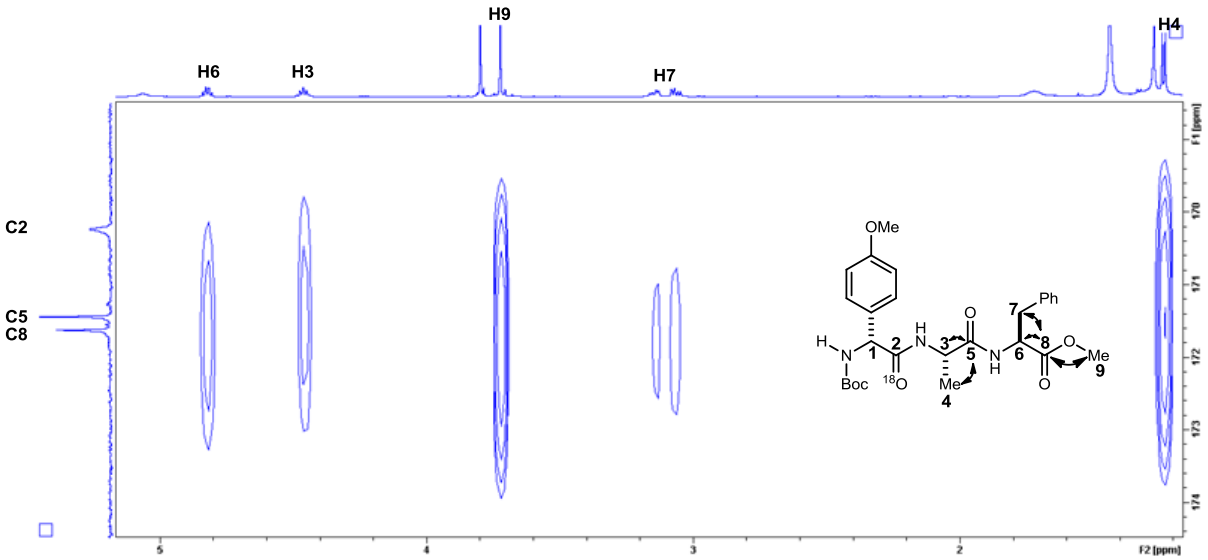

HMBC Analysis (Carbonyl Assignments):

C8 correlates to H6 and H9 indicating it is the ester carbonyl. C5 correlates to H3 and H4 indicating it is likely the unlabeled amide carbonyl, as the labeled amide carbonyl should not correlate to H4. C2 and the carbamate carbonyl shift of the Boc group (not shown) show no correlations, which is likely due to the broad nature of the carbon and proton shifts. C2 is likely to be the labeled amide carbonyl due to the other carbonyl shift being

much higher upfield (155 ppm), which would be expected for the carbamate carbonyl of the Boc group and not the amide.

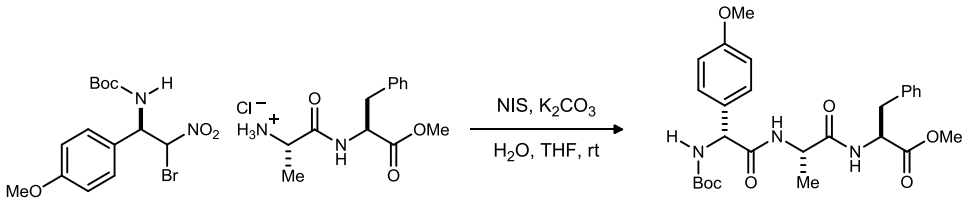

***N*-Boc-4-MeO-Phenylglycine-Ala-Phe-OMe (43)**

Following General Procedure A, the α-bromonitroalkane (20.0 mg, 50.0 μmol) and the ammonium salt of the Ala-Phe dipeptide (18.0 mg, 60.0 μmol) provided the tripeptide (single diastereomer), after flash column chromatography (40% ethyl acetate in hexanes), as a white solid (19.7 mg, 72%). $[\alpha]_D^{20}$ -38.1 (*c* 2.2, $CHCl_3$); R_f=0.17 (40% EtOAc/hexanes); mp =179-180 °C; IR (film) 3282, 2927, 1651, 1512, 1247, 1169 cm^{-1}; ^1H NMR (600 MHz, $CDCl_3$) δ 7.25 (m, 5H), 7.09 (d, *J* = 6.6 Hz, 2H), 6.85 (d, *J* = 9.0 Hz, 2H), 6.60 (br s, 1H), 6.36 (d, *J* = 7.8 Hz, 1H), 5.66 (br s, 1H), 5.06 (br s, 1H), 4.80 (ddd, *J* = 6.6, 6.6, 6.6 Hz, 1H), 4.45 (dq, *J* = 6.6, 6.6 Hz, 1H), 3.78 (s, 3H), 3.70 (s, 3H), 3.12 (dd, *J* = 13.8, 6.0 Hz, 1H), 3.03 (dd, *J* = 13.8, 6.6 Hz, 1H), 1.42 (s, 9H), 1.22 (d, *J* = 7.2 Hz, 3H); ^{13}C NMR (150 MHz, $CDCl_3$) ppm 171.6, 171.4, 170.2, 159.6, 155.1, 135.7, 130.0, 129.2, 128.6, 128.5, 127.2, 114.4, 80.1, 58.2, 55.3, 53.3, 52.3, 48.8, 37.7, 28.3, 17.9; HRMS (ESI): Exact mass calcd for $C_{27}H_{36}N_3O_7[M+H]^+$514.2548, found 514.2552.

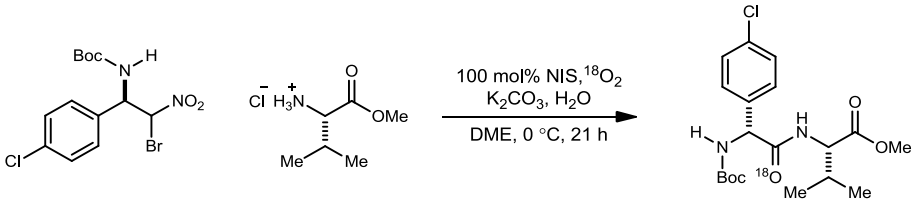

^{18}O-Labeled-*N*-Boc-4-Cl-Phenylglycine-Val-OMe (^{18}O-Labeled 44)

Following General Procedure B, the α-bromo nitroalkane (70 mg, 184 μmol) and ammonium salt of valine (37.1 mg, 221 μmol) provided the dipeptide (single diastereomer) after flash column chromatography (20% ethyl acetate in hexanes) as a yellow solid (44.7 mg, 60%). Spectroscopic data (^{1}H NMR, ^{13}C NMR, and IR) was in complete accord with that previously reported.[56] A shift in the IR carbonyl peak from 1661 cm^{-1} to 1646 cm^{-1} was observed. The ^{13}C NMR ^{16}O and ^{18}O carbonyl peaks were too close to approximate the ^{18}O incorporation. HRMS (ESI): Exact mass calcd for $C_{19}H_{27}ClN_2NaO_5$ $[M+Na]^+$ 421.1506 and $C_{19}H_{27}ClN_2NaO_4{}^{18}O$ $[M+Na]^+$ 423.1485, found 421.1495 and 423.1495. The relative intensities of these two peaks and their natural abundances were used to determine an 86% ^{18}O incorporation.

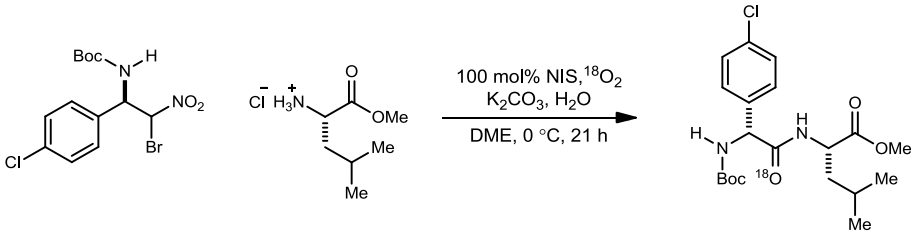

^{18}O-Labeled-*N*-Boc-4-Cl-Phenylglycine-Leu-OMe (^{18}O-Labeled 45)

Following General Procedure B, the α-bromo nitroalkane (70.0 mg, 184 μmol) and ammonium salt of alanine (40.1 mg, 221 μmol) provided the dipeptide (single diastereomer) after flash column chromatography (20% ethyl acetate in hexanes) as a

yellow solid (59.2 mg, 77%). Spectroscopic data (^{1}H NMR, ^{13}C NMR, and IR) was in complete accord with that previously reported.[56] A shift in the IR carbonyl peak from 1661 cm^{-1} to 1645 cm^{-1} was observed. The ^{13}C NMR ^{16}O and ^{18}O carbonyl peaks were too close to approximate the ^{18}O incorporation. HRMS (ESI): Exact mass calcd for $C_{20}H_{29}ClN_2NaO_5$ $[M+Na]^+$ 435.1663 and $C_{20}H_{29}ClN_2NaO_4{}^{18}O$ $[M+Na]^+$ 437.1642, found 435.1633 and 437.1655. The relative intensities of these two peaks and their natural abundances were used to determine a 92% ^{18}O incorporation.

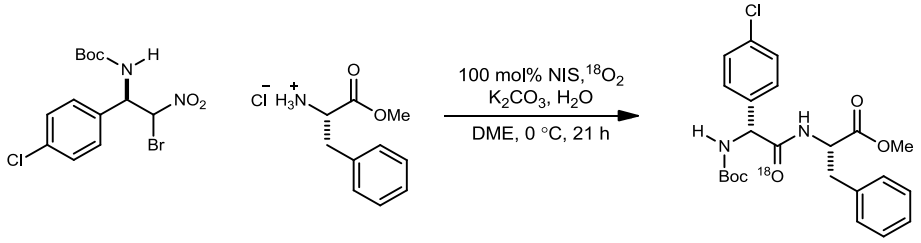

^{18}O-Labeled-*N*-Boc-4-Cl-Phenylglycine-Phe-Ome (^{18}O-Labeled 46)

Following General Procedure B, the α-bromo nitroalkane (70 mg, 184 μmol) and ammonium salt of phenylalanine (47.6 mg, 221 μmol) provided the dipeptide (single diastereomer) after flash column chromatography (20% ethyl acetate in hexanes) as a yellow solid (37.6 mg, 45%). Spectroscopic data (^{1}H NMR, ^{13}C NMR, and IR) was in complete accord with that previously reported.[56] A shift in the IR carbonyl peak from 1661 cm^{-1} to 1646 cm^{-1} was observed. The ^{13}C NMR ^{16}O and ^{18}O carbonyl peaks were too close to approximate the ^{18}O incorporation. HRMS (ESI): Exact mass calcd for $C_{23}H_{27}ClN_2NaO_5$ $[M+Na]^+$ 469.1506 and $C_{23}H_{27}ClN_2NaO_4{}^{18}O$ $[M+Na]^+$ 471.1488, found 469.1485 and 471.1495. The relative intensities of these two peaks and their natural abundances were used to determine a 90% ^{18}O incorporation.

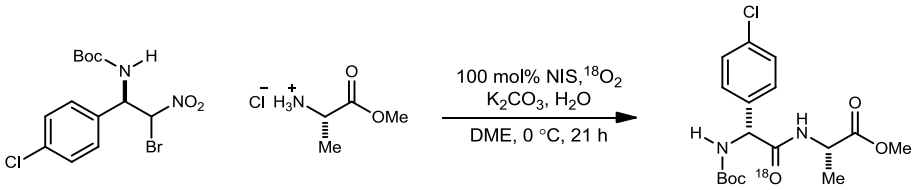

^{18}O-Labeled-*N*-Boc-4-Cl-Phenylglycine-Ala-Ome (^{18}O-Labeled 47)

Following General Procedure B, the α-bromo nitroalkane (70 mg, 184 μmol) and ammonium salt of alanine (29.8 mg, 221 μmol) provided the dipeptide (single diastereomer) after flash column chromatography (20% ethyl acetate in hexanes) as a yellow solid (49.0 mg, 71%). Spectroscopic data (^{1}H NMR, ^{13}C NMR, and IR) was in complete accord with that previously reported.[56] A shift in the IR carbonyl peak from 1662 cm^{-1} to 1645 cm^{-1} was observed. The ^{13}C NMR ^{16}O and ^{18}O carbonyl peaks were too close to approximate the ^{18}O incorporation. HRMS (ESI): Exact mass calcd for $C_{17}H_{23}ClN_2NaO_5$ $[M+Na]^+$ 393.1193 and $C_{17}H_{23}ClN_2NaO_4{}^{18}O$ $[M+Na]^+$ 395.1171, found 393.1170 and 395.1194. The relative intensities of these two peaks and their natural abundances were used to determine a 91% ^{18}O incorporation.

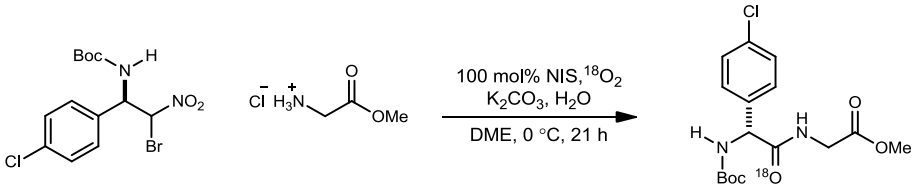

^{18}O-Labeled-*N*-Boc-4-Cl-Phenylglycine-Gly-Ome (^{18}O-Labeled 48)

Following General Procedure B, the α-bromo nitroalkane (75 mg, 198 μmol) and ammonium salt of glycine (29.8 mg, 237 μmol) provided the dipeptide (single diastereomer) after flash column chromatography (30% ethyl acetate in hexanes) as a yellow solid (43.8 mg, 62%). Spectroscopic data (^{1}H NMR, ^{13}C NMR, and IR) was in

complete accord with that previously reported.[56] A shift in the IR carbonyl peak from 1699 cm^{-1} to 1648 cm^{-1} was observed. The ^{13}C NMR ^{16}O and ^{18}O carbonyl peaks were too close to approximate the ^{18}O incorporation. HRMS (ESI): Exact mass calcd for $C_{16}H_{21}ClN_2NaO_5$ $[M+Na]^+$ 379.1037 and $C_{16}H_{21}ClN_2NaO_4{}^{18}O$ $[M+Na]^+$ 381.1014, found 379.1035 and 381.1049. The relative intensities of these two peaks and their natural abundances were used to determine a 91% ^{18}O incorporation.

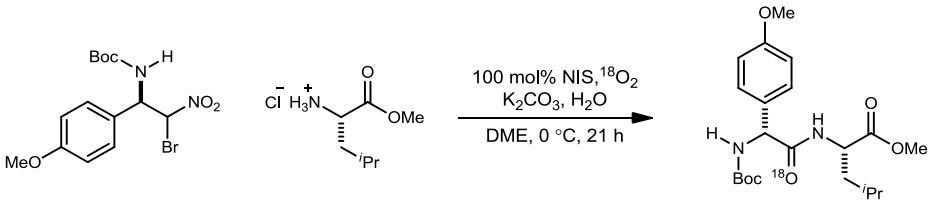

^{18}O-Labeled-*N*-Boc-4-OMe-Phenylglycine-Leu-OMe (^{18}O-Labeled 49)

Following General Procedure B, the α-bromo nitroalkane (70 mg, 187 μmol) and ammonium salt of leucine (40.7 mg, 224 μmol) provided the dipeptide (single diastereomer) after flash column chromatography (20% ethyl acetate in hexanes) as a viscous oil (37.5 mg, 49%). Spectroscopic data (^1H NMR, ^{13}C NMR, and IR) was in complete accord with that previously reported.[56] A shift in the IR carbonyl peak from 1664 cm^{-1} to 1646 cm^{-1} was observed. The ^{13}C NMR ^{16}O and ^{18}O carbonyl peaks were too close to approximate the ^{18}O incorporation. HRMS (ESI): Exact mass calcd for $C_{21}H_{32}N_2NaO_6$ $[M+Na]^+$ 431.2158 and $C_{21}H_{32}N_2NaO_5{}^{18}O$ $[M+Na]^+$ 433.2201, found 431.2141 and 433.2178. The relative intensities of these two peaks and their natural abundances were used to determine a 85% ^{18}O incorporation.

[56] Shen, B., Makley, D., Johnston, J. N. *Nature.* **2010**, *465*, 1027.

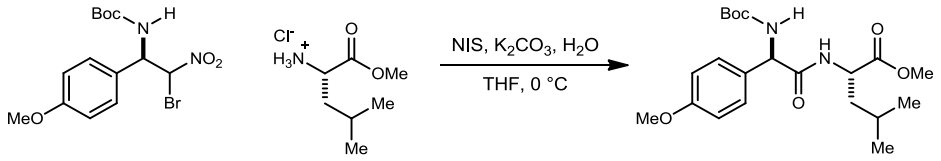

_N_-Boc-4-OMe-Phenylglycine-Leu-OMe (49)

Following General Procedure A, the α-bromo nitroalkane (25.0 mg, 67.0 μmol) and ammonium salt of leucine (14.6 mg, 80.4 μmol) provided the dipeptide (single diastereomer) after flash column chromatography (20% ethyl acetate in hexanes) as a yellow oil (20.8 mg, 76%). $[\alpha]_D^{20}$ -67.6 (*c* 1.1, $CHCl_3$); R_f = 0.17 (20% EtOAc/hexanes); IR (film) 3319, 2958, 2931, 1743, 1715, 1664, 1612, 1512, 1367 cm^{-1}; ^1H NMR (600 MHz, $CDCl_3$) δ 7.28 (d, *J* = 8.4 Hz, 2H), 6.87 (d, *J* = 8.4 Hz, 2H), 6.18 (d, *J* = 8.4 Hz, 1H), 5.65 (br s, 1H), 5.12 (br s, 1H), 4.60 (ddd, *J* = 9.0, 9.0, 4.8 Hz, 1H), 3.79 (s, 3H), 3.72 (s, 3H), 1.57 (ddd, *J* = 13.8, 8.4, 5.4 Hz, 1H), 1.45 (ddd, *J* = 14.4, 9.0, 5.4 Hz, 1H), 1.42 (s, 9H), 1.35 (m, 1H), 0.81 (d, *J* = 5.4 Hz, 3H), 0.80 (d, *J* = 4.8 Hz, 3H); ^{13}C NMR (150 MHz, $CDCl_3$) ppm 173.1, 170.1, 159.6, 155.0, 130.3, 128.5, 114.3, 80.0, 58.1, 55.3, 52.3, 50.8, 41.3, 28.2, 24.6, 22.7, 21.7; HRMS (ESI): Exact mass calcd for $C_{21}H_{32}N_2NaO_6$ $[M+Na]^+$ 431.2158, found 431.2137.

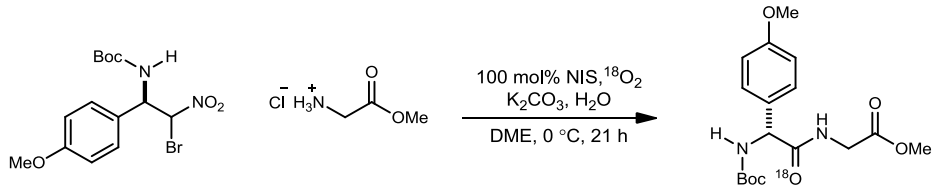

^{18}O-Labeled-*N*-Boc-4-OMe-Phenylglycine-Gly-OMe (^{18}O-Labeled 50)

Following General Procedure B (with the addition of a satd aq Na_2CO_3 wash), the α-bromonitroalkane (75.0 mg, 200 μmol) and ammonium salt of glycine (30.2 mg, 240

μmol) provided the dipeptide (single diastereomer) after flash column chromatography (30% ethyl acetate in hexanes) as a white solid (29.3 mg, 41%). Spectroscopic data (^{1}H NMR, ^{13}C NMR, and IR) was in complete accord with that previously reported. A shift in the IR carbonyl peak from 1669 cm^{-1} to 1647 cm^{-1} was observed. The ^{13}C NMR ^{16}O and ^{18}O carbonyl peaks were too close to approximate the ^{18}O incorporation. HRMS (ESI): Exact mass calcd for $C_{17}H_{24}N_2NaO_6$ $[M+Na]^+$ 375.1532 and $C_{17}H_{24}N_2NaO_5{}^{18}O$ $[M+Na]^+$ 377.1575, found 375.1507 and 377.1547. The relative intensities of these two peaks and their natural abundances were used to determine a 90% ^{18}O incorporation.

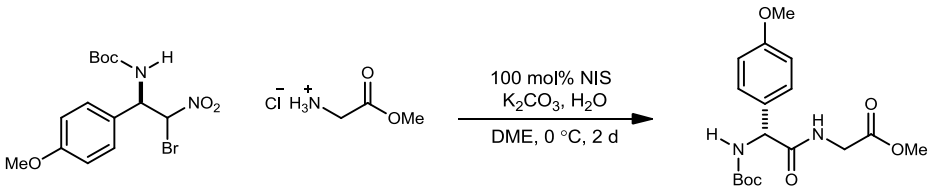

***N*-Boc-4-OMe-Phenylglycine-Gly-OMe (50)**

Following General Procedure A (with the addition of a satd aq Na_2CO_3 wash), the α-bromonitroalkane (30.0 mg, 80 μmol) and ammonium salt of glycine (12.1 mg, 96 μmol) provided the dipeptide (single diastereomer) after flash column chromatography (30% ethyl acetate in hexanes) as a white solid (9.3 mg, 33%). $[\alpha]_D^{20}$ -57.3 (*c* 0.95, $CHCl_3$); R_f = 0.08 (30% EtOAc/hexanes); mp 98-100 °C; IR (film) 3324, 2926, 2853, 1751, 1669, 1612, 1512, 1368, 1248 cm^{-1}; ^{1}H NMR (600 MHz, $CDCl_3$) δ 7.29 (d, *J* = 8.4 Hz, 2H), 6.88 (d, *J* = 9.0, 2H), 6.27 (br s, 1H), 5.65 (br s, 1H), 5.15 (br s, 1H), 4.07 (dd, *J* = 18.6, 5.4 Hz, 1H), 3.97 (dd, *J* = 18.6, 4.8 Hz, 1H), 3.79 (s, 3H), 3.73 (s, 3H), 1.41 (s, 9H); ^{13}C NMR (600 MHz, $CDCl_3$) ppm 170.6, 169.9, 159.7, 130.0, 128.6, 114.3, 80.4, 57.8, 55.3,

52.4, 41.4, 28.3. HRMS (ESI): Exact mass calcd for $C_{17}H_{24}N_2NaO_6$ $[M+Na]^+$ 375.1532, found 375.1517.

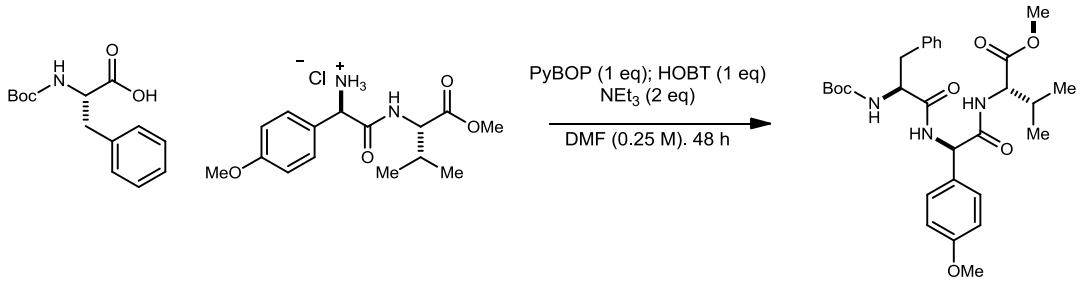

N-Boc-Phe-4-OMe-Phenylglycine-Val-OMe (63)

Boc-protected phenylalanine (48.0 mg, 181 µmol), PyBOP (113 mg, 218 µmol), and HOBt (30.0 mg, 218 µmol) were dissolved in anhydrous DMF (0.22 M) and allowed to stir for 10 minutes at room temperature. A solution of amine salt (72.0 mg, 218 µmol) and triethyl amine (91.0 µl, 652 µl) was added, and the reaction was allowed to stir for 48 hours at room temperature. The reaction was quenched with H_2O and extracted with methylene chloride, dried over $MgSO_4$, and concentrated. The residue was purified via flash column chromatography (30% ethyl acetate in hexanes) to afford the amide as a white solid (25.6 mg, 26%). $[\alpha]_D^{20}$ -32.3 (*c* 1.5, $CHCl_3$); R_f = 0.16 (30% EtOAc/hexanes); mp 166-170 °C; IR (film) 3298, 2966, 2931, 1741, 1695, 1645, 1513, 1459, 1368, 1308 cm^{-1}; ^1H NMR (600 MHz, $CDCl_3$) δ 7.25-6.92 (m, 9H), 6.79 (d, *J* = 8.7, 1H), 6.71 (d, *J* = 8.2, 1H), 5.62 (br s, 1H), 5.43 (br s, 1H), 4.51 (dd, *J* = 8.9, 5.2 Hz, 1H), 4.43 (br s, 1 H), 3.77 (s, 3H), 3.72 (s, 3H), 3.05 (m, 2 H), 2.04 (qqd, *J* = 6.7, 6.7, 5.4 Hz, 1H), 1.39 (s, 9H), 0.71 (d, *J* = 2.6 Hz, 3H), 0.70 (d, *J* = 2.6 Hz, 3H); ^{13}C NMR (600 MHz, $CDCl_3$) ppm 172.0, 170.5, 169.9, 159.3, 155.3, 136.5, 129.3, 129.2, 128.6, 128.3, 126.7, 114.0, 79.9, 57.1, 55.2, 52.2, 52.1, 38.7, 31.4, 28.24, 28.18, 18.7, 17.5. HRMS (ESI): Exact mass calcd for $C_{29}H_{39}N_3NaO_7$ $[M+Na]^+$ 564.2686, found 564.2694.

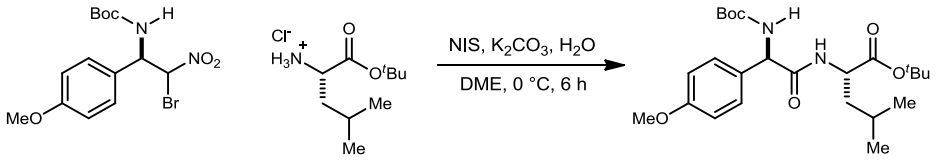

_N_-Boc-4-OMe-Phenylglycine-Leu-O^{t}Bu (79)

Following General Procedure A, the α-bromo nitroalkane (29.2 mg, 78.0 μmol) and ammonium salt of leucine *tert*-butyl ester (14.6 mg, 80.4 μmol) provided the dipeptide (single diastereomer) after flash column chromatography (20% ethyl acetate in hexanes) as a yellow solid (16.9 mg, 48%). $[\alpha]_D^{20}$ -64.1 (*c* 0.46, $CHCl_3$); R_f = 0.20 (20% EtOAc/hexanes); mp 72-76 °C; IR (film) 3322, 2964, 2932, 1720, 1667, 1612, 1512, 1368 cm^{-1}; ^1H NMR (600 MHz, $CDCl_3$) δ 7.28 (d, *J* = 8.4 Hz, 2H), 6.86 (d, *J* = 9.0 Hz, 2H), 6.08 (d, *J* = 8.4 Hz, 1H), 5.68 (br s, 1H), 5.09 (br s, 1H), 4.48 (ddd, *J* = 8.4, 8.4, 5.4 Hz, 1H), 3.79 (s, 3H), 1.51 (m, 2H), 1.45 (s, 9H), 1.40 (s, 9H), 1.36 (m, 1H), 0.81 (d, *J* = 6.0 Hz, 6H); ^{13}C NMR (150 MHz, $CDCl_3$) ppm 171.9, 169.8, 159.6, 130.2, 128.5, 114.3, 82.1, 55.3, 51.5, 41.6, 29.7, 28.3, 28.0, 24.7, 22.7, 21.9; HRMS (ESI): Exact mass calcd for $C_{24}H_{38}N_2NaO_6$ $[M+Na]^+$ 473.2628, found 473.2624.

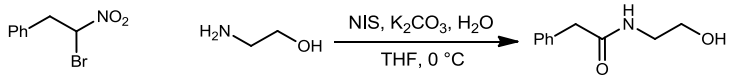

_N_-(2-Hydroxybutyl)-2-phenylacetamide (83)

Following General Procedure A, the α-bromo nitroalkane (30.8 mg, 134 μmol) and amine (9.7μl, 161 μmol) provided the amide after flash column chromatography (4% methanol in dichloromethane) as an off-white solid (20.8 mg, 86%). R_f = 0.37 (5% MeOH/CH_2Cl_2); mp 52-56 °C; IR (neat) 3290, 3063, 3029, 2920, 2850, 1645, 1604, 1583, 1495 cm^{-1}; ^1H NMR (600 MHz, $CDCl_3$) δ 7.28-7.26 (m, 2H), 7.22-7.21 (m, 1H), 7.19-7.17 (m, 2H),

6.02 (br s, 1H), 3.56 (t, *J* = 6.0 Hz, 2H), 3.49 (s, 2H), 3.27 (dt, *J* = 6.0, 6.0 Hz, 2H); ^{13}C NMR (600 MHz, $CDCl_3$) ppm 172.5, 134.6, 129.4, 129.0, 127.4, 62.1, 43.5, 42.6, 29.7; HRMS (ESI): Exact mass calcd for $C_{10}H_{14}NO_2$ $[M+H]^+$ 180.1019, found 180.1014

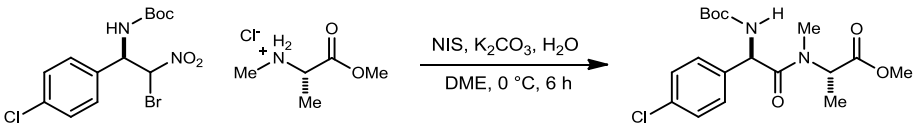

***N*-Boc-4-Cl-Phenylglycine-N-Me-Ala-OMe (112)**

Following General Procedure A, the α-bromo nitroalkane (26.1 mg, 69.0 μmol) and ammonium salt of *N*-methyl alanine (31.8 mg, 207 μmol) provided the dipeptide (single diastereomer) after flash column chromatography (10-25% ethyl acetate in hexanes) as a clear oil (8.6 mg, 33%). $[\alpha]_D^{20}$ -125 (*c* 0.2, $CHCl_3$); R_f = 0.13 (20% EtOAc/hexanes); IR (film) 3320, 2924, 2853, 1745, 1710, 1650, 1489, 1408,1367, 1244 cm^{-1}; ^{1}H NMR (600 MHz, $CDCl_3$)[57] δ 7.32 (s, 4H), 6.09 (d, *J* = 7.2 Hz, 1H), 5.53 (d, *J* = 7.2 Hz, 1H), 5.04 (q, *J*= 7.2 Hz, 1H), 3.73 (s, 3H), 2.80 (s, 3H), 1.40 (s, 9H), 1.32 (d, *J* = 7.8 Hz, 3H); ^{13}C NMR (150 MHz, $CDCl_3$) ppm 172.0, 170.0, 154.8, 136.3, 134.2, 129.2, 128.9, 79.9, 54.8, 53.5, 52.4, 31.9, 28.3, 14.3; HRMS (ESI): Exact mass calcd for $C_{18}H_{25}ClN_2NaO_5$ $[M+Na]^+$ 407.1350, found 407.1349.

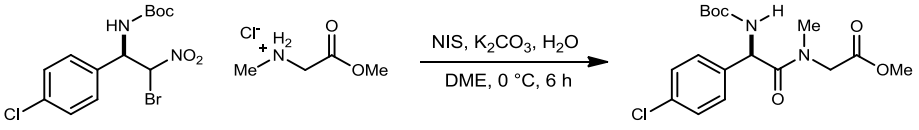

***N*-Boc-4-Cl-Phenylglycine-N-Me-Gly-OMe (116)**

Following General Procedure A, the α-bromo nitroalkane (25.0 mg, 66.0 μmol) and trifluroacetic acid salt of N-methylglycine (40.1 mg, 198 μmol) provided the dipeptide

[57] Compound was isolated as a 6:1 mixture of rotamers. Only the major rotamer is reported.

after flash column chromatography (20% ethyl acetate in hexanes) as a clear oil (13.6 mg, 56%). $[\alpha]_D^{20}$ -137 (*c* 0.5, $CHCl_3$); R_f = 0.21 (30% EtOAc/hexanes); IR (film) 3416, 3326, 2977, 2930, 1751, 1709, 1656, 1489, 1407, 1367 cm^{-1}; ^1H NMR (600 MHz, $CDCl_3$) δ 7.37 (d, *J* = 8.4 Hz, 2H), 7.33 (d, *J* = 8.4 Hz, 2H), 5.94 (d, *J* = 7.8 Hz, 1H), 5.59 (d, *J* = 7.8 Hz, 1H), 4.32 (d, *J* = 17.4 Hz, 1H), 3.94 (d, *J* = 17.4 Hz, 1H), 3.73 (s, 3H), 2.92 (s, 3H), 1.41 (s, 9H); ^{13}C NMR (150 MHz, $CDCl_3$) ppm 170.4, 169.1, 155.0, 135.9, 134.3, 129.4, 129.1, 80.0, 54.5, 52.2, 49.9, 36.3, 28.3; HRMS (ESI): Exact mass calcd for $C_{17}H_{23}ClN_2NaO_5$ $[M+Na]^+$ 393.1193, found 393.1174.